

---

# Polycrystalline Films of Microporous Materials on Different Substrates

---

Von der Naturwissenschaftlichen Fakultät der  
Gottfried Wilhelm Leibniz Universität Hannover

zur Erlangung des Grades

**Doktorin der Naturwissenschaften**  
**Dr. rer. nat.**

genehmigte Dissertation

von

Dipl.-Chem. Imke Bremer

geboren am 02. Februar 1983 in Twistringen

2013

Referent: Prof. Dr. Peter Behrens

Korreferent: Prof. Dr. Jürgen Caro

Tag der Promotion: 12.12.2013

## **Erklärung**

Hierdurch erkläre ich, dass ich meine Dissertation mit dem Titel „*Polycrystalline Films of Microporous Materials on Different Substrates*“ selbstständig verfasst und die benutzten Hilfsmittel und Quellen sowie gegebenenfalls zu Hilfeleistungen herangezogenen Institutionen vollständig angegeben habe.

Die Dissertation wurde nicht schon als Masterarbeit, Diplomarbeit oder andere Prüfungsarbeit verwendet.

Hannover, den 20.12.2013

Dipl.-Chem. Imke Bremer

---



## Abstract

This thesis addresses the synthesis and characterization of polycrystalline films of different microporous materials. It contains three chapters that are to be submitted as original research articles.

The first part deals with the synthesis of zeolitic membranes consisting of two active layers. Layers of sodalite, a promising material for the separation of hydrogen due to its narrow pores, were found to break during the necessary calcination process. The goal was to enhance the mechanical stability of the sodalite layer by introducing an additional layer of the more robust zeolite silicalite-1 that features a larger pore size. We have used seeding and secondary growth to successfully synthesize a hierarchical arrangement of a layered film of two microporous materials with different topologies on top of each other. Ultimately this concept did not enhance the stability of the sodalite layer, but offers an approach to other multilayer systems.

In the second part, the influence of monocarboxylic acid modulators on the synthesis of the metal-organic framework material UiO-66 was investigated. Up to now, this material has been available as an unstructured powder or as isolated nanocrystals only. For the generation of dense layers it would be of interest to have access to strongly intergrown multi-crystallite aggregates. We have found modulators which, in contrast to standard modulating agents, facilitate the formation of large and intergrown aggregates of UiO-66 and have compared the properties of the products synthesized with different modulators in terms of crystallinity, stability, and porosity.

These findings were used in the third part of this work for the preparation of polycrystalline layers of UiO-66 and also of a new material developed in our laboratory lately, PIZOF-2. In the course of this the influence of different substrate materials on the surface crystallization of Zr-containing MOFs was examined. An excellent transferability of the influence of surface properties of the support materials and of different modulators between the Zr-MOFs was demonstrated and reliable syntheses procedures for the deposition of Zr-MOF layers were found. With the gained knowledge layers of other PIZOFs should be easily producible. Different drying protocols were tested to improve the microstructure of the layers.

Though ultimately no crack free membranes could be obtained in this work, the layers are of interest as coatings for other applications in fields like sensing or biomedical applications.

**Keywords:** zeolites – metal-organic frameworks – Zr-MOFs – modulated synthesis – polycrystalline layers

---



## Kurzzusammenfassung

Diese Dissertation behandelt die Synthese und Charakterisierung von polykristallinen trägergestützten Membranen und Schichten verschiedener mikroporöser Materialien. Sie beinhaltet drei Kapitel, die als Original-Arbeiten veröffentlicht werden sollen.

Das erste Kapitel befasst sich mit der Synthese von zeolithischen Membranen, die zwei aktive Schichten enthalten. Schichten von Sodalith, der aufgrund seiner kleinen Poren ein vielversprechendes Material für die Trennung von Wasserstoff darstellt, zerbrechen während des notwendigen Calcinationsprozesses. Unser Ziel war es die mechanische Stabilität der Sodalith Schicht durch Einführen einer weiteren Schicht des robusteren und größerporigen Zeolithen Silicalit-1 zu verbessern. Dabei wurde die Methode des Impfens mit anschließendem Dickenwachstum verwendet, um erfolgreich die hierarchische Anordnung einer Doppelschicht aus zwei mikroporösen Materialien mit unterschiedlichen Topologien zu erzeugen. Auch wenn dieses Konzept jedoch letztlich nicht zu der erhofften Verbesserung der Stabilität der Sodalithschicht führte, bietet dieser Teil der Arbeit aber einen Ansatz für den Aufbau anderer Multischicht Systeme.

Im zweiten Teil wurde der Einfluss unterschiedlicher Monocarbonsäure-Modulatoren auf die Synthese des Metall-organischen Gerüsts UiO-66 untersucht. Bisher ist dieses Material nur in Form von unstrukturierten Pulvern oder als individuelle Nanopartikel erhältlich. Für die Herstellung dichter Schichten ist es jedoch von Interesse, Zugang zu stark verwachsenen Aggregaten von Kristallen zu haben. Wir haben Modulatoren gefunden, die, im Gegensatz zu den üblicherweise verwendeten Modulatoren, die Bildung von großen Aggregaten ineinander verwachsener Kristalle von UiO-66 ermöglichen. Die Eigenschaften der mit verschiedenen Modulatoren hergestellten Produkte wurden hinsichtlich ihrer Kristallinität, Stabilität und Porosität untersucht.

Diese Erkenntnisse wurden im dritten Teil für die Herstellung von polykristallinen Schichten von UiO-66 und PIZOF-2, einem neuen Material, das kürzlich in unseren Laboratorien hergestellt wurde, genutzt. Dabei wurde der Einfluss verschiedener Substrate auf die Kristallisation dieser Zr-MOFs untersucht. Eine ausgezeichnete Übertragbarkeit des Einflusses der Oberflächeneigenschaften der Trägermaterialien sowie der Wirkung verschiedener Modulatoren konnten für die beiden Zr-MOFs aufgezeigt werden. So wurden verlässliche Synthesewege für die Abscheidung von Zr-MOF-Schichten gefunden. Mit den gewonnenen Erkenntnissen sollten auch Schichten anderer PIZOFs leicht herzustellen sein. Verschiedene Trocknungsverfahren wurden getestet um die Mikrostruktur der Schichten zu verbessern. Obwohl letztendlich keine rissfreien Membranen erhalten werden konnten, sind die Schichten doch für mögliche Anwendungen in der Sensorik oder auch für biomedizinische Anwendungen von Interesse.

**Schlagnworte:** Zeolithe – Metall-organische Gerüste – Zr-MOFs – modulierte Synthese – polykristalline Schichten

---





## Danksagung

Zu Beginn möchte ich mich bei Prof. Dr. Peter Behrens für die Aufnahme in seinen Arbeitskreis und für die Betreuung meiner Doktorarbeit bedanken. Besonders zu schätzen weiß ich, dass er in Gesprächen stets die richtigen und vor allem motivierenden Worte gefunden hat, wann immer sich das Gefühl einstellte, mit seiner Arbeit nicht weiterzukommen.

Außerdem möchte ich mich bei Prof. Dr. Jürgen Caro für die Übernahme des Korreferats bedanken.

Ein besonderer Dank gebührt auch Dr. Simon Münzer, der mir den Einstieg in die Welt der Zeolithe sehr erleichtert hat und Dr. Andreas Schaate, der mich bei dem Wechsel auf das Gebiet der Zr-MOFs unterstützt hat, als Zeolithe schließlich aus der Mode kamen.

Einigen Mitarbeitern möchte ich noch einmal im Speziellen danken für ihren unermüdlichen Einsatz an verschiedenen Messgeräten. Georg Platz für das Erstellen passender Messfiles und die Durchführung der Messungen (wenn es sein musste auch am Wochenende) an den Sorptionsgeräten und natürlich auch Jann Lippke, der ebenso eifrig sorbiert, seit Georg uns verlassen hat. Für zahlreiche TG Messungen danke ich Andreas Schaate, Christian Schröder und Katharina Nolte. Bei Fabian Kempf möchte ich mich dafür bedanken, dass er mit großer Hingabe immer wieder versucht hat, meine unlösbaren Kristallstrukturen zu lösen und mir mit Rat und Tat bei der Zucht verbesserter (und dennoch nicht lösbarer) Kristalle und bei der Auswertung von NMR-Daten zur Seite stand. Bei Dr. Helge Bux und Lisa Diestel vom Arbeitskreis Caro möchte ich mich für die Durchführung der Permeationsmessungen bedanken.

Für die Synthese der PIZOF-Linker und das Anfertigen von NMR-Spektren möchte ich der Arbeitsgruppe von Prof. Dr. Adelheid Godt, insbesondere Thomas Preuße und Miriam Hülsmann, in Bielefeld danken.

Für die stets heitere Atmosphäre in Labor 020 danke ich Maria Schweinefuß, Philip Zerner und Katharina Nolte. Auch wenn ich nicht alle hier namentlich erwähnen kann, möchte ich dem gesamten AK Behrens für eine wunderbare Zeit danken, an die ich mich wohl immer gerne erinnern werde: Von den Kaffeepausen mit gemeinsamem Rätsel-Lösen über abenteuerliche Kanu-Fahrten auf der Örtze, Feierabendbiere mit mal mehr mal weniger fachlichen Diskussionen, Videoabende bis hin zu Besuchen auf der Pferderennbahn konnte man mit euch in jeder Lebenslage Spaß haben. Über die letzten Jahre ist so aus einem Arbeitskreis ein Freundeskreis (und manchmal sogar Mitbewohner) geworden, was durchaus keine Selbstverständlichkeit ist. Nicht zuletzt dank euch allen bin ich jeden Morgen gerne wieder zur Arbeit erschienen.

---

Bei Janosch möchte ich mich ganz besonders bedanken. Dafür, dass er mich unterstützt, manchmal auch getröstet und gelegentlich getriezt hat, wann immer es nötig war. Außerdem habe ich etwas sehr wichtiges von ihm gelernt: „Warum eigentlich nicht?“

Zuletzt möchte ich auch noch einmal meinen Eltern Jutta und Alex danken, ohne deren Unterstützung mein Studium und damit auch diese Arbeit sicher nicht möglich gewesen wären.

---

## Table of Contents

1	Introduction .....	1
1.1	Metal-Organic Frameworks .....	2
1.2	Synthesis Strategies for Metal-Organic Frameworks.....	7
1.2.1	Isorecticular Synthesis .....	7
1.2.2	Postsynthetic Modification.....	8
1.2.3	Modulated Synthesis of Metal-Organic Frameworks.....	9
1.3	Zirconium Containing Metal-Organic Frameworks.....	14
1.3.1	UiO-type MOFs .....	14
1.3.2	PIZOFs.....	18
1.3.3	MIL-140.....	22
1.4	Porosils and Porolites.....	23
1.4.1	Silicalite-1.....	25
1.4.2	Sodalite.....	26
1.5	Zeolite and MOF Membranes.....	29
1.5.1	Separation Principles .....	29
1.5.2	General Preparation Techniques .....	32
1.5.3	Zeolite-based Membranes.....	34
1.5.4	MOF-based Membranes .....	36
2	References .....	43
3	Results and Discussion.....	51
3.1	Preparation of Silica-Sodalite Layers on Top of Asymmetric $\alpha$ -Alumina Supports and on Silicalite-1 Membranes.....	51
3.2	Investigating the Influence of Different Monocarboxylic Acid Modulators on the Synthesis of Zr- <i>bdc</i> MOF (UiO-66).....	71
3.3	Deposition of Zr-MOF Layers on Different Ceramic Support Materials.....	87
4	Conclusion and Outlook.....	107
5	Curriculum Vitae .....	113
6	List of Publications.....	114

---



## 1 Introduction

The aim of this work is the preparation of thin films of different types of microporous materials on different substrates. Thin films of microporous materials play an important role in a variety of applications. When they are prepared as dense polycrystalline supported membranes, they may be used in gas or liquid phase separation as a cost- and energy-efficient alternative to other separation techniques like distillation or crystallization. For such an application the material requisitions are high. The active layer has to be dense, thin enough to ensure a high flux, yet thick enough to ensure a high selectivity; also, it has to be durable and stable under working conditions (which include increased temperature and pressure). For the construction of sensing devices supported films of microporous materials are of interest as well. In this case a material with a very specific uptake of, at best, only one kind of molecule into the pore system is desired. Another field of application of microporous thin films can be envisaged as active coatings in biomedicine. Porous coatings for example on implants can open the opportunity for a local drug release or tissue engineering.

A class of materials that can be used for such tasks are zeolites, because they are very stable under various conditions and available with different pore sizes. A drawback of zeolites however is their restricted chemical variability due to the (alumo-) silicate framework which is chemically very similar for this whole material class. Sodalite with its exceptionally small pore opening (2.8 Å) is of special interest for the separation of small molecules like hydrogen. Silica sodalite can only be synthesized with the use of organic molecules as structure-directing agents, which have to be removed after the synthesis to obtain an accessible pore system, which is of course a requirement to make use of the sodalite in membrane applications. Previous work on silica sodalite membranes in our laboratories had shown that this template removal step leads to cracked layers because temperatures of 1000 °C are necessary for this step. A mismatch in thermal expansion coefficients between ceramic support materials and sodalite is probably the reason for the formation of these cracks. It was an aim of this thesis to enhance the stability of the sodalite layer by introducing an additional layer of another zeolite between support and sodalite. The preparative means for the hierarchical

---

construction of a two-layered zeolite membrane, which had not been reported before, had to be developed.

Metal-organic frameworks (MOFs) are porous materials that offer a much broader range of chemical versatility than zeolites, because of their modular composition and their character as organic-inorganic hybrid materials. The sub-class of Zr-containing MOFs features an exceptionally high chemical and thermal stability which is not self-evident for many MOFs but of course a requirement for most applications. An aim of this thesis was the preparation of supported layers of this relatively new class of materials. The Zr-MOF UiO-66 was investigated as a model substance to find reliable and reproducible synthesis routes to yield strongly intergrown multi-crystallite aggregates of a sufficient size. With the gained knowledge the influence of different support materials on the film growth was investigated.

According to these topics, the main part of this thesis is organized in three chapters which are presented in the form of original research articles in sections 3.1 (preparation of two-layered zeolite films), 3.2 (investigations on the synthesis of the Zr-bdc MOF), and 3.3 (deposition of Zr-MOF layers). Chapter 3 is preceded by a general introduction into topics related to the work presented there. Finally, in chapter 4 some general conclusions and an outlook on possible future work are presented.

## **1.1 Metal-Organic Frameworks**

Metal-organic frameworks (MOFs) are in principle a relatively young class of crystalline organic-inorganic hybrid materials. More frequently the term refers to only the porous representatives of this class of materials in particular, which are also called by the more precise term porous coordination polymers (PCPs).<sup>[1,2]</sup> The term MOF was first used in the year 1995 by the group of YAGHI.<sup>[3,4]</sup> MOFs consist of metal clusters or discrete metal ions that are coordinated by multidentate (at least bidentate) organic ligands (the so called linkers) so that framework structures are formed. (Fig.1) Thereby structures can be built up that may contain cavities and large inner surfaces. The metal complexes are often called secondary building units (SBUs). The term SBU originates from zeolite chemistry and marks the structure

---

motifs that are necessary to completely build up the different zeolite topologies.<sup>[5]</sup> In this respect the term SBU for the metal complexes in MOFs is misleading, since not only the complexes but in addition to that the linkers are necessary for a complete depiction of the MOF structure. To further use the term SBU in MOF chemistry the meaning of the abbreviation could be altered to structural building unit, which would capture the actual situation much better.

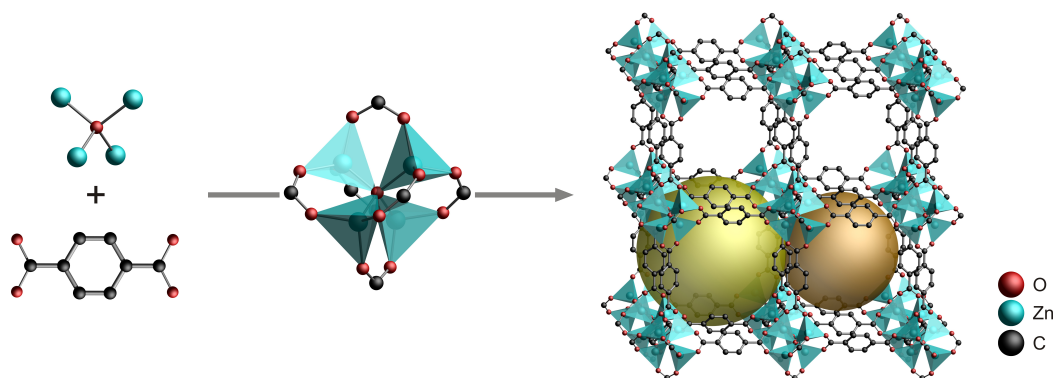


**Fig. 1:** Construction principle of a metal-organic framework illustrated with the example of MOF-5: a central oxygen atom is tetrahedrally coordinated by four zinc atoms, which in turn are coordinated pair wise by carboxylate functionalities of the terephthalic acid linkers. The formed tetrahedral nodes (SBUs) form a cubic structure when combined with the linear linkers. In this structure alternating larger (yellow, diameter: 15.1 Å) and smaller (orange, diameter: 11.8 Å) pores are present.<sup>[6]</sup>

The SBUs can contain different metal ions and can exhibit diverse coordinations. Thereby a large number of possible geometries in these inorganic nodes becomes available. (Fig. 2) Generally all metal ions capable of forming coordination bonds may be used in the inorganic building block. But the most frequently used ones are  $\text{Fe}^{2+}$ ,  $\text{Fe}^{3+}$ ,  $\text{Zn}^{2+}$ ,  $\text{Ni}^{2+}$ ,  $\text{Co}^{2+}$ ,  $\text{Mg}^{2+}$  or  $\text{Al}^{3+}$ . By adding different linkers (Fig. 3), a variable number of SBUs can be linked in different spatial arrangements depending on the number of coordinating moieties and their geometrical alignment. Most linkers used in MOF synthesis contain either oxygen or nitrogen atoms that are able to coordinate to the metal ions. Thus a pool of structure motifs is available from which new compounds can be assembled.

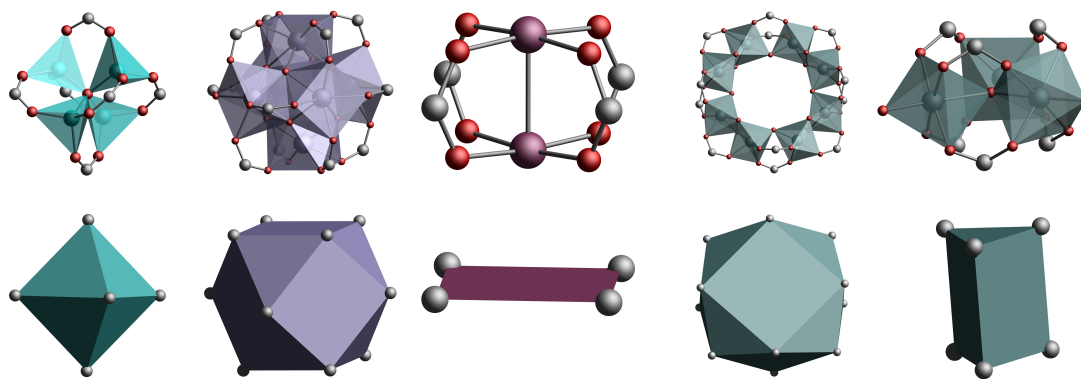


**Fig. 2:** Examples of SBUs found in carboxylate based MOFs with the corresponding geometric building units depicted as polyhedra formed by the carbon atoms of the carboxylate functionalities. From left to right: 6-fold (octahedrally) coordinated SBU of MOF-5,<sup>[6]</sup> 12-fold (cuboctahedrally) coordinated SBU of the UiO-MOFs,<sup>[7]</sup> 4-fold (quadratic) coordinated paddle-wheel SBU of HKUST-1,<sup>[8]</sup> 12-fold (compressed cuboctahedrally) coordinated SBU of CAU-1,<sup>[9]</sup> 6-fold (trigonal prismatic) coordinated SBU of MIL-88.<sup>[10]</sup>

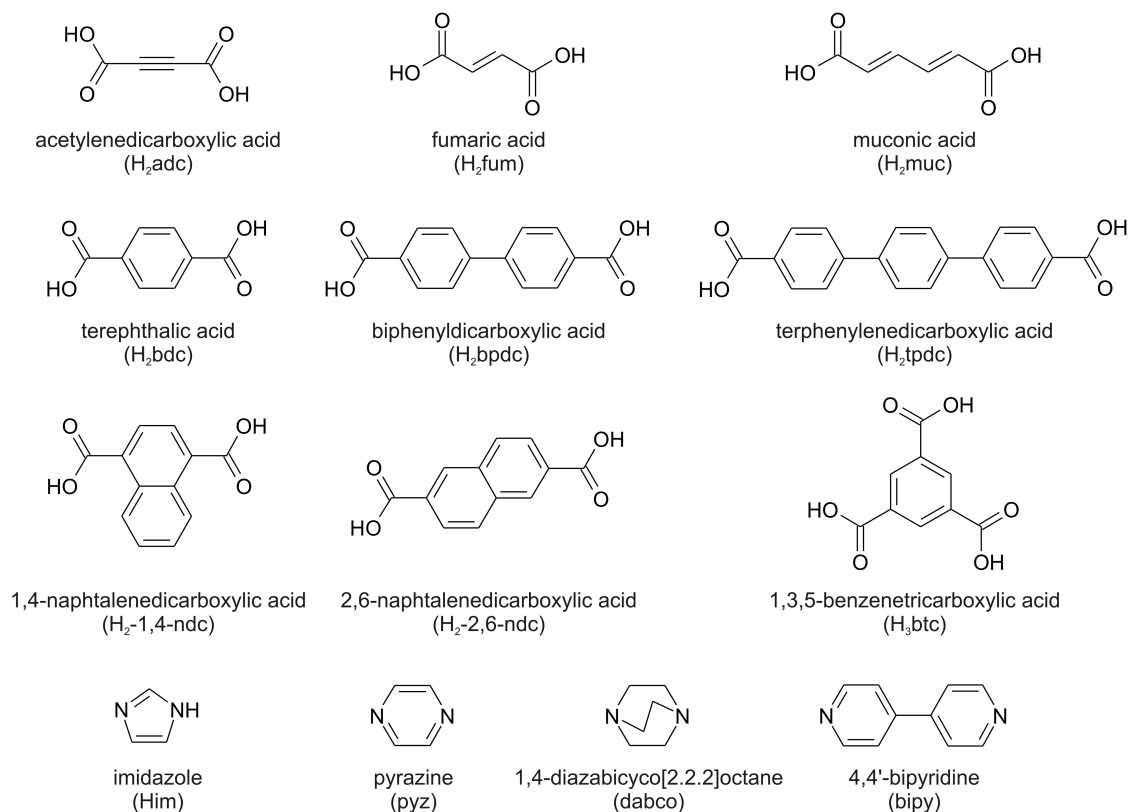


**Fig. 3:** Examples for commonly used linkers in MOF synthesis with their denotations and abbreviations.

This modular construction of metal-organic frameworks is often presented as an important advantage of this class of materials. But it has to be considered that the



different building units cannot simply be combined randomly and a selective formation of a new structure runs smoothly very rarely. Instead the composing of new structures often demands a screening of many different experimental parameters which is usually done in a high-throughput setup. Nonetheless the properties of MOFs with regard to pore sizes and properties of the pore volume (e.g. hydrophilic / hydrophobic) can be tuned by design of the linker. With the means of organic chemistry different functional groups may be added to the linker or linkers of a desired length to accomplish a designated pore size can be synthesized.

In comparison to purely inorganic microporous materials like zeolites or active carbons the stability of MOFs in respect to heating or exposure to chemicals is generally lower. This is due to the hybrid character of MOFs. Some MOFs, especially those with carboxylate linkers, are prone especially to hydrothermal conditions.<sup>[11]</sup> MOF-5 for example, which is probably the best-known and most popular representative of its kind, is not even stable towards ambient humidity of more than 4 % of water and cannot be handled in air, because the water molecules coordinate to the zinc ions and thereby destroy the SBUs.<sup>[12,13]</sup> A whole subclass of MOFs, the so-called zeolitic imidazolate frameworks (ZIFs), show a better stability not only towards water and other chemicals like alcohols, benzene or aqueous sodium hydroxide solution but also the thermal stability of some ZIFs is exceptionally high.<sup>[11,14]</sup> These materials consist of discrete divalent cations (e.g.  $\text{Zn}^{2+}$ ,  $\text{Co}^{2+}$ ) linked by bidentate imidazolate derivatives. Due to the tetrahedral coordination and an angle of approximately  $145^\circ$  formed between metal - imidazolate linker - metal, which is similar to the oxygen-silicon-oxygen angle found in zeolites, ZIFs show crystal structures based on zeolitic topologies.<sup>[15]</sup> Another class of MOFs with outstanding thermal and chemical stability are the zirconium based MOFs of the UiO (Universitetet i Oslo) and also of the PIZOF (porous interpenetrated zirconium organic frameworks) type. Since these are a major topic in this work, they are described in more detail in chapter 1.3.

When investigating different zeolites, it was often observed that the effective aperture sizes of the pores calculated from crystallographic data were smaller than those derived from permeation experiments. These findings were explained with a thermally induced breathing motion of the pores, which means that the

---

distributions of oxygen to oxygen distances across the apertures are becoming broader.<sup>[16]</sup> The aperture sizes of a number of MOFs underlie a certain dynamic as well. This may either be caused by a rotation or tilting of the organic linkers around a bond or by a reversible contraction or expansion of the whole network (called breathing effect in MOFs).<sup>[17]</sup> The most famous example of a breathing MOF is probably MIL-53 ( $\text{Cr}^{\text{III}}(\text{OH})$  bdc) found by the group of FÉREY.<sup>[18]</sup> In this structure chains of corner sharing chromium-oxygen octahedra are linked by terephthalate ions. Thus linear one dimensional channels are formed. Upon heating to 300 °C all guest molecules are released and the structure is fully expanded. With the uptake of water the structure closes with shrinkage in  $a$ -direction and expansion in  $b$ -direction (Fig. 4). This phenomenon is caused by the formation of hydrogen bonds between the water molecules and OH-groups linked to the chromium atom. The opening and closing of the structure also takes place during the adsorption and desorption of  $\text{CO}_2$ .<sup>[19]</sup> In this case a certain pressure is needed to expand the structure which then happens abruptly. That is why this pressure is called gate opening pressure.

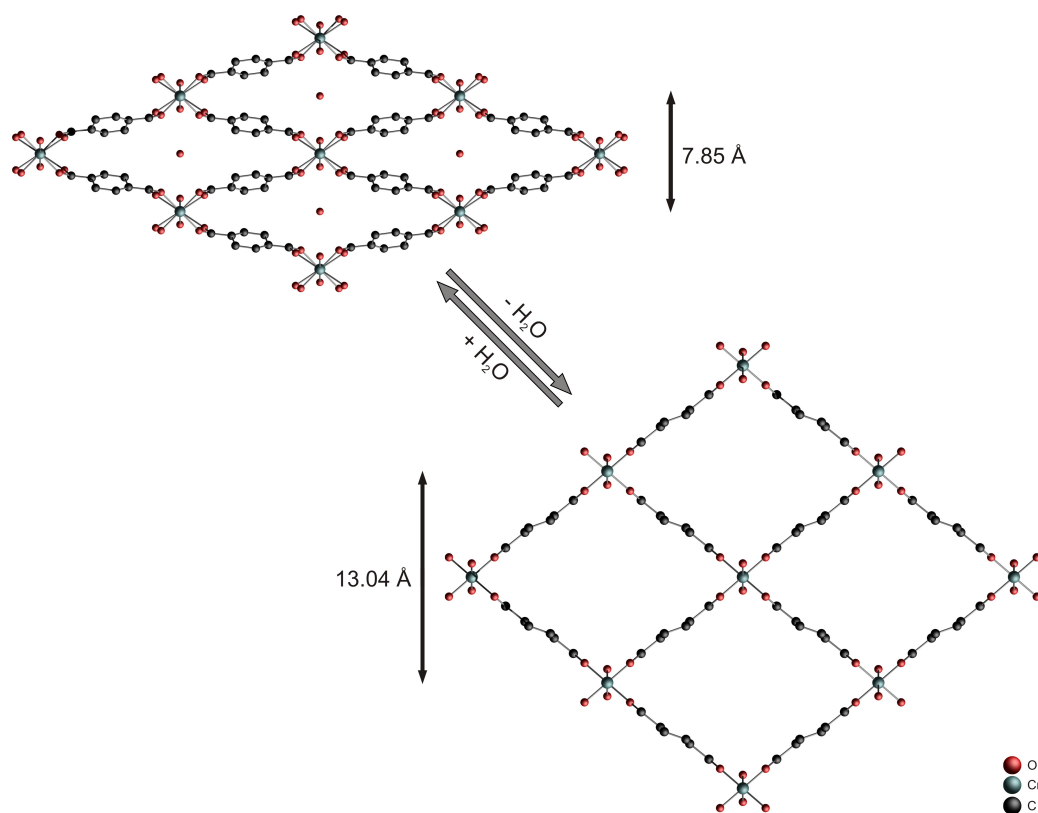


**Fig. 4:** The structure of MIL-53 (view along  $c$ -axis) expands upon removal of water molecules and contracts upon release vice versa. The shrinkage is caused by the formation of strong hydrogen-bonds between the OH-groups that are coordinated to the Cr-atoms and the water molecules.<sup>[18]</sup>

## 1.2 Synthesis Strategies for Metal-Organic Frameworks

### 1.2.1 Isorecticular Synthesis

The term isorecticular synthesis was coined by YAGHI *et al.* and describes a synthesis strategy in which the pore size and also functionality of an existing MOF topology is varied systematically.<sup>[20,21]</sup> It is therefore first of all necessary to retain the inorganic connector and the connectivity of the linker. YAGHI also claimed the necessity of sticking closely to defined reaction conditions so that the same building blocks would be formed from the educts during the course of reaction.<sup>[21]</sup> Following these principles they were able to produce a whole series of isorecticular MOFs (IRMOFs) based on the already existing cubic structure of MOF-5, which was renamed into IRMOF-1 in the course of these findings.<sup>[20]</sup> 16 different linear dicarboxylic acids were used in combination with the previously described zinc-SBU, varying not only the length but also the functionality of the linkers. Thereby a family of materials with the same topology was created with different pore sizes, pore volumes and crystal densities. Moreover it could be shown that a hydrophobic functionalization of the bdc-linker enhances the methane uptake of the final MOF. This shows that by using isorecticular synthesis materials with desired properties can be designed.

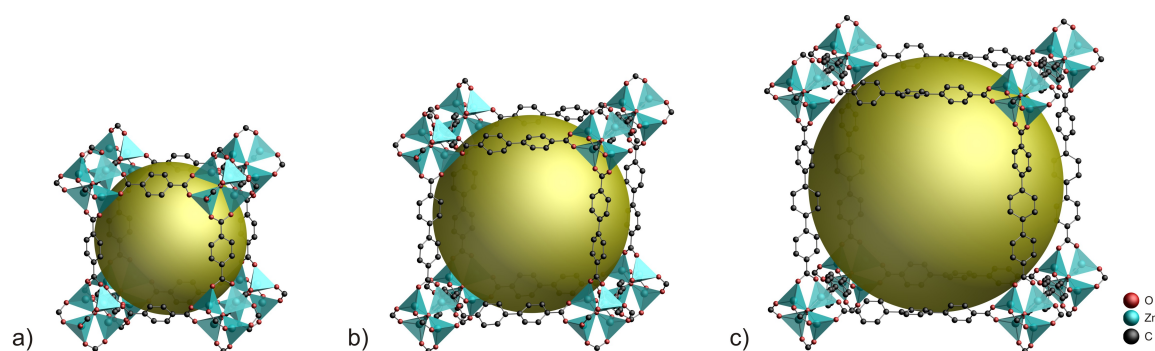


**Fig. 5:** Three examples of the IRMOF series: a) IRMOF-1 (also known as MOF-5) with bdc<sup>2-</sup> as linker, b) IRMOF-10 with bpdc<sup>2-</sup> as linker and c) IRMOF-16 with tpdc<sup>2-</sup> as linker. The free volume is indicated by the yellow balls.

A smaller homologue of the IRMOF series with acetylenedicarboxylic acid linkers (later named IRMOF-0) was not accessible with the same solvothermal synthesis as the other IRMOFs because of the thermal instability of this acid. It is known to decompose upon heating. After a room temperature synthesis for MOF-5 was

discovered (with an addition of triethylamine to deprotonate the linker), the group of YAGHI succeeded in synthesizing IRMOF-0 eventually.<sup>[22]</sup> Other than MOF-5 IRMOF-0 exhibits a doubly interpenetrated structure, each framework showing the same topology as the other IRMOFs.

Another approach to isorecticular synthesis was reported by FÉREY and co-workers in the MIL-88 series. The parental MIL-88A consists of trimeric iron SBUs (see Fig. 2) linked by fumarate.<sup>[23]</sup> It was synthesized by the so called “controlled SBU” approach: the isolated trimeric Fe-SBU can be prepared with acetate ligands, which are then exchanged with the desired linker in a low temperature reaction (< 100 °C) while the SBUs remain intact. This route was successfully transferred to the longer 2,6-naphthalene dicarboxylate linker with the yield of MIL-88C.<sup>[24]</sup>

Further examples for isorecticular materials are the zirconium based UiO-66 to -68 series and the PIZOFs (porous interpenetrated zirconium organic frameworks), which are structurally related to the previous. (see chapter 1.3)

### 1.2.2 Postsynthetic Modification

Even functional groups that may not withstand the synthesis conditions of the MOF (which are mostly solvothermal conditions) or may interfere with the formation of the desired material can be incorporated into the final product by postsynthetic modification (PSM) under mild conditions. A large part of the toolbox of organic synthesis may be applied and therefore materials with tailored properties for different applications can be developed from existing MOFs. In general different types of PSM are known.<sup>[25,26]</sup> This starts with rather simple modifications involving non-covalent interactions which includes guest exchange and ion exchange. It was shown by LEE *et al.*<sup>[27]</sup> but also by YAGHI *et al.*<sup>[4]</sup> in 1995 that metal organic frameworks could release guest molecules under retention of the framework and would readily reabsorb the same or even other guest molecules. Depending on the framework charge MOFs may also undergo both anion<sup>[28]</sup> and cation<sup>[29]</sup> exchange other than zeolites which are limited to cation exchange due to the anionic charge of zeolite networks. Another type of PSM is a modification based on coordinative interactions. This can mean an exchange of

---

ligands at the metal centers, which is possible for example in HKUST-1 where the axial aqua ligands on the paddle-wheel unit can be replaced by other molecules like pyridine<sup>[8]</sup> or similarly in MIL-100 where methanol is inserted.<sup>[30]</sup> An alternative modification by coordinative interactions is the introduction of additional metal centers by coordinating metals to free coordination sites at the linkers.<sup>[31,32]</sup>

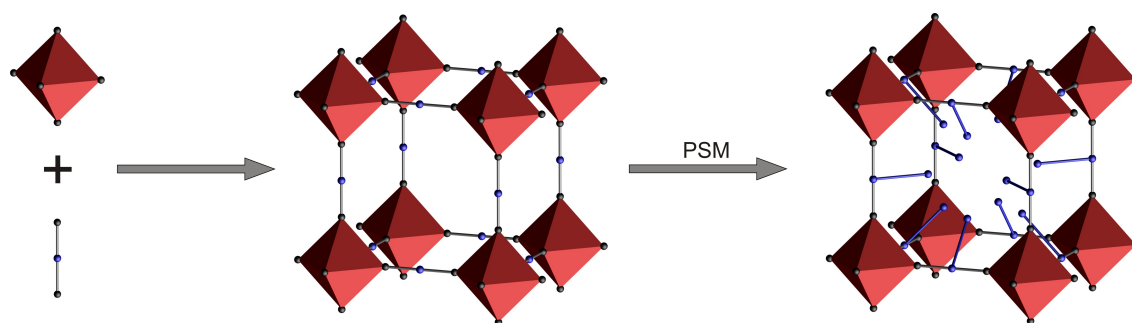


**Fig. 5:** General schematic illustration of postsynthetic modification (PSM) of porous MOFs by covalent bonds: After the crystalline product is formed, functional moieties are added in a second reaction step.

The most powerful way of PSM is based on covalent bonds. In this case, reactive moieties on the linkers are used to form new bonds and thereby decorate the pores with new residues that may change the chemical properties of the framework (Fig. 5). The most commonly used strategy in covalent PSM targets amino-groups which can readily be introduced into various MOFs by using amino-functionalized linkers. It was shown by COHEN and co-workers that the amino groups in IRMOF-3 (the amino-substituted version of MOF-5) can be reacted with various anhydrides to form amides<sup>[33,34]</sup> or with isocyanates to generate urea derivatives.<sup>[35]</sup> Other types of reactions like imine condensation,<sup>[36]</sup> bromination,<sup>[37]</sup> reduction,<sup>[38]</sup> or click reactions<sup>[39,40]</sup> have also been shown to be successful in postsynthetic modification of MOFs.

### 1.2.3 Modulated Synthesis of Metal-Organic Frameworks

The nucleation and also the growth rate in MOF synthesis can be selectively affected by different ways of modulation. Since MOFs are coordination compounds one way of influencing the reaction is by coordination modulation which involves the addition of monodentate ligands to the reaction mixture which compete for

coordination sites at the metal atom with the bridging ligands. Another way is deprotonation modulation since in most reactions leading to the formation of MOFs, the linkers (e.g. imidazole linkers or carboxylic acid-based linkers) have to be deprotonated.<sup>[41]</sup> First systematic investigations concerning the coordination modulation were done by the group of KITAGAWA. They explored the influence of monodentate ligands on the formation of HKUST-1.<sup>[42]</sup> As a competitive ligand dodecanoic acid was used. They observed that the crystal sizes of the final products increased with increasing amount of modulator. It was also asserted that the addition of the modulator strongly affected the nucleation but not the growth which remained fast. With higher amounts of modulator more copper can be bound into complexes and less copper is available for the reaction leading to the formation of HKUST-1. With the decreasing supersaturation of the metal precursor, the nucleation rate is decreased, and with fewer nuclei larger crystals are formed. Another example studied by the group of KITAGAWA is the influence of a competitive ligand on the formation of the pillared-layer MOF  $\text{Cu}_2(\text{ndc})_2\text{dabco}$ .<sup>[43]</sup> In this MOF two-dimensional layers of dicopper clusters linked by the dicarboxylates are connected by the pillaring amine ligand dabco. In their work they have shown that the addition of a monocarboxylic acid (acetic acid) as a competitive ligand to the naphthalene dicarboxylate linkers would inhibit the growth of the crystals only in the *a,b* plane. With this synthesis strategy they were able to suppress the growth of distinct crystal faces and rod-shaped nanocrystals were obtained. These examples show that modulation allows control over crystal size and also crystal shape.

A modulated synthesis was also recently applied to the formation of Zr-MOFs by our group.<sup>[44]</sup> Since different isolated molecular Zr-complexes are known which are terminated by monocarboxylic acids and the structures of which are very similar to the final SBU of these MOFs, we assumed that the addition of monocarboxylic acids might lead to the formation of these complexes in solution before the ligands are exchanged against the dicarboxylate linkers. This assumption is very similar to the controlled SBU concept of FÉREY<sup>[23]</sup> with the difference that the complexes were not isolated prior to the formation of the framework. Different zirconium-carboxylate clusters are described in literature<sup>[45-48]</sup> which all contain the same core consisting of  $\text{Zr}_6(\mu_3\text{O})_4(\mu_3\text{OH})_4^{12+}$

---

clusters. The six zirconium atoms in this core-complex are arranged in an octahedron and the oxide and hydroxide ions are capping the faces of this octahedron (Fig. 6 a). When complexes are formed with sterically demanding carboxylates, for example pivalate ( $\text{Bu}^t\text{COO}^-$ ), 12 of these carboxylates are bridging the edges of the Zr-octahedron (Fig. 6 b) to form a highly symmetric complex in which all Zr-atoms are coordinated square-antiprismatically by oxygen (Fig. 6 c).<sup>[48]</sup>

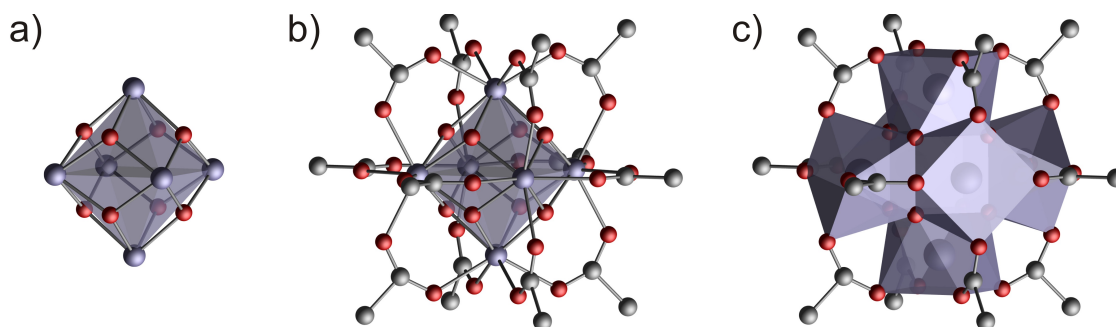


Fig. 6: a) The inner  $\text{Zr}_6\text{O}_4(\text{OH})_4^{12+}$  cluster consisting of octahedrally arranged Zr-atoms and O-atoms capping the faces of the octahedron; b) 12 carboxylate functionalities are bridging the edges of the Zr-octahedron in the final  $\text{Zr}_6\text{O}_4(\text{OH})_4(\text{OOCR})_{12}$  complex (with  $\text{R} = \text{Bu}^t, \text{C}(\text{CH}_3)_2\text{Et}$ ); c) each Zr-atom is coordinated square-antiprismatically by oxygen. The organic moieties of the carboxylates are omitted for clarity.<sup>[48]</sup>

The group of SCHUBERT performed some research on the use of smaller and sterically less demanding carboxylates in this kind of Zr-complexes. In the resulting coordination compounds, the outer coordination sphere is different from the one described before, while the inner coordination remains unchanged. In contrast to the symmetrical complex described before, where only one coordination mode of the carboxylates is present, there are in fact three different coordination modes when for example isobutyrate (ib) is used as carboxylate ligand.<sup>[47]</sup> Three carboxylates are chelating Zr-atoms that are all situated on one triangular face of the octahedron. On the opposite face there is one carboxylate that is mono-coordinating, while the remaining eight carboxylates are edge-bridging. The open coordination site resulting from the mono-hapto carboxylate is filled by water or other protic solvents (Fig. 7).

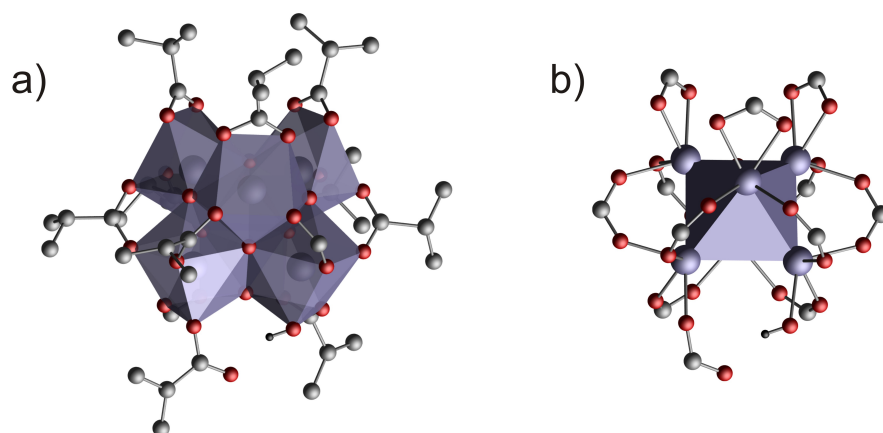


Fig. 7: a) Structure of the  $\text{Zr}_6\text{O}_4(\text{OH})_4(\text{ib})_{12}(\text{H}_2\text{O})$  complex; b) all three chelating carboxylates are situated on one triangular face of the Zr-octahedron, while the mono-coordinating ligand is located on the opposite face.<sup>[47]</sup>

This type of structure was also found in complexes with other ligands like  $\text{Zr}_6\text{O}_4(\text{OH})_4(\text{bz})_{12}(\text{PrOH})$  and  $\text{Zr}_6\text{O}_4(\text{OH})_4(\text{me})_{12}(\text{PrOH})$  (bz = benzoate, me = methacrylate).<sup>[45]</sup> These kinds of complexes obviously possess higher energies than the highly symmetric complexes with only bridging ligands. These complexes are most likely stabilized by solvent effects and H-bonded carboxylic acids.<sup>[46]</sup> In their work the SCHUBERT-group also made the observation, that an exchange of carboxylate ligands in the complexes with other ligands from solution is feasible and compounds with mixed ligands were obtained, e.g.  $\text{Zr}_6\text{O}_4(\text{OH})_4(\text{me})_8(\text{ib})_4(\text{BuOH})$ .<sup>[47]</sup> By removal of the solvent it is in this case possible to remove the butanole from the complex. With this removal the coordination mode of the mono-hapto carboxylate changes to a bridging coordination. It was assumed that this process is reversible and that an exchange of ligands happens accordingly in this obviously activated position.<sup>[47]</sup>

These observations led us to the assumption that similar complexes with monodentate carboxylates are formed in a modulated synthesis of Zr-containing MOFs prior to the formation of the final frameworks. The addition of a high excess of monocarboxylic acids would probably ensure that most of the Zr-atoms become coordinated by “modulating” ligands and are thus bound in isolated complexes. By stepwise ligand-exchange reactions with dicarboxylic acid linkers the network of the MOF is then slowly built up. This would lead to a reduced nucleation rate and thus to the formation of larger crystals. This behavior could best be observed in a modulated synthesis of UiO-66 with modulation by benzoic acid.<sup>[44]</sup> This acid was



chosen for its structural and chemical similarity to the bdc-linker present in the UiO-66. Nonetheless a similar effect was observed with the use of other monocarboxylic acids like formic acid or acetic acid. In all cases not only a size variation in the final products was observed but also the effect that with increasing amounts of modulator the intergrowth of the crystals, which is especially pronounced when no modulator is used, is suppressed. It has to be mentioned that an influence on the final size of the products is not achieved with every Zr-containing MOF. Especially in the synthesis of PIZOFs, this size modulation is not found. This shows that the quite simple explanation given for the size modulation observed for UiO-66 is probably not sufficient for all Zr-MOFs. But it was observed in our laboratory that the addition of modulators to the synthesis of different Zr-MOFs at least leads to higher crystallinity in almost all cases.<sup>[44, 49-51]</sup> Also, the synthesis procedures become more reproducible and robust. Another interesting observation arises when functionalized acids are used as modulators. In such cases the surface characteristics of the growing particles are probably changed and some properties of the product, e.g. the intergrowth of crystallites, can be influenced. This behavior is discussed in chapter 3.2.

---

## 1.3 Zirconium Containing Metal-Organic Frameworks

### 1.3.1 UiO-type MOFs

The first zirconium-containing MOFs were published by the group of LILLERUD in 2008.<sup>[7]</sup> They reported of a new isorecticular series of metal-organic frameworks with a new Zr-SBU. The structure of the SBU is the same as in the isolated  $Zr_6O_4(OH)_4(OOCBu^t)_{12}$  complex described in chapter 1.2.3.<sup>[48]</sup> Since these complexes offer 12 connection points for carboxylic acids, the emerging building block shows the same connectivity as for example metals in cubic close packings. That is why the framework that comes to be when the SBUs are connected by linear dicarboxylic acids is comparable to an extended ccp structure as depicted in Fig. 8. In analogy to that, octahedral and tetrahedral cavities can be found in the network. The three isorecticular Zr-MOFs containing the non-functional linkers terephthalic acid, biphenylene dicarboxylic acid and terphenylene dicarboxylic acid (Fig. 9) were named UiO-66, UiO-67 and UiO-68, respectively, after the university at which they were discovered, the University of Oslo (Universitetet i Oslo). Since terphenylene dicarboxylic acid is nearly insoluble in DMF, which is commonly used as solvent in Zr-MOF syntheses, we were unable to synthesize UiO-68 in our laboratories.

By the method of fitting a sphere inside the cavity without touching the framework atoms, the pore sizes can be estimated. In UiO-66 the diameters of these spheres amount to 1.1 and 0.8 nm for the octahedral and tetrahedral voids, respectively. All pores in the structure are accessible via triangular windows. The size of the windows is often given by the diameter of a sphere that may pass the window. Using this model, window sizes of 0.6, 0.8 and 1.0 nm are given for UiO-66, -67 and -68.<sup>[7]</sup>

---

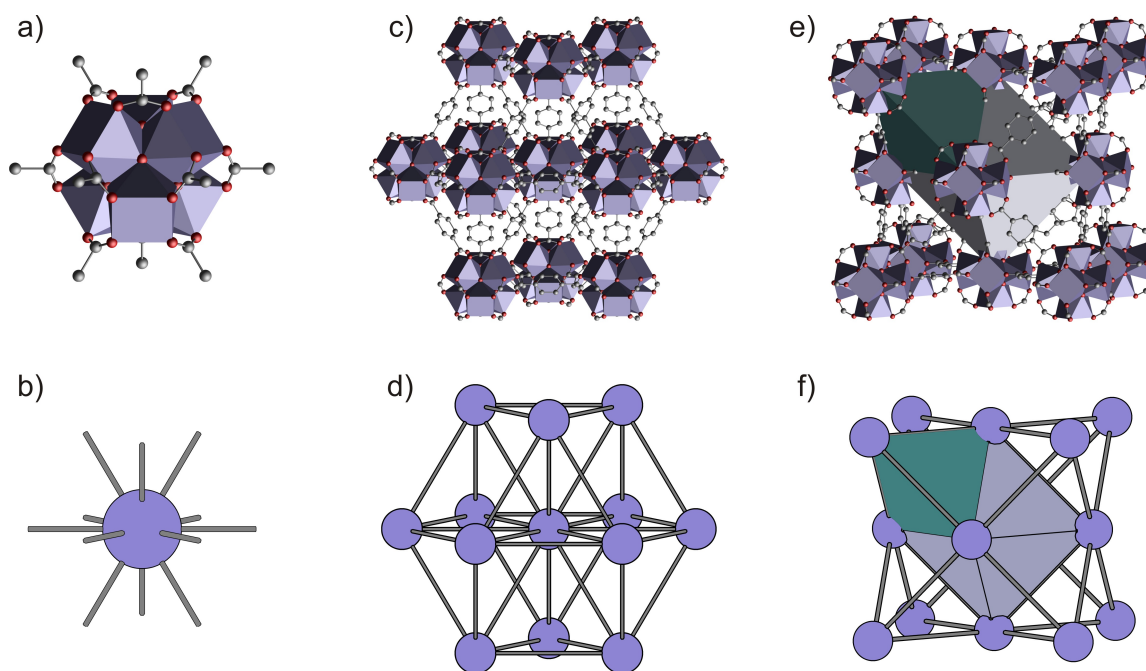


Fig. 8: a) and b) The SBU found in Zr-MOFs offers 12 connection points for carboxylates; c) and d) because of the 12-fold connectivity, the structure formed when the SBUs are connected via linear dicarboxylic acids is comparable to an extended cubic close packing; e) and f) accordingly, the final network contains octahedral and tetrahedral cavities as does a ccp structure.<sup>[7]</sup>

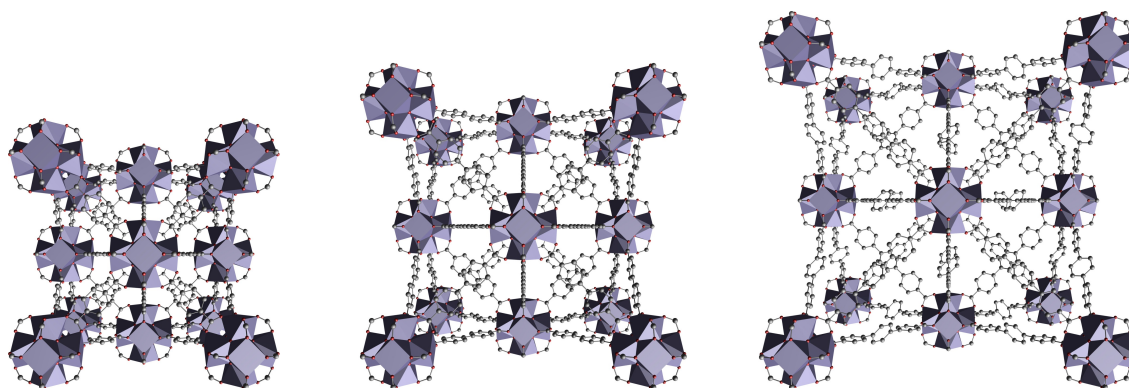
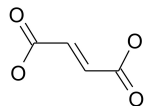
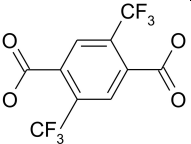
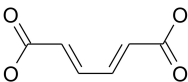
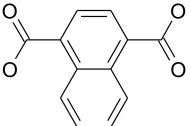
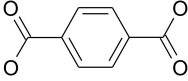
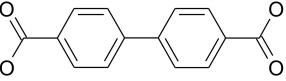
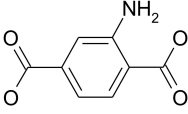
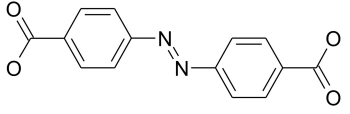
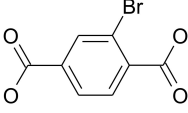
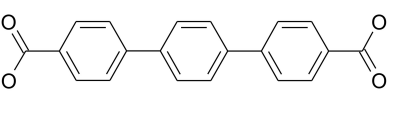
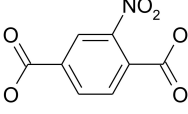
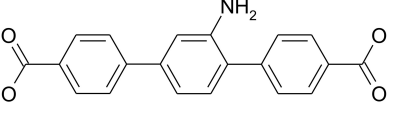


Fig. 9: The isoreticular UiO-series: UiO-66 containing terephthalic acid linkers, UiO-67 containing biphenylene dicarboxylic acid linkers and UiO-67 containing terphenylene dicarboxylic acid linkers.<sup>[7]</sup>

Over the last few years, a number of Zr-MOFs with UiO-analogue structures were published containing different linear dicarboxylic acids. A summary of the different linkers used so far is given in Table 1. When looking at the different linkers it becomes obvious that most of the dicarboxylic acids that lead to the successful formation of UiO-like frameworks are relatively short. That is probably owned to the fact that the use of longer linkers causes problems in the synthesis. In our laboratory we were able to produce Zr-MOFs containing longer linkers only by a

modulated synthesis. Otherwise, products showing low crystallinity were produced.

Table 1: Linkers leading to the formation of UiO-type metal-organic frameworks.

Designation	linker	Ref.	designation	linker	Ref.
Zr-fum		[50]	Zr-bdc-(CF <sub>3</sub> ) <sub>2</sub>		[54]
Zr-muc		[52]	Zr-1,4-ndc		[53]
Zr-bdc (UiO-66)		[7]	Zr-bpdc (UiO-67)		[7]
Zr-bdc-NH <sub>2</sub>		[53]	Zr-abdc		[49]
Zr-bdc-Br		[53]	Zr-tpdc (UiO-68)		[7]
Zr-bdc-NO <sub>2</sub>		[53]	Zr-tpdc-NH <sub>2</sub>		[44]

A rule of thumb states that the higher the charge of the metal ions, the more stable the final MOF becomes. That is why Zr<sup>4+</sup>-containing MOFs, especially those with unfunctionalized linkers, show an exceptionally high thermal stability of up to 540 °C (UiO-66 and also UiO-67).<sup>[7]</sup> Following the decomposition products of UiO-66 by MS measurements, benzene can be detected in the gas phase at this temperature. This shows that the weakest point of the structure is the C-C bond between the carboxylate group and the benzene ring and not the inorganic brick or the coordination bond as one might presume.<sup>[7]</sup> Of course the thermal stability is dependent on the kind of linker in the structure. Zr-bdc-NH<sub>2</sub> and Zr-bdc-NO<sub>2</sub> show a lower decomposition temperature than the analogues UiO-66, Zr-bdc-Br or Zr-1,4-ndc.<sup>[53,56]</sup> That is because these functionalized linkers are prone to combustion at lower temperatures. Prior to the complete destruction of the framework by combustion of the linker, the inorganic brick will release water to

form dehydroxylated inner complexes of  $Zr_6O_6$  instead of  $Zr_6O_4(OH)_4$ . This dehydroxylation starts at a temperature of approx. 100 °C, is completed at 300 °C and is fully reversible.<sup>[7,55,56]</sup> The dehydroxylation affects the structure of the Zr-cluster in so far as a squeezing of the Zr-octahedron occurs along one diagonal of the octahedron (Fig. 10). This process can be monitored by IR spectroscopy, where the band contributed by the vibration of isolated hydroxyl groups disappears, and EXAFS analysis, where the squeezing of the Zr-octahedron and thereby the change in interatomic distances can be found.<sup>[55]</sup> Since almost no changes occur in the PXRD pattern of the dehydroxylated material, it is safe to assume that the compression of the SBUs takes place in an unordered fashion. If this was an ordered process, the symmetry of the resulting framework would be lowered resulting in changes in the PXRD pattern. After the dehydroxylation process, each Zr-atom is only 7-fold coordinated by oxygen which leaves one open coordination site with LEWIS acidic character. These open metal sites are often accountable for catalytic activity. That is why a possible catalytic application of the dehydroxylated UiO-66 and Zr-bdc-NH<sub>2</sub> was successfully tested in a cross-aldol condensation in the synthesis of jasminaldehyde. In this reaction dehydroxylated Zr-bdc-NH<sub>2</sub> proved most suitable with very good selectivity and yield.<sup>[56]</sup>

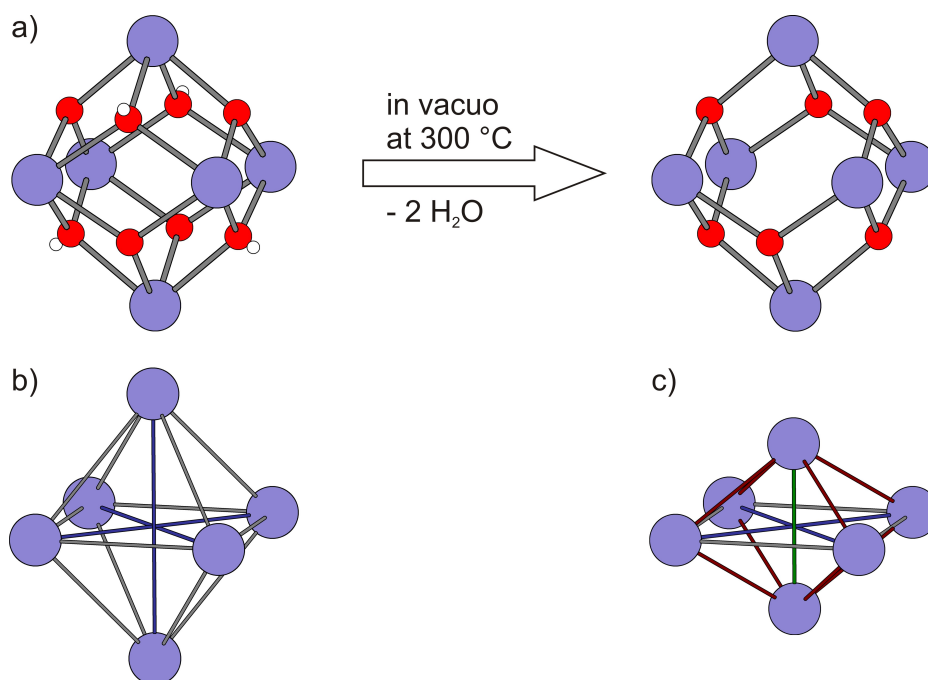


Fig. 10: The inner core of the Zr-SBU is able to expel two molecules of water when heated up to a temperature of 300 °C (a). This leads to a contraction of the previously regular Zr-octahedron (b) along one diagonal (c). The figure was reproduced from ref. [55].

UiO-MOFs not only feature an unprecedented thermal stability but also a very good chemical stability which makes these materials promising candidates for potential applications for example in catalysis or separation. The framework remains intact after immersing the material in solvents like water, benzene, acetone, ethanol or DMF.<sup>[55]</sup> Even in an aqueous HCl solution (pH value of 1) the Zr-MOFs do not dissolve. Only in NaOH solution (pH value of 14) most UiO-MOFs are transformed into less crystalline or even amorphous materials.<sup>[57]</sup> It is remarkable to note that Zr-bdc-NO<sub>2</sub> does not dissolve in NaOH, which shows that the functionalities situated on the linker have an influence not only on the thermal but also the chemical stability.

Other functionalizations of the linker in UiO-MOFs are accessible via postsynthetic modifications. As mentioned in chapter 1.2.2 the most commonly used starting material for this task is an amine-carrying linker, in this case Zr-bdc-NH<sub>2</sub>.<sup>[53,58,59]</sup> It may be transformed into different amides by reaction with anhydrides<sup>[53,58]</sup> or to hemiaminal or azaridine with acetaldehyde.<sup>[59]</sup> It is also possible to convert the Zr-bdc-Br compound into Zr-bdc-CN by reaction with copper cyanide under microwave irradiation in only 10 minutes.<sup>[60]</sup> A synthesis of the Zr-bdc-CN-MOF can be done by an alternative route using CN-bdc directly in the synthesis of the framework. Since this linker is commercially not available it has to be synthesized in a three step reaction thus leading to an expenditure of reaction time of 98 h in contrast to approx. 24 h with the use of PSM.<sup>[60]</sup> This example clearly shows the potential power of postsynthetic modification.

### 1.3.2 PIZOFs

A new class of Zr-MOFs, showing close structural relation to the UiO-MOFs, are the porous interpenetrated Zr-organic frameworks (PIZOFs). These MOFs contain the same SBU as the UiO-MOFs but they are connected by much longer oligo-phenylene ethynylene dicarboxylic acids, resulting in an interpenetrated yet porous structure.<sup>[49]</sup>

Examining an isolated framework of the PIZOF structure, it exhibits the same cubic arrangement of the SBUs as the UiO-MOFs (see section 1.3.1). In contrast to the

---

shorter linkers in the UiO-MOFs, the long linkers in the PIZOFs exhibit a higher degree of flexibility. That is why the resulting tetrahedral cavities in the PIZOF framework are no longer equal like in the UiO-MOFs, but two different kinds can be found alternating in the structure due to a bending of the linkers. All four linkers bordering one tetrahedral cavity are either bent towards the center of the tetrahedron, resulting in a concave void, or bent away from the center, resulting in a convex void.

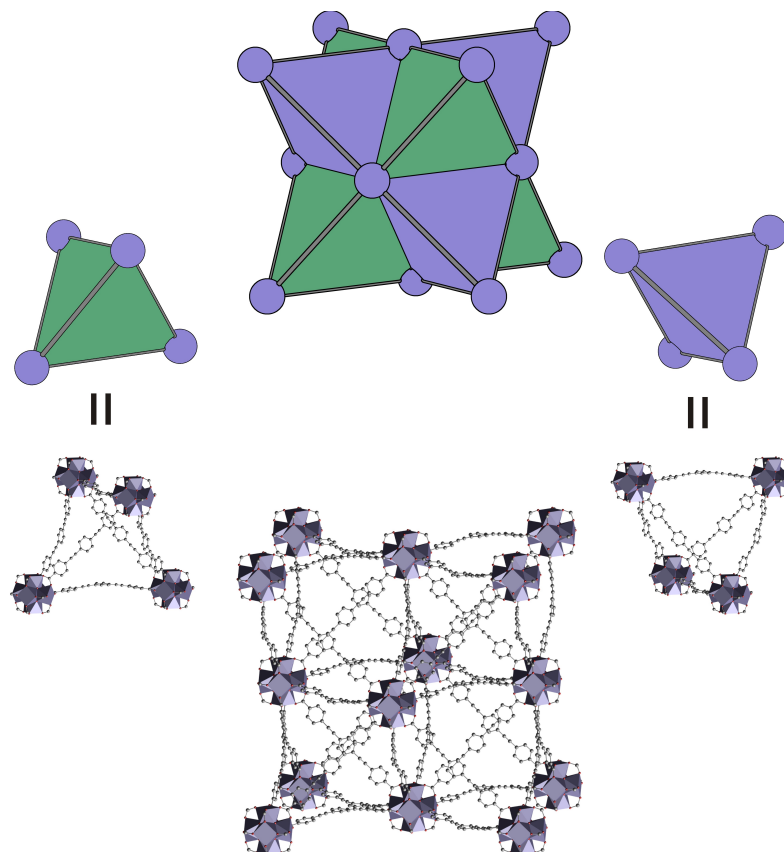


Fig. 11: Topological representation of one isolated PIZOF framework. Similar to UiO-MOFs the Zr-SBUs are arranged in an expanded cubic close packing. In contrast to UiO-MOFs, the tetrahedral cavities of PIZOFs are not equivalent, but two different kinds are present. Due to a bending of the long linkers, smaller concave tetrahedral voids (green) and larger convex ones (purple) are alternating in the structure.<sup>[44]</sup>

The concave tetrahedral voids host SBUs of a second framework, which has exactly the same structure as the first one. Both frameworks are interpenetrating each other without any point of connection. By this interpenetration the octahedral cavities which are present in the ‘first’ framework become limited to tetrahedral cavities of the ‘second’ framework (Fig. 12).

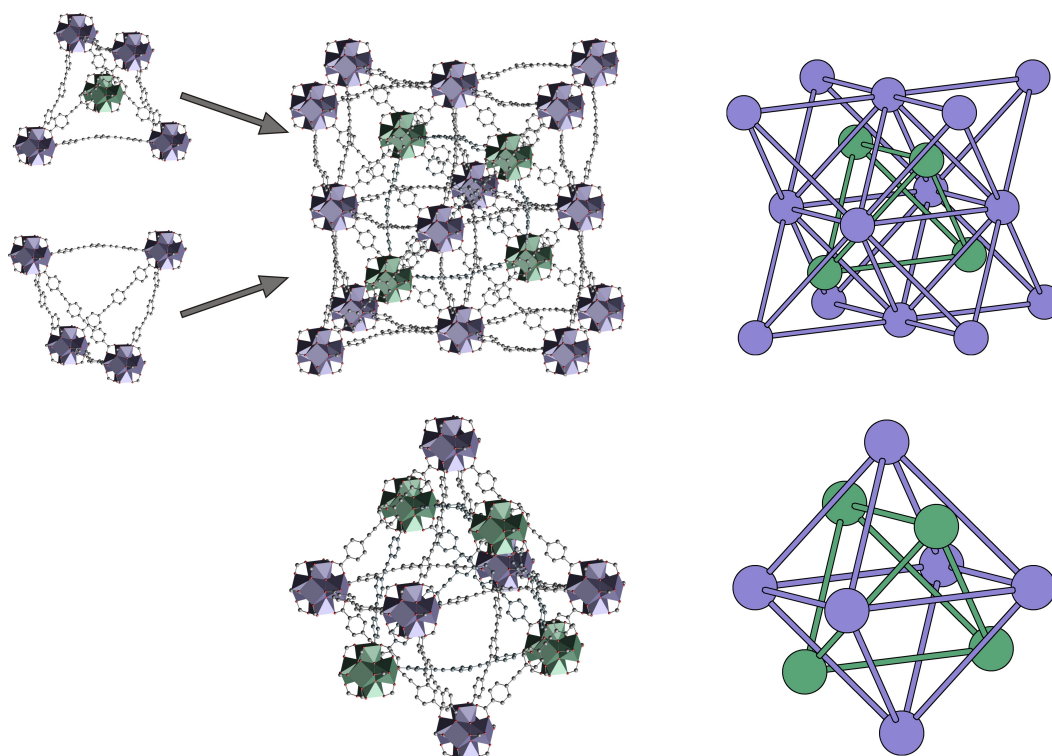


Fig. 12: The concave tetrahedral cavities are hosting SBUs of a second framework (shown in green for easier distinction). By the interpenetration all octahedral cavities are reduced to tetrahedral ones.

A major advantage of PIZOFs is the high variability of the linkers. They may be functionalized at the central phenylene ring with all kinds of moieties which can withstand the reaction conditions (120 °C in DMF). Regardless of the type of functionalization isostructural MOFs are obtained, even with such very long alkyl chains consisting of up to 16 atoms (Fig. 13). These side chains are pointing into the convex tetrahedral cavities. The accessibility of the pores was proven by Ar sorption experiments.<sup>[44]</sup> It is also possible to perform postsynthetic modifications on the functional groups of the side chains. For example, it was shown for PIZOF-3 ( $R' = \text{OCH}_3$ ,  $R'' = \text{OCH}_2\text{C}\equiv\text{CH}$ , see Fig. 13) that a copper catalyzed click reaction (1,3-dipolar cycloaddition between azide and alkyne moieties) can be performed postsynthetically, and PIZOF-8 ( $R' = \text{OCH}_3$ ,  $R'' = \text{O}(\text{CH}_2)_3\text{furan}$ ) can be reacted in a Diels-Alder cycloaddition.<sup>[40]</sup>

With long side chains the pores are almost filled by the residues of the linker. For example in PIZOF-11 (with two *O*-undecyl residues on the linkers) the pore volume is filled with what can possibly be considered as an immobilized polymer-like structure. Hints for this were taken from Ar sorption experiments carried out



in our laboratory. In these experiments a hysteresis, which is uncommon for microporous materials, was detected. A similar hysteresis however can be found in sorption isotherms of microporous polymers.<sup>[61]</sup> That is why we assume that PIZOFs with long side chains might combine the rigid framework of MOFs with a polymer-like structure inside the pores. These polymers would therefore be unable to swell unlike common polymers.

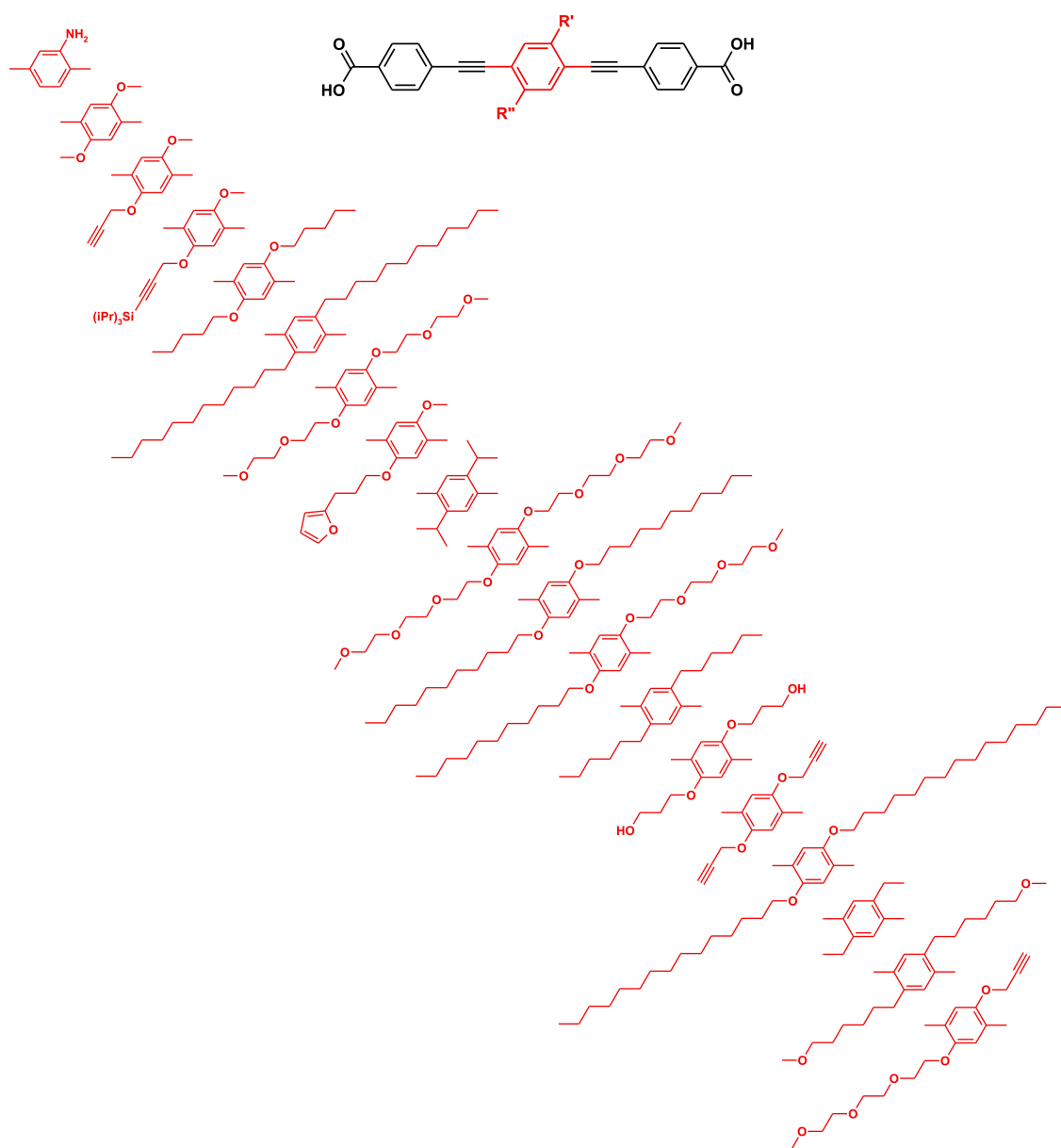


Fig. 13: Pool of linkers used to date to produce PIZOFs. Different side chains can be attached on the central phenylene ring of the oligo-phenylene ethynylene dicarboxylic acid linkers. The resulting MOFs are denoted PIZOF-1 to PIZOF-19 (from top to bottom).

### 1.3.3 MIL-140

A new series of zirconium-containing MOFs which was recently reported is the MIL-140.<sup>[62]</sup> In contrast to other Zr-MOFs like UiO-type MOFs and PIZOFs it contains a chain-like SBU with 7-fold coordinated zirconium. When these chains are connected by dicarboxylic acid linkers, a porous network with channel-like pores arises. Up to now there are four dicarboxylic acids which are known to form this structure: terephthalic acid (MIL-140A), 2,6-naphthalene dicarboxylic acid (MIL-140B), 4,4'-biphenyle dicarboxylic acid (MIL-140C) and 3,3'-dichloro-4,4'-azobenzene dicarboxylic acid (MIL-140D).

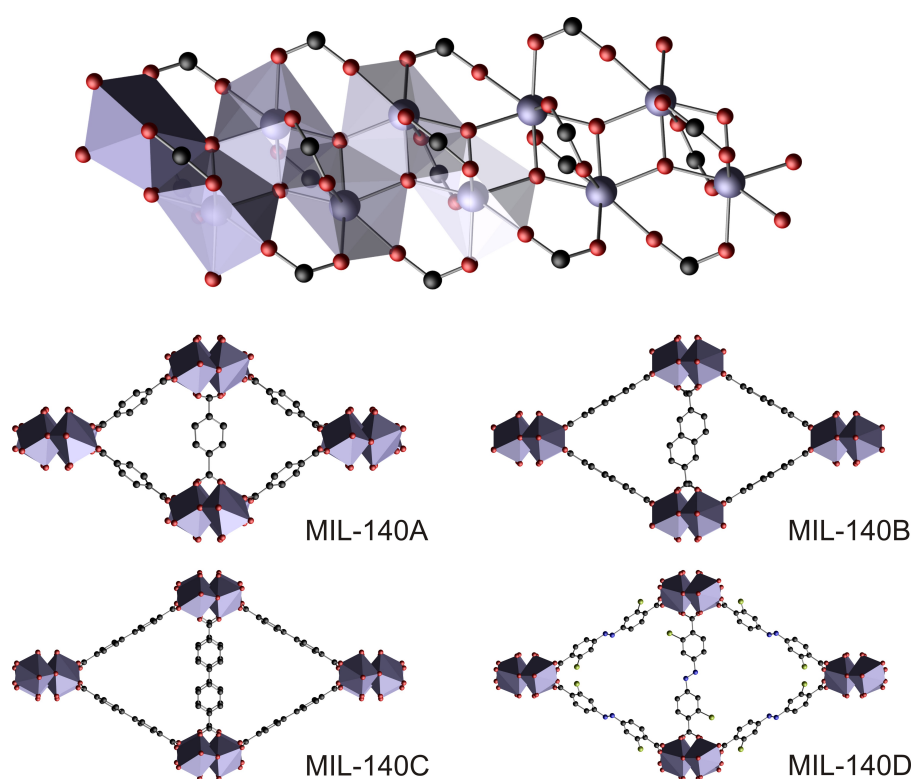


Fig. 14: The isoreticular MIL-140 series contains a chain of 7-fold coordinated Zr-atoms as SBU. These chains can be linked together by different dicarboxylic acids to form a porous MOF with channel like pores.<sup>[62]</sup>

The MIL-140 series can typically be synthesized using a higher reaction temperature than for the UiO-type MOFs (220 °C instead of 120 °C).

## 1.4 Porosils and Porolites

Tectosilicates are built up from corner sharing  $[TO_4]$ -tetrahedra, the so-called primary building units ( $T$  = mainly Si, Al, but also other tetrahedrally coordinated atoms are possible like Ge, Ga, B etc.). The tetrahedra are linked together to form secondary building units, which are structures featuring rings which may contain up to 20  $T$ -atoms, but consist at least of four. These secondary building units are sufficient to describe the whole framework of porous tectosilicates. The porous tectosilicates can be divided into porosils, which contain solely Si as  $T$ -atoms in the network, and porolites, which contain Al in addition to Si. By replacing silicon atoms by aluminum atoms in the structure, a negative charge of the framework is established. This is neutralized by the insertion of positively charged ions like  $H^+$ ,  $Na^+$ ,  $K^+$ ,  $Ca^{2+}$  etc. into the pores. Both porolites and porosils can be subdivided into two families with either open or more dense (nevertheless porous) structures. The former contains channel-like cavities with at least 8-ring (this means that eight  $T$ -atoms form a ring) windows and the latter contains only cage-like cavities with maximal 6-ring windows. The first are marked by the prefix “zeo”, the latter by the prefix “clathra”. This classification is summarized in Fig. 15.

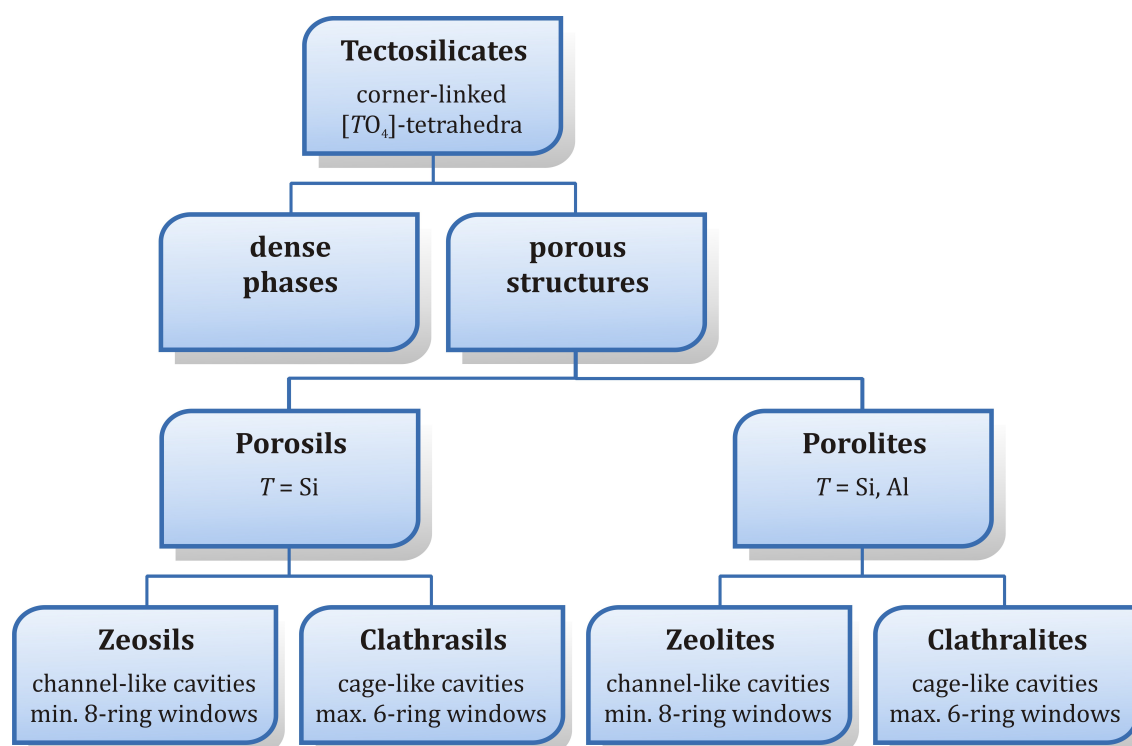


Fig. 15: Classification of tectosilicates.<sup>[63]</sup>

This classification is often not applied consequently and the term zeolite is frequently used as a notion for all kinds of porous tectosilicates.

There are a number of naturally occurring porous tectosilicates. Since the first discovery of zeolites in 1756 by the Swedish mineralogist CRONSTEDT, approximately 40 natural zeolites have been found.<sup>[64]</sup> Natural zeolites contain alkali or alkaline earth metal cations for charge balancing. Besides natural zeolites there are synthetic zeotype materials. Each of the up to date 201 known structures is assigned a three letter code.<sup>[65]</sup> Some of them have structures analogue to natural zeolites, while most of them do not have a naturally occurring counterpart and may contain both inorganic and organic cations. Because of their porosity and intracrystalline void space porous tectosilicates have found a number of applications as adsorbents and catalysts soon after their first synthesis in the late 1940s.<sup>[66]</sup> They are able to discriminate molecules based on their shape and size. The most important technical application of zeolites is probably their use as cracking catalysts in oil refinement.

The synthesis of zeotypes proceeds most often in a basic solution to make sure that the silicate and also the aluminate species are dissolved. A synthesis in acidic solution is also possible when fluoride is used as a mineralizing agent.<sup>[67]</sup> Either way, some additional species is needed in the synthesis solution to initiate the formation of porous materials. Without such a space filler, structure-directing agent (SDAs) or template, dense structures would be formed. In synthetic zeolites this role is most often taken on by organic molecules. The classification into the three mentioned categories was first suggested by DAVIS and LOBO.<sup>[64]</sup> Most zeolitic materials can be synthesized with a variety of different organic molecules. This is what is called space filling. In contrast to this a true structure-directing agent is defined as a single organic species that leads to a specific structure. This is for example the case in the synthesis of hexagonal faujasite (EMT) which can be synthesized in the presence of 18-crown-6.<sup>[68,69]</sup> However, other organic molecules have been shown to lead to the formation of EMT, for example polyquaternium-6,<sup>[70]</sup> but in these cases no phase pure product is obtained, EMT is always mixed with FAU. Compared to SDAs true templates are found even more rarely. To speak of templating mechanisms, the resulting zeolite structures must not only adopt the fitting geometric structure, but also has to strongly interact with the organic

---

molecule. This is the case for example in ZSM-18 that is templated by a triquaternary ammonium cation  $(C_{18}H_{30}N_3)^{3+}$  (tri-quat).<sup>[71]</sup> The cages of ZSM-18 show the same 3-fold rotational symmetry as the tri-quat molecule that resides in these cages. By NMR studies it could even be shown that the host-guest interactions in the material are sufficiently high to not even allow rotation of the templating molecule, which is otherwise the usual case for molecules residing in zeolite cages.<sup>[72]</sup> These enhanced interactions distinguish templating from structure direction. A more recent example for true templating can be found in the chiral gallogermate zeolite  $[Ni(en)_3][Ga_2Ge_4O_{12}]$ .<sup>[73]</sup> The chirality of the used  $[Ni(en)_3]^{2+}$  cation is transferred to the structure in the form of chiral cages.

#### 1.4.1 Silicalite-1

Silicalite-1 is a purely siliceous zeosil that possesses the MFI topology. The aluminum containing zeolite counterpart is called ZSM-5 (Zeolite Socony Mobil - 5). There is also a naturally occurring mineral with MFI topology that is called mutinaite:  $Na_3Ca_4(Si_{85}Al_{11})O_{192} \cdot 60H_2O$ .<sup>[74]</sup> The structure of ZSM-5 was disclosed in 1978 using single crystal and powder X-ray data.<sup>[75]</sup> As SBU it contains exclusively 5-1 rings.<sup>[5]</sup> The channel system of the material comprises two intersecting channels formed from 10 *T*-atoms each. Straight channels are running parallel to [010] and sinusoidal channels running parallel to [100] cross the first ones as shown in Fig. 15. The space filler that is most often used in the synthesis of silicate or aluminosilicate MFI is the tetrapropylammonium cation, but other molecules like for example di- and tri-quaternary ammonium cations can also be used.<sup>[76]</sup>

The main use of materials with MFI topology is that of ZSM-5 in acid-catalyzed organic syntheses such as the isomerization and alkylation of hydrocarbons. In particular it is used for the selective synthesis of *para*-xylene. This can be accomplished via different pathways. The disproportionation of toluene,<sup>[77,78]</sup> the alkylation of toluene with methanol,<sup>[77,79]</sup> or the isomerization of xylenes<sup>[77]</sup> can be used to yield *p*-xylene with high selectivities over ZSM-5 as catalyst. The explanation for this behavior is that the channels of MFI with a diameter of approx. 6 Å allow an unhindered diffusion of *p*-xylene (kinetic diameter of ca. 5.8 Å)

---

whereas the diffusion of *o*- and *m*-xylene is much slower (kinetic diameter of approx. 6.8 Å).<sup>[80]</sup>

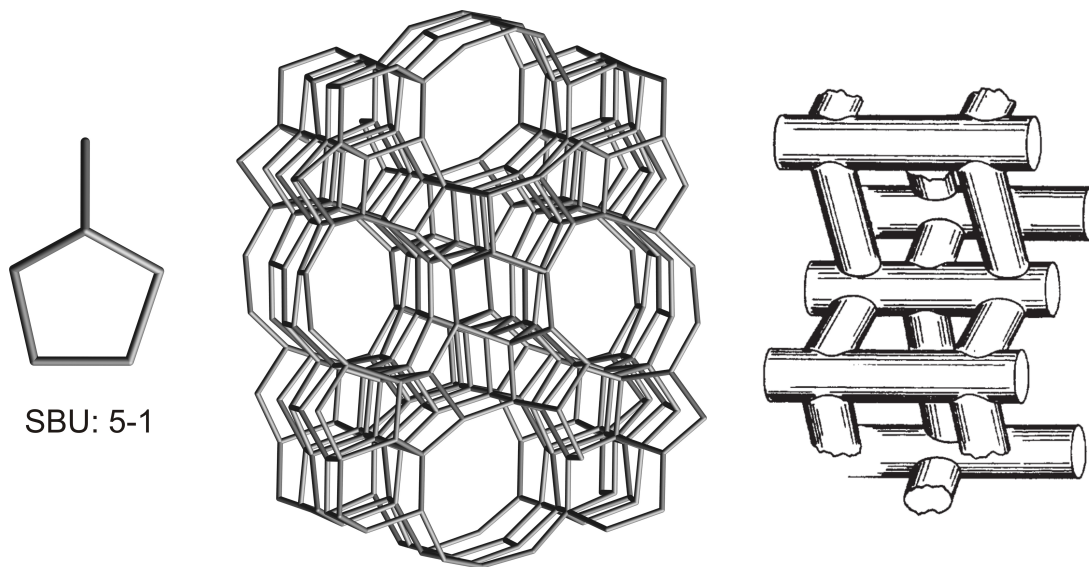


Fig. 16: The structure of silicalite-1 is built up from 5-1 SBUs (left). The MFI topology (middle) has straight 10-ring channels parallel to  $[010]$  and intersecting sinusoidal 10-ring channels parallel to  $[100]$ . The topological picture (right, viewed along  $[010]$ ) shows only  $T$ -atoms as knots and the oxygen bridges as lines. Structural data from ref. [65]. Right: Depiction of the channel system of MFI.<sup>[75]</sup>

### 1.4.2 Sodalite

The structure of sodalite is built up from a single SBU, the 6-ring. These 6-rings can be put together to form the composite building unit that is present in several other zeolites as well, the so called sodalite- or  $\beta$ -cage. In SOD, these  $[4^66^8]$ -polyhedra are connected directly via the 4-rings. In the cubic unit cell one of these polyhedra is found on each vertex. Thereby another sodalite-cage is formed in the middle of the elementary cell. This is shown in fig. 16. Since SOD does not contain window sizes larger than 6-rings it is classified as a clathrasil or clathralite depending on the aluminum content. Most species trapped inside the sodalite cages during synthesis cannot leave the material afterwards. For example colored anions can be trapped inside the structure, which are unable to leak out. That is why certain sodalites make up for high quality pigments. Ultramarine pigments are sodalites with an Al/Si ratio of 1:1 (which is the highest possible ratio according to LÖWENSTEIN'S rule) containing polysulfide anions ( $S_2^-$ : yellow-green,  $S_3^-$ : blue,  $S_4^-$ : red) which

account for the color of the pigment. Ultramarines are available in different colors like blue, green, pink or violet. Natural ultramarine blue is the chromophoric component in lapis lazuli and is one of the rarely found natural blue pigments that are light-fast and bleach resistant. The polysulfide anions are protected from chemical reactions (for example with oxygen) by the framework of the clathralite.

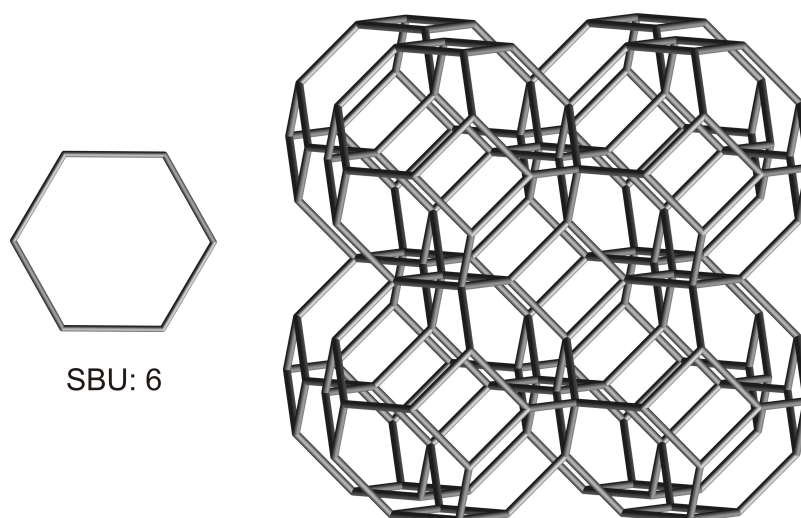


Fig. 17: The SBU found in SOD is a 6-ring (left). The topological picture of the SOD-structure (right) shows only *T*-atoms as knots and the oxygen bridges as lines. Structural data from ref. [65].

Sodalites can be synthesized using organic molecules as space fillers instead of alkali ions. These can be charged molecules as it is the case for the tetramethyl ammonium (TMA) ion.<sup>[81]</sup> One TMA ion occupies each sodalite cage so that the Al/Si ratio is reduced to 1:5 in order to keep charge balance. The unit cell composition is therefore  $[(\text{CH}_3)_4\text{N}]_2[\text{Al}_2\text{Si}_{10}\text{O}_{24}]$ . Pure silica sodalites are available using uncharged space fillers like ethylene glycole,<sup>[82]</sup> 1,3,5-trioxane,<sup>[83]</sup> 1,3-dioxolane,<sup>[84]</sup> ethylenediamine,<sup>[85]</sup> ethanolamine,<sup>[85]</sup> ethylamine,<sup>[86]</sup> and pyrrolidine.<sup>[86]</sup>

Owing to the small window diameter of sodalite of approx. 2.8 Å, only very small molecules like helium, ammonia, water or hydrogen (kinetic diameters of 2.6 – 2.9 Å) may pass through the pores of the material. It therefore seems to be a well suited material for example in the separation of H<sub>2</sub> in dehydrogenation processes or as water selective membranes. Until now different aluminosilicate sodalite membranes have been reported in the literature.<sup>[87-90]</sup> XU and coworkers have reported of a hydroxy sodalite membrane that shows a permselectivity for H<sub>2</sub>/*n*-C<sub>4</sub>H<sub>10</sub> of more than 1000.<sup>[87]</sup> This separation factor demonstrates how

powerful sodalite can be in hydrogen separation. The applicability of hydroxy sodalite films in the dehydration of water/alcohol mixtures was demonstrated by KAPTEIJN and coworkers.<sup>[90]</sup>

Sodalite was also investigated as a material for the storage of hydrogen. At elevated pressures and temperatures hydrogen can enter the cages of the material through the 6-ring windows and is captured inside the structure after cooling the material to room temperature. Compared to other materials (like for example certain MOFs) both the calculated and the measured storage capacities are rather low. For hydroxy sodalite they are 0.10 wt% (calculated) and 0.26 wt% (measured), for silica sodalite they are even lower: 0.08 wt% (calculated) and 0.15 wt % (measured).<sup>[91]</sup>

---



## 1.5 Zeolite and MOF Membranes

Compared to other separation techniques like rectification or crystallization a separation using membranes is much more energy- and thereby also more cost-efficient in technical applications. That is why a lot of research activity is present in this field. For separation tasks materials with defined pore sizes are desired. Therefore zeolites and the younger class of metal organic frameworks seem to be suitable materials.

### 1.5.1 Separation Principles

Membranes are defined as structures through which mass transports can occur. This can be caused by different driving forces like gradients in pressure, concentration or electrical potential.<sup>[92]</sup> However to achieve a selection, not only a mass transfer but also a semipermeable character of the membrane has to be ensured. In the easiest case it arises from a discrimination of size in analogy to a simple sieve. Considering small particles on a molecular level this effect is called molecular sieving. For this effect a porous material with defined pore sizes in the same size range as the species that have to be separated is necessary. For a gas separation, which will be discussed in more detail here, pores with sizes of a few angstroms are needed. This requirement is met by zeolites but also by a younger class of hybrid materials, the metal-organic frameworks.

The separation of gaseous species with the use of membranes is called gas permeation. The driving force is a difference in partial pressure on both sides of the membrane. The side which is loaded with the gas mixture that is to be separated is called the feed side. The side on which the products of the separation are obtained is called the permeate side. The needed pressure difference can either be accomplished by an excess pressure on the feed side, that is by applying a feed pressure to the membrane, or by a negative pressure on the permeate side, which means evacuation of the permeate.

---

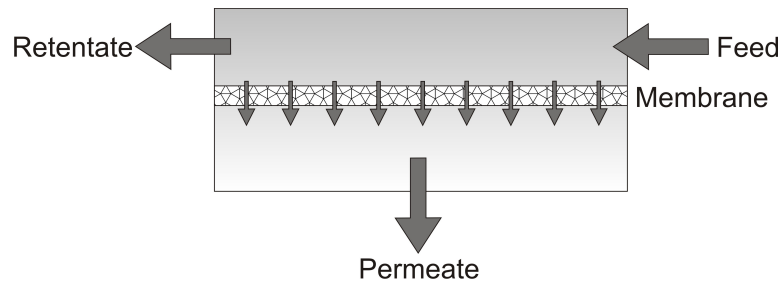


Fig. 18: Depiction of a membrane setup clarifying the terms feed, retentate and permeate.

Characteristic properties of a membrane are the separation factor and the flux through the active layer. Both variables are sought to be as high as possible, although the separation factor plays a much more important role for it is a material property whereas a low flux can be compensated by employing a larger membrane area. With the use of permeation measurements both terms can be appraised. For that purpose a feed of known composition is applied to the membrane and the composition of the permeate is detected. The flux  $J$  is given by the number of transported material (e.g. the number of transported moles) per time and membrane area. If two components  $i$  and  $j$  are investigated the separation factor arises from the ratio of the composition of the permeate ( $P$ ) in relation to the composition of the feed ( $F$ ).

$$S_{ij} = \frac{w_{iP}/w_{jP}}{w_{iF}/w_{jF}}$$

$S$ : separation factor

$w$ : weight percent

The transport of a species through a porous membrane can be separated into several steps. At first the species have to be adsorbed on the feed-side, then a diffusion step through the active layer takes place, before desorption of the gas on the permeate-side occurs. Because of these events the performance of a membrane with regard to a certain separation task is not only dependent of the size of the gas-molecules in relation to the pore size of the active layer (which would be a mere molecular sieving effect), but is also contingent upon other factors like hydrophilic/hydrophobic interactions or VAN-DER-WAALS interactions, which can play an important role during the sorption processes.

It is generally assumed that sorption of a gas species is a rather fast process compared to the diffusion through the membrane. This means that diffusion is the

rate limiting step in gas permeation. Caused by the pressure difference between both sides of the membrane and under the assumption that adsorption and desorption proceed fast, a gradient in concentration is established through the membrane layer. The flux through the active separation layer can therefore be calculated using the empirically found FICK'S first law.

$$J_i = -D_i \cdot \text{grad } c_i = -D_i \cdot \frac{\partial c_i}{\partial z}$$

$J$ : Flux

$D$ : diffusion coefficient

$c$ : concentration

$z$ : direction of diffusion

A simplified linear form of FICK'S first law can be used, because in the mass transport through a membrane, only the  $z$  direction perpendicular to the surface of the active layer is of interest. The diffusion coefficient, that is assumed to be a constant, can show a noticeable dependency on the concentration. Moreover in systems with more than one gas species the diffusion coefficient is different from the one for the pure substance.

A borderline case of diffusion occurs when the mean free path of the gas becomes larger than the pore diameter, that is when the KNUDSEN number becomes larger than 1.

$$Kn = \frac{\lambda}{d_{\text{pore}}} \gg 1$$

$Kn$ : Knudsen number

$\lambda$ : mean free path

$d_{\text{pore}}$ : pore diameter

In this case the so-called KNUDSEN diffusion commences, which is characterized by the fact that gas molecules collide with pore walls more often than with other gas molecules. For linear pores the KNUDSEN diffusion coefficient amounts to:

$$D_{Kn} = \frac{4}{3} d_{\text{pore}} \sqrt{\frac{8RT}{\pi M}}$$

$R$ : ideal gas constant,  $8.314 \text{ J} \cdot \text{mol}^{-1} \cdot \text{K}^{-1}$

$T$ : absolute temperature

$M$ : molar mass of the gas

One can see that with constant temperature and unchanging pore diameter, the diffusion coefficient is only dependent on the molar mass of the gas. The higher the mass becomes, the slower the diffusion proceeds. According to this the ideal separation factor of a binary mixture, which can be calculated as the quotient of the single gas permeations, is formed as the square root of the ratio of the molar masses of the two gases.

$$\alpha_{Kn} = \sqrt{\frac{M_{\text{gas1}}}{M_{\text{gas2}}}}$$

$\alpha$ : ideal separation factor

A separation by KNUDSEN diffusion is not of interest in industrial application, because in most separation tasks molecules of similar weight have to be separated. In these cases the separation factors reached with KNUDSEN diffusion are too low. Knudsen diffusion occurs mostly when pore diameters of approx. 1 – 20 nm are present. Grain boundaries lie in this size range. So when KNUDSEN separation factors are measured in permeation experiments it is a good hint that the active layer is not completely dense.

### 1.5.2 General Preparation Techniques

Since the research in the field of zeolite membranes has been going on for approximately three decades whereas MOF membranes came up much later, most preparation techniques were first used and optimized for zeolites. First attempts in making use of the porous structure of these materials for separation tasks was as fillers embedded in polymer membranes.<sup>[93,94]</sup> A difficulty that still remains in the production of these so-called mixed matrix membranes (MMMs) with zeolite particles is the integration of the particles into the organic matrix. The inorganic nature of zeolites makes it difficult to control the homogenous distribution in the polymer.<sup>[95,96]</sup> The hybrid character and the possibilities of differently functionalized linkers of MOFs makes these porous solids promising in applications in MMMs. The main disadvantage of MMMs remains their low thermal stability due to the organic polymer matrix. Purely inorganic membranes feature a much better thermal stability. These can be free standing membranes that are

---

often prepared on a PTFE substrate and removed from it after synthesis to form a self supported film.<sup>[97,98]</sup> It is also possible to form free standing layers without these temporary substrates for example at the interface of two liquids. Following this idea, MFI layers can be formed at the interface between an aqueous and an organic phase<sup>[99]</sup> or on a mercury surface.<sup>[100]</sup> Unsupported thin layers of crystalline materials like zeolites are often brittle and their potential in application is therefore limited. That is why most reported membranes are crystallized on porous substrates that are permeable and are not removed after synthesis. As support materials ceramics like  $\alpha$ -Al<sub>2</sub>O<sub>3</sub>,  $\gamma$ -Al<sub>2</sub>O<sub>3</sub> or TiO<sub>2</sub>, stainless steel, glass or quartz are commonly used.

For the preparation of supported membranes (either zeolitic materials or MOFs) two different synthesis approaches are commonly pursued. The active layer may either be grown directly in an *in situ* crystallization in only one step or a layer of seed crystals that is first deposited on the support may be grown into a dense layer in a two step synthesis. The advantages of an *in situ* crystallization are obviously the underlying simplicity and the time saving aspect. On the other hand it can be difficult to gain control over nucleation and growth in a one step reaction. It is important to produce enough nucleation sites on the support to achieve a dense layer after the growth process. Therefore it can be beneficial to decouple the nucleation and the growth step by employing a seeding and secondary growth step. Using this concept it is easier to gain control over the size and orientation of the crystals in the final membrane. In a first step crystallites of the desired material are formed and applied to the substrate. Thereby it is assured that enough nucleation sites are present and a dense film can be grown with a small layer-thickness in the secondary growth step.

Since supported layers of zeolitic and MOF materials are a main topic of this work, the preparation of these membranes is discussed separately and in more detail in the following chapters.

---

### 1.5.3 Zeolite-based Membranes

The defined pore sizes and geometries characteristic for zeolites make these materials suited for separation tasks. The size of these cavities and channels decides over which molecules may be separated. Fig. 19 gives an overview over the kinetic diameters of some small molecules in comparison to the pore sizes of a few selected zeolitic topologies. Not only the pore sizes but the Si/Al ratio (that makes the materials either hydrophobic or hydrophilic) and the chemical stability play an important role and have to be taken into account as well when trying to find a suited material for a specific separation.

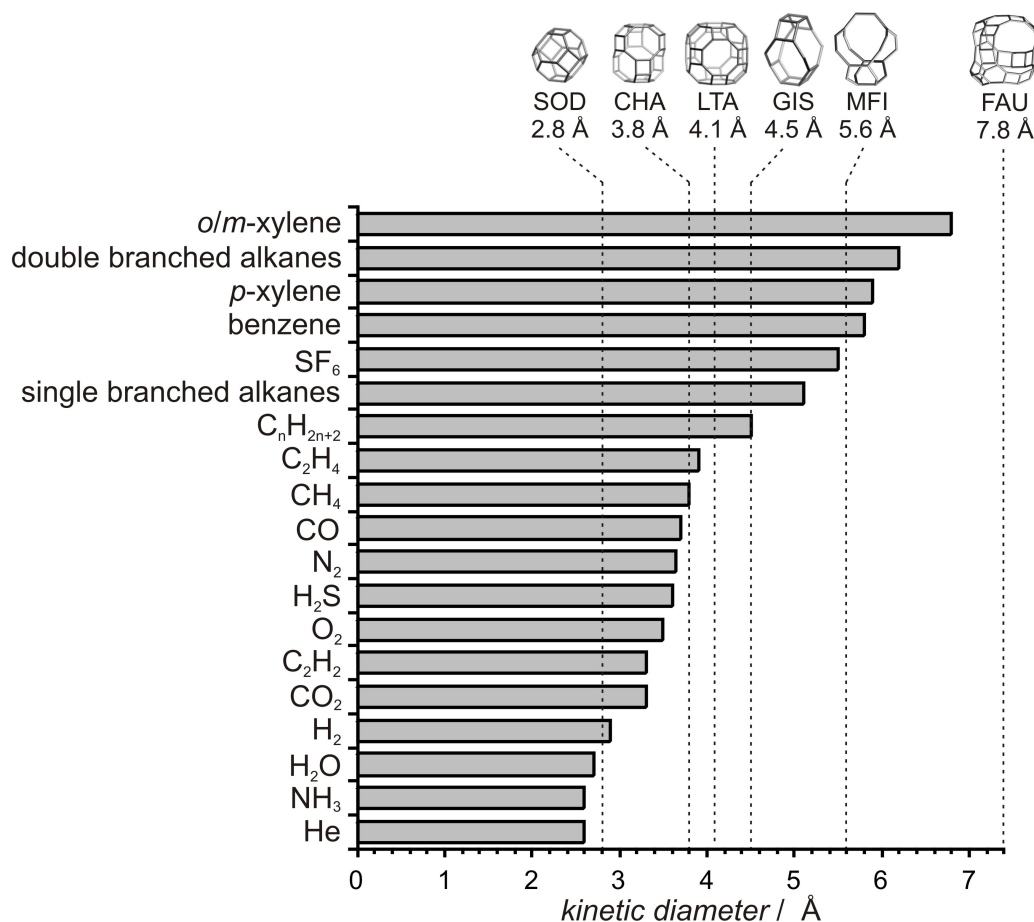


Fig. 19: Comparison of kinetic diameter of small molecules with the effective pore sizes of some zeolitic topologies (reproduced from ref [101]).

Among all the different topologies the most often investigated one in membrane research activities is MFI.<sup>[102]</sup> A possible field of application for aluminum-poor MFI membranes is the separation of *n*-butane and *iso*-butane, which was studied by a number of researchers.<sup>[103-105]</sup> A selectivity for *n*-butane over *iso*-butane is observed with ideal separation factors of up to 90 and mixture separation factors

of approx. 50.<sup>[105]</sup> Another example of shape-selectivity in MFI membranes can be found in the separation of methanol from methyl *t*-butyl ether with a mixture separation factor of 250.<sup>[106]</sup> Another kind of separation that has already found application in industrial scale is the dewatering of organic solvents. It is based on the hydrophilic character of aluminum rich zeolites and not on a molecular sieving effect. In 2000 the first large scale LTA membrane plant was developed and built by Mitsui Engineering and Shipbuilding Co. Ltd. It is used for the dewatering of alcohols with an initial concentration of 90 wt. % and yields 530 L/h with a final water contents of 0.2 wt. %.<sup>[107]</sup> Similar plants using LTA membranes for the dewatering of organic solvents were built by other companies as well (Smart and Inocermic, Busan Nanotech Research Institute, Nanjing Jiushi Hi-Tech Co.).<sup>[108]</sup>

There are various examples for laboratory scale *in situ* crystallization in zeolitic membrane preparation. A lot of research activity in the 1990s has shown that different zeolitic materials may be grown on various supports using the simple *in situ* crystallization, e.g. mordenite (MOR) on stainless steel or PTFE plates,<sup>[109]</sup> MFI on  $\alpha$ -alumina<sup>[110]</sup> or silicon wafers,<sup>[111]</sup> P-type zeolite (GIS) on  $\alpha$ -alumina,<sup>[112]</sup> A-type zeolite (LTA) on quartz.<sup>[113]</sup> In some cases it is beneficial for the final quality of the membrane when a pre-treatment of the support is carried out prior to the synthesis of the active layer. In zeolite membrane synthesis the number of OH-groups on the surface of the support is crucial to ensure a high nucleation site density. Ceramic supports may therefore be treated with sodium hydroxide solution. A way to produce hydroxyl groups on porous TiO<sub>2</sub> supports is the use of UV radiation. This concept was developed by VAN DER BERG *et al.* and it led to increased nucleation of zeolite A.<sup>[114,115]</sup> The kind of support chosen for a specific material also plays an important role. For the synthesis of porosil membranes for example the use of alumina supports always leads to a contamination of the porosil with aluminum. The aluminum may either diffuse directly into the silica material from the support for example in calcination processes or through the reaction solution when the support is partially dissolved.<sup>[116]</sup>

When using the seeding and secondary growth mechanism, the quality of the support becomes less important because nucleation sites are applied in the seeding step. When directly comparing *in situ* crystallization and seeded growth, the latter often leads to higher quality membranes.<sup>[117]</sup> The most delicate step of

---

this procedure is the attachment of seed crystals to the support material. There are several means of doing so. The quickest and simplest way of seeding is probably to rub the support with a powder of the desired zeolite.<sup>[118,119]</sup> Since a seeding step by rubbing is fast and cost-efficient, it can easily be transferred to large-scale productions. Another quite simple way of seeding is by dip-coating.<sup>[120]</sup> The seed crystals may even be deposited in an oriented way by dipping, which results in an oriented layer after secondary growth.<sup>[121]</sup> To achieve an oriented layer the seed crystals do not necessarily have to be oriented, but a competitive growth can lead to a preferred orientation of the crystals as well.<sup>[122]</sup> This kind of growth is often observed in MFI layers.<sup>[123]</sup> Adhesion between seed crystals and support can be enhanced by using electrostatic attraction. In this case the surface charge of seeds and support has to be opposing. If this is not an intrinsic property of the materials, the surface of either the support or the seeds or even both can be modified using charged molecules like for example different polymers or silanes.<sup>[124,125]</sup> By employing a suitable surface modification, a covalent attachment of the seed crystals can also be achieved.<sup>[125]</sup> These few examples give a little insight into the various means of zeolitic membrane production. Since they have proven successful some of these concepts have been transferred to MOF membranes as well.

#### **1.5.4 MOF-based Membranes**

Unlike zeolite membranes, of which a few have already found their way into industrial application, the research on MOF membranes is in a much earlier stadium. Compared to zeolites MOFs cover a wider range of pore sizes (from micropores up to mesopores) and surface properties and are therefore highly promising materials for membranes based separations.

There are several challenges that have to be considered in the production of MOF based membranes. Similar to zeolitic membranes the MOF layer may crack during or after the synthesis. Since MOFs are crystalline materials they tend to be brittle. Cracks may form when thermal stress is applied for example when cooling the materials after the synthesis that is carried out under elevated temperatures most often. Several types of MOF layers like HKUST-1,<sup>[127]</sup> MOF-5,<sup>[128,129]</sup> or ZIF-69<sup>[130]</sup> have therefore been reported to require a slow natural cooling after the synthesis.

---



Another process step in which cracks may form is during drying. Surface tension at the solid/liquid interface in grain boundaries or in pores causes capillary stress in the films that leads to the formation of cracks. Two possible ways of reducing the capillary stress are to either dry the materials at nearly saturated conditions<sup>[127]</sup> (and thereby decreasing the drying rate) or to introduce a surfactant to the film surface to reduce the solid/liquid surface tension.<sup>[131]</sup> Another thing besides the formation of cracks that has to be taken care of is a sufficient bonding between the support material and the MOF layer. Whereas silica species can readily bind to hydroxyl groups present on ceramic supports this is not necessarily the case for MOFs. Some linkers like dicarboxylates or imidazole species, that are unsubstituted in the 2 position, have been shown to bind covalently to alumina supports.<sup>[132,133]</sup>

In general the fabrication techniques for MOF membranes are similar to those described for zeolite membranes in section 1.5.3. Either *in situ* growth or seeding and subsequent secondary growth are commonly used. As mentioned before the bonding between the MOF and the native substrates (mostly ceramic ones like titania or alumina) is commonly weak. That is why there are only few publications describing a successful *in situ* growth of MOF membranes on untreated supports. MOF-5 and ZIF-69 have been grown on unmodified  $\alpha$ -Al<sub>2</sub>O<sub>3</sub> supports by LIU and coworkers.<sup>[128,130]</sup> Another example for *in situ* growth on untreated supports was reported by BUX *et al.* They used a microwave synthesis for the production of ZIF-8 membranes on bare titania supports.<sup>[134]</sup> A modification of the substrate prior to the *in situ* growth of the MOF is reported more frequently. In the case of different ZIFs like ZIF-22 and ZIF-90 the group of CARO has shown that 3-aminopropyltriethoxysilane (APTES) covalently bound to an alumina support can facilitate the attachment of the ZIFs to the support.<sup>[135,136]</sup> For ZIF-7 and ZIF-8 JEONG and coworkers have reported another way of modifying the alumina support that has proven helpful for the fabrication of membranes of these materials. They have dropped a solution of the linker onto the heated substrate. The solvent was rapidly evaporated and the imidazole linkers were covalently bound to the surface by the formation of Al-N bonds.<sup>[137]</sup> These linkers are then used for the anchoring of the ZIF. When choosing a suited support material for a MOF layer one can make use of the fact that MOFs are formed via coordinative bonds between metal and linker.

---

The group of QUI has shown for a zinc and a copper MOF that substrates consisting of the accordant metal can be used as both support and metal source.<sup>[138,139]</sup> The copper containing MOF HKUST-1 was grown on a oxidized copper mesh so that an essentially free standing membrane was formed.<sup>[139]</sup>

Similar to zeolite membranes, MOF membranes fabricated via seeding and secondary growth often show enhanced properties, because this synthesis procedure allows for a better control over characteristics like film thickness, crystal orientation and density of grain boundaries. Unlike zeolitic seed crystals, that can be attached covalently to ceramic supports by a simple calcination step, MOF nanocrystals are often sensitive in respect to elevated temperatures and do not interact with the substrates strongly. For ZIF-8 however a simple seeding by rubbing was reported to yield good quality membranes after the secondary growth process.<sup>[140]</sup> Much more frequently a more delicate seeding procedure is necessary. For MMOF (Cu(hfipbb)(H<sub>2</sub>hfipbb)<sub>0.5</sub>; H<sub>2</sub>hfipbb = 4,4'(hexafluoro-isopropyl idene)-bis (benzoic acid)) and different ZIFs the use of polyethylene-imine (PEI) as a polymer binder is required to attach the MOF to the substrates.<sup>[141-143]</sup> For the fabrication of MMOF membranes the alumina supports were first dip-coated with PEI before the seed crystals were rubbed onto the PEI layer. This step proved necessary to produce uniform membranes.<sup>[141]</sup> In the case of ZIF-7<sup>[142]</sup> and ZIF-8<sup>[143]</sup> a suspension containing the seed crystals and PEI was used in a dip coating process. In all three cases the seeds are linked to the alumina supports by H-bonds of the PEI, which means that the crystals are not directly attached to the support. Of course the strength of attachment is only as high as the strength of attachment of both the support and the seeds to the PEI binder. Another way of seeding was reported by the group of JEONG for HKUST-1. They have developed a thermal seeding process in which a suspension of HKUST-1 is dropped onto the hot (200 °C) support.<sup>[127]</sup> They have shown that it is mandatory for a sufficient linkage of the seeds that the suspension contains the precursor chemicals of the MOF in addition to the seeds. When only the HKUST-1 seeds are present in the suspension during thermal seeding, the seeds do not remain on the support after ultrasonic treatment. A technique called reactive seeding was introduced by LEE *et al.* for MIL-53 membranes.<sup>[144]</sup> It features two solvothermal reaction steps. First a seed layer is produced in an *in situ* growth process and in a second solvothermal

---

reaction step the seeds are grown into a dense film. A similar fabrication pathway was reported under the name of “microwave-induced thermal deposition”. In this case the support is seeded by *in situ* growth using a rapid microwave synthesis.<sup>[129,145]</sup>

Because of the larger pore sizes of MOFs, bigger molecules compared to zeolitic membranes could probably be separated in a liquid phase adsorptive separation. Contrary to this thought MOF based membranes (most of which are ZIF membranes) have up to date mainly been tested for the separation of small gases like hydrogen, methane and carbon dioxide. A summary of single gas permeances of small gases through exemplary MOF membranes is shown in Table 2. For the separation of H<sub>2</sub> from other gases, MOFs with small micropores seem to be ideal candidates. That is why ZIFs with small pore sizes (ZIF-7: 3.0 Å, ZIF-8: 3.4 Å, ZIF-22: 3.0 Å) have been extensively explored for this purpose. For ZIF-8 no sharp cutoff in the permeance of gases larger than the calculated pore size was found due to framework flexibility. Nonetheless the data evaluated by the group of CARO and by JEONG and coworkers have shown that ZIF-8 is indeed capable of separating hydrogen from other gases like methane.<sup>[134,137]</sup> For the smaller pored ZIF-7 and ZIF-22 a cutoff between H<sub>2</sub> and CO<sub>2</sub> was observed.<sup>[135,146]</sup> Both materials could be very promising in practical hydrogen separation. However some MOFs with larger pore sizes have shown surprisingly good performances in the separation of H<sub>2</sub> as well. For example HKUST-1 (pore size ca. 9 Å) membranes synthesized on copper nets exhibit separation factors far beyond KNUDSEN diffusion.<sup>[139]</sup> The same material crystallized on  $\alpha$ -alumina supports shows separation factors lower than the previously mentioned one.<sup>[127]</sup> This might be due to the porous nature of the support or diffusion through grain boundaries (which once more underlines the importance of control over the microstructure of membranes). Membranes made of MOF-5 (with a pore size of approx. 15 Å) exhibit KNUDSEN behavior in the permeance of small gases.<sup>[128]</sup> This is not surprising since the pores are much larger than the tested gases.

---

Table 2: Single gas permeances of exemplary MOF membranes.

MOF	$T / ^\circ\text{C}$	$d / \mu\text{m}$	permeance at $\sim 1 \text{ atm} / 10^{-8} \text{ mol m}^{-2} \text{ s}^{-1} \text{ Pa}^{-1}$					ideal separation factor				Ref.
			$\text{H}_2$	$\text{CH}_4$	$\text{N}_2$	$\text{CO}_2$	$\text{H}_2 / \text{CH}_4$	$\text{H}_2 / \text{N}_2$	$\text{H}_2 / \text{CO}_2$			
MOF-5	25	40	80	39	30	25	2	2.7	3.2	[129]		
MOF-5	25	25	285	103.3	80	66.7	2.8	3.6	4.3	[128]		
MOF-5	25	85	131.7	56.7	40	33.3	2.3	3.3	4	[128]		
ZIF-7	220	1.5	4.55	0.31	0.22	0.35	14.7	20.7	13	[146]		
ZIF-7	200	1.5	7.4	1.18	1.1	1.1	6.3	6.7	6.7	[142]		
ZIF-8	20	5	-	472	-	2430	-	-	-	[140]		
ZIF-8	25	20	17.3	1.33	1.49	4.45	13	11.6	3.9	[137]		
ZIF-8	25	2.5	36	7.8	9	14	4.6	4	2.6	[147]		
ZIF-8	25	40	6.04	0.48	0.52	1.33	12.6	11.6	4.5	[134]		
ZIF-22	50	40	20.2	3.02	2.84	2.38	6.7	7.1	8.5	[135]		
ZIF-69	25	50	6.5	1.85	-	2.5	3.5	-	2.6	[130]		
ZIF-90	200	20	25	1.57	1.98	3.48	15.9	12.6	7.2	[136]		
MMOF	25	20	1.6	-	0.35	0.35	-	4.6	4.6	[141]		
MMOF	190	20	0.2	-	0.01	0.04	-	20	5	[141]		
HKUST-1	25	60	125.3	16.1	-	27.4	7.8	-	4.6	[139]		
HKUST-1	25	25	74.8	25.7	20.3	14.8	2.9	3.7	5.1	[148]		
HKUST-1	25	25	200	80	50	50	2.5	4	4	[127]		
HKUST-1	190	25	110	20	15		5.5	7.3		[127]		

Up to now Zr-based MOFs have not been synthesized as polycrystalline supported membranes. However MAURIN and coworkers have explored thermodynamic and kinetic behavior of CO<sub>2</sub>/CH<sub>4</sub> gas mixtures within UiO-66 with a combination of experimental and computational methods.<sup>[149]</sup> They have explored both coadsorption and codiffusion of CO<sub>2</sub> and CH<sub>4</sub>. Compared to single gas adsorption, the CH<sub>4</sub> uptake in a gas mixture is drastically decreased while that of CO<sub>2</sub> is only slightly affected. This means that there is an adsorption selectivity for carbon dioxide over methane. In addition to that they found an interesting diffusion behavior. The diffusivity of methane increases with an increasing amount of CO<sub>2</sub> in the material. Since molecular dynamic simulations have shown that CO<sub>2</sub> diffuses about five times slower than CH<sub>4</sub>, one can state that in UiO-66 the slower molecule enhances the mobility of the faster one. This behavior can be explained by the presence of two different types of pores in UiO-66: octahedral voids and tetrahedral voids. CO<sub>2</sub> molecules possess a higher affinity to the tetrahedral voids than CH<sub>4</sub>. Simulations of diffusion pathways for both species lead to a jump sequence of tetrahedral – octahedral – tetrahedral. When both species are present, the CH<sub>4</sub> molecules are “pushed” out of tetrahedral void more frequently by the stronger adsorbing CO<sub>2</sub>. These results indicate that UiO-66 may be a promising material for CO<sub>2</sub>/CH<sub>4</sub> gas mixture separation. Since it can be expected that the presence of functional groups would enhance the affinity of CO<sub>2</sub> even more, computational exploration of differently functionalized UiO-66 MOFs was carried out by the same group.<sup>[150]</sup> Adsorption selectivities have indeed been shown to increase with increasing polarity of functional groups on the linkers in the sequence: -CF<sub>3</sub>, -Br, -NO<sub>2</sub>, -NH<sub>2</sub>, -(OH)<sub>2</sub>, -SO<sub>3</sub>H, -CO<sub>2</sub>H.

First experiments with UiO-66 and UiO-66-NH<sub>2</sub> as fillers in mixed matrix membranes have been done by KALIAGUINE and coworkers.<sup>[151]</sup> They have incorporated nanoparticles of these materials in polyimide matrices and evaluated the properties of the resulting MMMs in single gas permeances of CO<sub>2</sub> and CH<sub>4</sub>. They have observed that the ideal selectivity is higher with the UiO-66-NH<sub>2</sub> fillers compared to the neat polymer whereas it stays nearly unchanged with UiO-66 fillers. The CO<sub>2</sub>/CH<sub>4</sub> (50/50%) mixed gas selectivities reported were slightly lower than the ideal selectivities as expected for all tested materials.

---



## 2      References

- [1] G. Férey, *Chem. Soc. Rev.* **37** (2008) **191**.
- [2] S. Kitagawa, R. Kitaura, S. Noro, *Angew. Chem. Int. Ed.* **43** (2004) **2334**.
- [3] O.M. Yaghi, H. Li, *J. Am. Chem. Soc.* **117** (1995) **10401**.
- [4] O.M. Yaghi, G. Li, H. Li, *Nature* **378** (1995) **703**.
- [5] Ch. Baerlocher, L.B. McCusker, D.H. Olson, *Atlas of Zeolite Framework Types*, 6<sup>th</sup> Ed., Elsevier, Amsterdam, 2007.
- [6] H. Li, M. Eddaoudi, M. O’Keeffe, O.M. Yaghi, *Nature* **402** (1999) **276**.
- [7] J.H. Cavka, S. Jakobsen, U. Olsbye, N. Guillou, C. Lamberti, S. Bordiga, K.P. Lillerud, *J. Am. Chem. Soc.* **130** (2008) **13850**.
- [8] S.S.-Y. Chui, S.M.-F. Lo, J.P.H. Charmant, A.G. Orpen, I.D. Williams, *Science* **283** (1999) **1148**.
- [9] T. Ahnsfeldt, N. Guillou, D. Gunzelmann, I. Margiolaki, T. Loiseau, G. Férey, J. Senker, N. Stock, *Angew. Chem. Int. Ed.* **48** (2009) **5163**.
- [10] T. Loiseau, L. Lecroq, C. Volkringer, J. Marrot, G. Férey, M. Haouas, F. Taulelle, S. Bourrelly, P.L. Llewellyn, M. Latroche, *J. Am. Chem. Soc.* **128** (2006) **10223**.
- [11] J.J. Low, A.I. Benin, P. Jakubczak, J.F. Abrahamian, S.A. Faheem, R.R. Willis, *J. Am. Chem. Soc.* **131** (2009) **15834**.
- [12] S.S. Kaye, A. Dailly, O.M. Yaghi, J.R. Long, *J. Am. Chem. Soc.* **129** (2007) **14176**.
- [13] J.A. Greathouse, M.D. Allendorf, *J. Am. Chem. Soc.* **128** (2006) **10678**.
- [14] K.S. Park, Z. Ni, A.P. Côté, J.Y. Choi, R. Huang, F.J. Uribe-Romo, H.K. Chae, M. O’Keeffe, O.M. Yaghi, *Proc. Natl. Acad. Sci. U. S. A.* **103** (2006) **10186**.
- [15] A. Phan, C.J. Doonan, F.J. Uribe-Romo, C.B. Knobler, M. O’Keeffe, O.M. Yaghi, *Acc. Chem. Res.* **43** (2010) **58**.
- [16] M.W. Deem, J.M. Newsam, J.A. Creighton, *J. Am. Chem. Soc.* **114** (1992) **7198**.
- [17] G. Férey, C. Serre, *Chem. Soc. Rev.* **38** (2009) **1380**.
- [18] C. Serre, F. Millange, C. Thouvenot, M. Noguès, G. Marsolier, D. Louër, G. Férey, *J. Am. Chem. Soc.* **124** (2002) **13519**.
-

- [19] C. Serre, S. Bourrelly, A. Vimont, N.A. Ramsahye, G. Maurin, P.L. Llewellyn, M. Daturi, Y. Filinchuk, O. Leynaud, P. Barnes, G. Férey, *Adv. Mater.* **19** (2007) **2246**.
- [20] M. Eddaoudi, J. Kim, N. Rosi, D. Vodak, J. Wachter, M. O'Keeffe, O.M. Yaghi, *Science* **295** (2002) **469**.
- [21] O.M. Yaghi, M. O'Keeffe, N.W. Ockwig, H.K. Chae, M. Eddaoudi, J. Kim, *Nature* **423** (2003) **705**.
- [22] D.J. Tranchemontagne, J.R. Hunt, O.M. Yaghi, *Tetrahedron* **64** (2008) **8553**.
- [23] C. Serre, F. Millange, S. Surblé, G. Férey, *Angew. Chem. Int. Ed.* **43** (2004) **6286**.
- [24] S. Surblé, C. Serre, C. Mellot-Draznieks, F. Millange, G. Férey, *Chem. Commun.* (2006) **284**.
- [25] Z. Wang, S.M. Cohen, *Chem. Soc. Rev.* **38** (2009) **1315**.
- [26] K.K. Tanabe, S.M. Cohen, *Chem. Soc. Rev.* **40** (2011) **498**.
- [27] D. Venkataraman, G.B. Gardner, S. Lee, J.S. Moore, *J. Am. Chem. Soc.* **117** (1995) **11600**.
- [28] B.F. Hoskins, R. Robson, *J. Am. Chem. Soc.* **112** (1990) **1546**.
- [29] Y. Liu, G. Li, X. Li, Y. Cui, *Angew. Chem. Int. Ed.* **46** (2007) **6301**.
- [30] A. Vimont, J.-M. Goupil, J.-C. Lavalley, M. Daturi, S. Surblé, C. Serre, F. Millange, G. Férey, N. Audebrand, *J. Am. Chem. Soc.* **128** (2006) **3218**.
- [31] C.-D. Wu, A. Hu, L. Zhang, W. Lin, *J. Am. Chem. Soc.* **127** (2005) **8940**.
- [32] S.S. Kaye, J.R. Long, *J. Am. Chem. Soc.* **130** (2008) **806**.
- [33] Z. Wang, S.M. Cohen, *J. Am. Chem. Soc.* **129** (2007) **12368**.
- [34] K.K. Tanabe, Z. Wang, S.M. Cohen, *J. Am. Chem. Soc.* **130** (2008) **8508**.
- [35] E. Dugan, Z. Wang, M. Okamura, A. Medina, S.M. Cohen, *Chem. Commun.* (2008) **3366**.
- [36] M.J. Ingleson, J.P. Barrio, J.-B. Guilbaud, Y.Z. Khimyak, M.J. Rossiensky, *Chem. Commun.* (2008) **2680**.
- [37] Z. Wang, S.M. Cohen, *Angew. Chem. Int. Ed.* **47** (2008) **4699**.
- [38] W. Morris, C.J. Doonan, H. Furukawa, R. Banerjee, O.M. Yaghi, *J. Am. Chem. Soc.* **130** (2008) **12626**.
- [39] T. Gadzikwa, G. Lu, C.L. Stern, S.R. Wilson, J.T. Hupp, S.T. Nguyen, *Chem. Commun.* (2008) **5493**.
- [40] P. Roy, S. Schaate, P. Behrens, A. Godt, *Chem. Eur. J.* **18** (2012) **6979**.
-



- [41] J. Cravillon, R. Nayuk, S. Springer, A. Feldhoff, K. Huber, M. Wiebcke, *Chem. Mater.* **23** (2011) **2130**.
- [42] S. Diring, S. Furukawa, Y. Takashima, T. Tsuruoka, S. Kitagawa, *Chem. Mater.* **22** (2010) **4531**.
- [43] T. Tsuruoka, S. Furukawa, Y. Takashima, K. Yoshida, S. Isoda, S. Kitagawa, *Angew. Chem. Int. Ed.* **48** (2009) **4739**.
- [44] A. Schaate, P. Roy, A. Godt, J. Lippke, F. Waltz, M. Wiebcke, P. Behrens, *Chem. Eur. J.* **17** (2011) **6645**.
- [45] G. Kickelbick, P. Wiede, U. Schubert, *Inorg. Chim. Acta* **284** (1999) **1**.
- [46] P. Walther, M. Puchberger, F.R. Kogler, K. Schwarz, U. Schubert, *Phys. Chem. Chem. Phys.* **11** (2009) **3640**.
- [47] F.R. Kogler, M. Jupa, M. Puchberger, U. Schubert, *J. Mater. Chem.* **14** (2004) **3133**.
- [48] A. Piszczek, A. Radtke, A. Grodzicki, A. Wojtczak, J. Chojnacki, *Polyhedron* **26** (2007) **679**.
- [49] A. Schaate, P. Roy, T. Preuße, S.J. Lohmeier, A. Godt, P. Behrens, *Chem. Eur. J.* **17** (2011) **9320**.
- [50] G. Wißmann, A. Schaate, S. Lilienthal, A.M. Schneider, I. Bremer, P. Behrens, *Microporous Mesoporous Mater.* **152** (2012) **64**.
- [51] A. Schaate, S. Dühnen, G. Platz, S. Lilienthal, A.M. Schneider, P. Behrens, *Eur. J. Inorg. Chem.* (2012) **790**.
- [52] V. Guillerm, S. Gross, C. Serre, T. Devic, M. Bauer, G. Férey, *Chem. Commun.* **46** (2010) **767**.
- [53] S.J. Garibay, S.M. Cohen, *Chem. Commun.* **46** (2010) **7700**.
- [54] C. Zlotea, D. Phanon, M. Mazaj, D. Heurtaux, V. Guillerm, C. Serre, P. Horcajada, T. Devic, E. Magnier, F. Cuevas, G. Férey, P.L.Llewellyn, M. Latroche, *Dalton Trans.* **40** (2011) **4879**.
- [55] L. Valenzano, B. Civalieri, S. Chavan, S. Bordiga, M.H. Nilsen, S. Jakobsen, K.P. Lillerud, C. Lamberti, *Chem. Mater.* **23** (2011) **1700**.
- [56] F. Vermoortele, R. Ameloot, A. Vimont, C. Serre, D. De Vos, *Chem. Commun.* **47** (2011) **1521**.
- [57] M. Kandiah, M.H. Nilsen, S. Usseglio, S. Jakobsen, U. Olsbye, M. Tilset, C. Larabi, E.A. Quadrelli, F. Bonino, K.P. Lillerud, *Chem. Mater.* **22** (2010) **6632**.
-

- [58] M. Kandiah, S. Usseglio, S. Svelle, U. Olsbye, K.P.Lillerud, M. Tilset, *J. Mater. Chem.* **20** (2010) **9848**.
- [59] W. Morris, C.J. Doonan, O.M. Yaghi, *Inorg. Chem.* **50** (2011) **6853**.
- [60] M. Kim, S.J. Garibay, S.M. Cohen, *Inorg. Chem.* **50** (2011) **729**.
- [61] J. Weber, J. Schmidt, A. Thomas, W. Böhlmann, *Langmuir* **26** (2010) **15650**.
- [62] V. Guillerm, F. Ragon, M. Dan-Hardi, T. Devic, M. Vishnuvarthan, B. Campo, A. Vimont, G. Clet, Q. Yang, G. Maurin, G. Férey, A. Vittadini, S. Gross, C. Serre, *Angew. Chem.* DOI: 10.1002/ange.201204806.
- [63] F. Liebau, H. Gies, R.P. Gunawardane, B. Marler, *Zeolites* **6** (1986) **373**.
- [64] M.E. Davis, R.F. Lobo, *Chem. Mater.* **4** (1992) **756**.
- [65] Ch. Baerlocher, L.B. McCusker, <http://www.iza-structure.org/databases/> Database of Zeolite Structures (August 2012).
- [66] D.W. Breck, *Zeolite Molecular Sieves: Structure, Chemistry, and Use*, Wiley, New York, 1973.
- [67] J.L. Guth, H. Kessler, J.M. Higel, J.M. Lamblin, J. Patarin, A. Seive, J.M. Chezcau, R. Wey, *ACS Symp. Ser.* **398** (1989) **176**.
- [68] J.P. Arhancet, M.E. Davis, *Chem Mater.* **3** (1991) **567**.
- [69] M.W. Anderson, K.S. Pachis, F. Prébin, S.W. Carr, O. Terasaki, T. Ohsuna, V. Alfreddson, *J. Chem. Soc., Chem. Commun.* (1991) **1660**.
- [70] S. Liu, L. Li, C. Li, X. Xiong, F.-S. Xiao, *J. Porous Mater.* **15** (2008) **295**.
- [71] S.L. Lawton, W.J. Rohrbaugh, *Science* **247** (1990) **1319**.
- [72] S.B. Hong, H.M. Cho, M.E. Davis, *J. Phys. Chem.* **97** (1993) **1622**.
- [73] Y. Han, Y. Li, J. Yu, R. Xu, *Angew. Chem. Int. Ed.* **50** (2011) **3003**.
- [74] E. Galli, G. Vezzalini, S. Quartieri, A. Alberti, M. Franzini, *Zeolites* **19** (1997) **318**.
- [75] G.T. Kokotailo, S.L. Lawton, D.H. Olson, W.M. Meier, *Nature* **272** (1978) **437**.
- [76] L.W. Beck, M.E. Davis, *Microporous Mesoporous Mater.* **22** (1998) **107**.
- [77] W.W. Kaeding, G.C. Barile, M.M. Wu, *Catal. Rev: Sci. Eng.* **26** (1984) **597**.
- [78] T.-C. Tsai, S.-B. Liu, I. Wang, *Appl. Catal., A* **181** (1999) **355**.
- [79] Y. Chen, W.W. Kaeding, F.G. Dwyer, *J. Am. Chem. Soc.* **101** (1979) **6783**.
- [80] M.A. Snyder, M. Tsapatsis, *Angew. Chem.* **119** (2007) **7704**.
- [81] Ch. Baerlocher, M.W. Meier, *Helv. Chim. Acta* **52** (1969) **1853**.
- [82] D.M. Bibby, M.P. Dale, *Nature* **317** (1985) **157**.
- [83] J. Keijsper, C.J.J. Den Ouden, M.F.M. Post, *Stud. Surf. Sci. Catal.* **49** (1989) **237**.
-

- 
- [84] G. van der Goor, P. Behrens, J. Felsche, *Microporous Mater.* **2** (1994) **501**.
- [85] C.M. Braunbarth, P. Behrens, J. Felsche, G. van der Goor, G. Wildermuth, *Zeolites* **16** (1996) **207**.
- [86] U. Werthmann, B. Marler, H. Gies, *Microporous Mesoporous Mater.* **39** (2000) **549**.
- [87] X. Xu, Y. Bao, C. Song, W. Yang, J. Liu, L. Lin, *Microporous Mesoporous Mater.* **75** (2004) **173**.
- [88] S.-R. Lee, Y.-H. Son, A. Julbe, J.-H. Choy, *Thin Solid Films* **495** (2006) **92**.
- [89] A. van Niekerk, J. Zah, J.C. Breytenbach, H.M. Krieg, *J. Membr. Sci.* **300** (2007) **156**.
- [90] S. Khajavi, J.C. Jansen, F. Kapteijn, *J. Membr. Sci.* **326** (2009) **153**.
- [91] A.W.C. van der Berg, S.T. Bromley, J.C. Wojdel, J.C. Jansen, *Microporous Mesoporous Mater.* **87** (2006) **235**.
- [92] W.J. Koros, Y.H. Ma, T. Shimidzu, *Pure & Appl. Chem.* **68** (1996) **1479**.
- [93] D.R. Paul, D.R. Kemp, *J. Polym. Sci.: Symposium* **41** (1973) **79**.
- [94] D.R. Kemp, D.R. Paul, *J. Polym. Sci., Part B: Polym. Phys.* **12** (1974) **485**.
- [95] M.W. Anderson, K.S. Pachis, J. Shi, S.W. Carr, *J. Mater. Chem.* **2** (1992) **255**.
- [96] R. Mahajan, R. Burns, M. Schaeffer, W.J. Koros, *J. Appl. Polym. Sci.* **86** (2002) **881**.
- [97] S. Husain, W. Koros, *J. Membr. Sci.* **288** (2007) **195**.
- [98] H. Lee, P.K. Dutta, *Microporous Mesoporous Mater.* **38** (2000) **151**.
- [99] V. Tricoli, J. Sefcik, A.V. McCormick, *Langmuir* **13** (1997) **4193**.
- [100] Y. Kiyozumi, F. Mizukami, K. Maeda, M. Toba, S. Niwa, *Adv. Mater.* **8** (1996) **517**.
- [101] E.E. McLeary, J.C. Jansen, F. Kapteijn, *Microporous Mesoporous Mater.* **90** (2006) **198**.
- [102] Y.S. Lin, I. Kumakiri, B.N. Nair, H. Alsyouri, *Sep. Purif Methods* **31** (2002) **379**.
- [103] W.J.W. Bakker, F. Kapteijn, J. Poppe, J.A. Moulijn, *J. Membr. Sci.* **117** (1996) **57**.
- [104] A. Bai, M.-D. Jia, L. Falconer, R.D. Noble, *J. Membr. Sci.* **105** (1995) **79**.
- [105] Z.A.E.P. Vroon, K. Keizer, H. Verwij, A.J. Burggraaf, *J. Membr. Sci.* **113** (1996) **293**.
-

- 
- [106] M. Noack, P. Kölsch, J. Caro, M. Schneider, P. Toussaint, I. Sieber, *Microporous Mesoporous Mater.* **35-36** (2000) **253**.
- [107] Y. Morigami, M. Kondo, J. Abe, H. Kita, K. Okamoto, *Sep. Purif. Technol.* **25** (2001) **251**.
- [108] J. Gascon, F. Kapteijn, B. Zornoza, V. Sebastián, C. Casado, J. Coronas, *Chem. Mater.* **24** (2012) **2829**.
- [109] S. Yamazaki, K. Tsutsumi, *Microporous Mater.* **5** (1995) **245**.
- [110] J. Dong, K. Wagner, Y.S. Lin, *J. Membr. Sci.* **148** (1998) **233**.
- [111] J.C. Jansen, G.M. van Rosmalen, *J. Cryst. Growth* **128** (1993) **1150**.
- [112] J. Dong, Y.S. Lin, *Ind. Eng. Chem. Res.* **37** (1998) **2404**.
- [113] S. Yamazaki, K. Tsutsumi, *Microporous Mater.* **4** (1995) **205**.
- [114] A.W.C. van der Berg, L. Gora, J.C. Jansen, T. Maschmeyer, *Microporous Mesoporous Mater.* **66** (2003) **303**.
- [115] A.W.C. van der Berg, L. Gora, J.C. Jansen, M. Makkee, T. Maschmeyer, *J. Membr. Sci.* **224** (2003) **29**.
- [116] M. Pan, Y.S. Lin, *Microporous Mesoporous Mater.* **43** (2001) **319**.
- [117] G. Xomeritakis, A. Gouzinis, S. Nair, T. Okubo, M. He, R.M. Overney, M. Tsapatsis, *Chem. Eng. Sci.* **54** (1999) **3521**.
- [118] K. Kusakabe, T. Kuroda, A. Murata, S. Morooka, *Ind. Eng. Chem. Res.* **36** (1997) **649**.
- [119] I. Kumakiri, T. Yamaguchi, S. Nakao, *Ind. Eng. Chem. Res.* **38** (1999) **4682**.
- [120] M.P. Bernal, G. Xomeritakis, M. Tsapatsis, *Catal. Today* **67** (2001) **101**.
- [121] L.C. Boudreau, M. Tsapatsis, *Chem. Mater.* **9** (1997) **1705**.
- [122] A.-J. Bons, P.D. Bons, *Microporous Mesoporous Mater.* **62** (2003) **9**.
- [123] A. Gouzinis, M. Tsapatsis, *Chem Mater.* **10** (1998) **2497**.
- [124] L.C. Boudreau, J.A. Kuck, M. Tsapatsis, *J. Membr. Sci.* **152** (1999) **41**.
- [125] G.S. Lee, Y.-J. Lee, K.B. Yoon, *J. Am. Chem. Soc.* **123** (2001) **9769**.
- [126] K. Ha, Y.-J. Lee, H.J. Lee, K.B. Yoon, *Adv. Mater.* **12** (2000) **1114**.
- [127] V. Varela-Guerrero, Y. Yoo, M.C. McCarthy, H.-K. Jeong, *J. Mater. Chem.* **20** (2010) **3938**.
- [128] Y. Liu, Z. Ng, E.A. Khan, H.-K. Jeong, C.-B. Ching, Z. Lai, *Microporous Mesoporous Mater.* **118** (2009) **296**.
- [129] Y. Yoo, Z. Lai, H.-K. Jeong, *Microporous Mesoporous Mater.* **123** (2009) **100**.
- [130] Y. Liu, E. Hu, E.A. Khan, Z. Lai, *J. Membr. Sci.* **353** (2010) **36**.
-

- [131] Y. Yoo, V. Varela-Guerrero, H.-K. Jeong, *Langmuir* **27** (2011) **2652**.
- [132] S. Bertazzo, K. Rezwan, *Langmuir* **26** (2010) **3364**.
- [133] S. Aguado, J. Canivent, D. Farrusseng, *Chem. Commun.* **46** (2010) **7999**.
- [134] H. Bux, F. Liang, Y. Li, J. Cravillon, M. Wiebcke, J. Caro, *J. Am. Chem. Soc.* **131** (2009) **16000**.
- [135] A. Huang, H. Bux, F. Steinbach, J. Caro, *Angew. Chem. Int. Ed.* **49** (2010) **4958**.
- [136] A. Huang, W. Dou, J. Caro, *J. Am. Chem. Soc.* **132** (2010) **15562**.
- [137] M.C. McCarthy, V. Varela-Guerrero, G.V. Barnett, H.-K. Jeong, *Langmuir* **26** (2010) **14636**.
- [138] X. Zou, G. Zhu, I.J. Hewitt, F. Sun, S. Qui, *Dalton Trans.* (2009) **3009**.
- [139] H. Guo, G. Zhu, I.J. Hewitt, S. Qui, *J. Am. Chem. Soc.* **131** (2009) **1646**.
- [140] S.R. Venna, M.A. Carreon, *J. Am. Chem. Soc.* **132** (2010) **76**.
- [141] R. Ranjan, M. Tsapatsis, *Chem. Mater.* **21** (2009) **4920**.
- [142] Y.-S. Li, F.-Y. Liang, H. Bux, A. Feldhoff, W.-S. Yang, J. Caro, *Angew. Chem. Int. Ed.* **49** (2010) **548**.
- [143] H. Bux, A. Feldhoff, J. Cravillon, M. Wiebcke, Y.-S. Li, J. Caro, *Chem. Mater.* **23** (2011) **2262**.
- [144] Y. Hu, X. Dong, J. Nan, W. Jin, X. Ren, N. Xu, Y.M. Lee, *Chem. Commun.* **47** (2011) **737**.
- [145] Y. Yoo, H.-K. Jeong, *Chem. Commun.* (2008) **2441**.
- [146] Y. Li, F. Liang, H. Bux, W. Yang, J. Caro, *J. Membr. Sci.* **354** (2010) **48**.
- [147] Y. Pan, Z. Lai, *Chem. Commun.* **47** (2011) **10275**.
- [148] J. Nan, X. Dong, W. Wang, W. Jin, N. Xu, *Langmuir* **27** (2011) **4309**.
- [149] Q. Yang, A.D. Wiersum, H. Jobic, V. Guillerm, C. Serre, P.L. Llewellyn, G. Maurin, *J. Phys. Chem. C* **115** (2011) **13768**.
- [150] Q. Yang, A.D. Wiersum, P.L. Llewellyn, V. Guillerm, C. Serre, G. Maurin, *Chem. Commun.* **47** (2011) **9603**.
- [151] O.G. Nik, X.Y. Chen, S. Kaliaguine, *J. Membr. Sci.* **413-414** (2012) **48**.
-



### 3 Results and Discussion

#### 3.1 Preparation of Silica-Sodalite Layers on Top of Asymmetric $\alpha$ -Alumina Supports and on Silicalite-1 Membranes

##### *Preface*

This section deals with the synthesis of silica sodalite membranes. Because of its narrow pore size, sodalite membranes are of interest in the separation of small gases especially hydrogen. Membranes were produced on asymmetric  $\alpha$ -alumina supports by using a two step synthesis consisting of a seeding step by electrostatic adhesion of sodalite nanocrystals and a secondary growth process. The main difficulty in obtaining template free sodalite layers is the calcination process that requires high temperatures of 1000 °C to fully empty the narrow pores. These harsh conditions result in the formation of cracks in the sodalite layer, which of course makes them unusable as membranes. The cracks probably occur because of a mismatch in the thermal expansion between the support material and the active layer. We have tried to overcome these problems by introducing a layer of a more robust and larger pore zeolite in between the alumina and the sodalite to hopefully act as a mediator between the two materials. For that purpose we have chosen silicalite-1.

This section will be submitted as an original research article. The authors are Imke Bremer, Simon Münzer, Helge Bux, Jürgen Caro and Peter Behrens. Dr. S. Münzer synthesized and analyzed the SOD nanocrystals as well as the ET-SOD layers. Dr. H. Bux from the workgroup of Prof. Dr. J. Caro of the Institute of Physical Chemistry and Electrochemistry of the Leibniz University Hannover performed the single gas permeation measurements.

---





## Preparation of Silica-Sodalite Layers on Top of Asymmetric $\alpha$ -Alumina Supports and on Silicalite-1 Membranes

Imke Bremer,<sup>1</sup> Simon Muenzer,<sup>1</sup> Helge Bux,<sup>2</sup> Juergen Caro,<sup>2</sup> and Peter Behrens<sup>1</sup>

<sup>1</sup> Institute of Inorganic Chemistry, Leibniz University Hannover, Callinstr. 9, 30167 Hannover

<sup>2</sup> Institute of Physical Chemistry and Electrochemistry, Leibniz University Hannover, Callinstr. 3A, 30167 Hannover

### Abstract

The preparation of purely silicious sodalite membranes on asymmetric  $\alpha$ -alumina support discs using a two-step crystallization was investigated. Severe cracks occurred in these layers during the calcination process possibly due to a mismatch in the thermal expansion coefficients of the support and the sodalite. We tried to solve these problems by introducing a layer of another zeolite between the support and sodalite. For that purpose silicalite-1 was chosen. Therefore TPA-MFI membranes with a thickness of approx. 2.5  $\mu\text{m}$  were prepared and characterized. On top of these sodalite layers were successfully synthesized using a seeded synthesis with a “dropping and brushing” seeding procedure. Although the additional zeolite layer did not solve the problems we were facing in the calcination step, this work is a good example for a fabrication of multi-zeolite layers which could serve in possible application as for example combined shape-selective and catalyzing membranes.

### Keywords

silicalite-1 membrane – sodalite membrane – double zeolite layer – seeded synthesis

### Introduction

A relatively modern method for the separation of mixtures of materials in a continuous way lies in the use of supported molecular sieving membranes in which zeolites form the active separation layer in the form of a thin layer on top of a meso- or macroporous substrate. Separation processes like distillation, crystallization etc. can be replaced by separation via zeolite membranes which feature lower energy consumption among other advantages. Because of their

---

defined pore sizes and their excellent thermal and chemical stability inorganic microporous materials possess significant advantages in technical separation processes over other materials like organic polymers.

The ongoing interest in this area of research is reflected in the increasing number of publications. First industrial applications of a zeolite-A membrane are realized in the dehydration of ethanol and isopropanol.<sup>[1]</sup> Other zeolite membranes of the structure types of FAU,<sup>[2-9]</sup> MOR,<sup>[10-14]</sup> FER,<sup>[15-16]</sup> AFI,<sup>[17-20]</sup> SOD,<sup>[21-27]</sup> and the most often prepared MFI<sup>[28-32]</sup> are currently being prepared in laboratory scale and analyzed and optimized in respect to their separation properties.

Acting on the assumption of a selective separation caused by sieving effects, separation of small atoms and molecules like He, H<sub>2</sub>O, NH<sub>3</sub> and H<sub>2</sub> ( $\varnothing$  2.6 – 2.9 Å) from gas mixtures with molecules that possess a kinetic diameter in the range of 3.0 – 3.8 Å (N<sub>2</sub>, O<sub>2</sub>, CO, CO<sub>2</sub>, H<sub>2</sub>S, n-alkenes) is possible only with membranes made from zeolites that have pore openings smaller than eight-ring windows. In this regard the hydrogen separation in dehydrogenation reactions is of special interest. For example the dehydrogenation of propane or butane is run equilibrium controlled under industrial conditions. By removing the formed hydrogen the conversion degree can be increased significantly.<sup>[33-35]</sup> Sodalite possesses six membered rings as pore opening windows with a dynamic diameter of approx. 2.8 Å and would therefore meet the requirements for such separations. Purely siliceous materials are of special interest for membrane applications. Because of their uncharged network no ionic interactions can occur between the membrane materials and the separated substances. Purely siliceous sodalite can only be synthesized with the use of structure directing agents (SDAs). In contrast to channel-like structures of zeolites with larger pores like MFI, LTA, or FAU diffusion processes in the narrow pored cage-like sodalite structure are strongly hindered, which makes the removing of the SDAs demanding both in time and temperature. For that reason only aluminosilicate sodalite membranes were synthesized in the past, which can be produced without any further template when using high sodium concentrations.<sup>[21-27]</sup> These alkali ions are situated in the sodalite cages for charge equalization and are inhibiting helium from entering the pores. Because of this pore blocking effect and the fact that phases other than sodalite often occur when trying to produce aluminosilicate sodalite membranes<sup>[22-25]</sup> it would be better to use organic templates to synthesize a siliceous sodalite membrane. Here we report of such syntheses of silica-sodalite layers on asymmetric alumina support discs by a two step crystallization (seeding of nanocrystals onto the support and second crystallization), the problems we were facing when trying to calcine these and the attempt to overcome the problems in calcination by introducing a layer of silicalite-1 (MFI) between the alumina support and the sodalite layer.

---

## Experimental

### *Preparation of alumina supported silica-sodalite membranes*

For seeding of the asymmetric  $\alpha$ -Al<sub>2</sub>O<sub>3</sub> support discs (18 x 1 mm, Inocermic, Germany) aluminosilica sodalite nanoparticles prepared with tetramethylammonium hydroxide as SDA (TMA-AlSi-SOD) with a diameter of 20 – 50 nm were used. TMA-AlSi-SOD particles were prepared according to a method previously published by us.<sup>[36]</sup> Seeding was realized by electrostatic adhesion. For that purpose a 2.5 wt % suspension of the nanoparticles in 0.1 M ammonia was prepared. The pH value was adjusted to 6.5 by addition of 0.1 M hydrochloric acid. The alumina disc was then immersed into this suspension for 5 min, rinsed thoroughly with deionized water and dried under reduced pressure.

Synthesis solution for the second crystallization of silica sodalite was prepared by mixing water, ethylamine (ET, purum, 70 % in H<sub>2</sub>O, Fluka) and fumed silica Cabosil M-5 (Riedel-de Haën) to yield a final gel composition of SiO<sub>2</sub> : 25 ET : 100 H<sub>2</sub>O. Second crystallization took place under hydrothermal conditions. The synthesis gel was filled into a Teflon-lined stainless steel autoclave, the seeded alumina support was placed into the solution at an angle of 75° to avoid sedimentation of particles onto the support. The autoclave was placed into a convection oven at 170 °C for 24 h.

### *Preparation of alumina supported silicalite-1 membranes*

Asymmetric  $\alpha$ -Al<sub>2</sub>O<sub>3</sub> support discs were seeded with silicalite-1 nanoparticles prepared with tetrapropylammonium hydroxide as SDA (TPA-MFI). TPA-MFI nanoparticles were prepared by mixing deionized water, sodium hydroxide (purum, Acros Organics), tetrapropylammonium hydroxide (TPAOH, purum, ca. 20 % in H<sub>2</sub>O, Sigma-Aldrich) and tetraethoxysilane (puriss, Fluka) to result in a composition of 25 SiO<sub>2</sub> : 9 TPAOH : 0.16 NaOH : 495 H<sub>2</sub>O. The synthesis solution was stirred at 80 °C for 96 h to yield particles with a diameter of 80 – 100 nm.<sup>[37]</sup> For seeding a 2.5 wt% suspension of the nano-TPA-MFI in 0.1 M ammonia was dropped onto the alumina disc to form a thin liquid film. The disc was then dried and the excess of particles was brushed off the support (“dropping and brushing” method).

For second crystallization a synthesis solution was prepared by mixing deionized water, tetraethoxysilane (puriss, Fluka) and tetrapropylammonium hydroxide (TPAOH, purum, ca. 20 % in H<sub>2</sub>O, Sigma-Aldrich) to yield a composition of SiO<sub>2</sub> : 0.3 TPAOH : 420 H<sub>2</sub>O.<sup>[38]</sup> A Teflon-lined stainless steel autoclave was filled with the solution, the seeded support was positioned at an angle of 75° in the solution to avoid sedimentation of particles onto the support and the autoclave was placed in a convection oven at 130 °C for 24 h.

---

The template was removed from silicalite-1 membranes by heating up to 350 °C for 6 h before further heating to 450 °C for 6 h with heating rates of 0.3 K min<sup>-1</sup> and a cooling rate of 0.5 K min<sup>-1</sup>.

#### *Preparation of silica-sodalite films on top of silicalite-1 membranes*

Nano-TMA- $\text{AlSi-SOD}$  was seeded onto Silicalite-1 membranes by the previously described “dropping and brushing” method. Second crystallization of silica-sodalite was done according to the synthesis procedure described in section ‘*Preparation of alumina supported silica-sodalite membranes*’.

#### *Methods*

X-ray powder diffraction patterns were collected on a StadiP diffractometer (STOE) using  $\text{Cu K}\alpha_1$  radiation. X-ray diffraction patterns of membranes were collected on a Theta-Theta diffractometer (STOE) using  $\text{Cu K}\alpha_1$  radiation. When applicable, Scherrer’s equation was used to calculate the particle size. A silicon standard was measured under the same conditions to determine the reflection broadening caused by the instrumental setup.

For the collection of SEM images a JEOL JSM-6700F field-emission scanning electron microscope (FE-SEM) was used. The SEM was operated with an acceleration voltage of 2 kV at a working distance of 8 mm using a LEI-detector and 3 mm using a SEI-detector respectively. Nanoscale samples were prepared by suspending the material in ethanol and dropping the suspension on a graphite block. All other samples were prepared by attaching them to a brass holder with an adhesive graphite pad.

Zeta potentials of colloidal suspensions of TMA- $\text{AlSi-SOD}$ , TPA-MFI and  $\alpha\text{-Al}_2\text{O}_3$  were measured at different pH-values using a Malvern Zetasizer Nano ZS to determine the pH-value suitable for electrostatic adhesion of the different materials.

Gas separation properties of the membranes were tested in single gas permeation experiments. For the measurements the coated ceramic discs were mounted in a measuring cell sealed with rubber rings. A gas pressure of 0.5 bar was applied to one side of the membrane and the flow through the layer was measured in volume per time using a bubble counter. From the flow in moles per time ( $D$ ), the permeable area ( $A$ ) and the transmembrane pressure ( $\Delta p$ ) of 0.5 bar the permeances ( $P$ ) for different gases were calculated:  $P_{(\text{gas})} = D / A \cdot \Delta p$ .

## Results and Discussion

### *Alumina supported silica-sodalite layers*

For seeding of the asymmetric  $\text{Al}_2\text{O}_3$  support discs sodalite nanoparticles synthesized with TMAOH as SDA were used. Comparison of the collected powder diffraction pattern (Fig. 1) with the corresponding powder diffraction file (pdf-card [22-1809]) shows that a phase pure sodalite was obtained. The size of the particles can be calculated as approx. 53 nm from the broadening of the reflections using Scherrer's equation. The SEM micrograph of the sample (Fig. 1, inset) reveals a particle size between 30 – 80 nm and a cubic shape which is typical for sodalite crystals. In this size range of particles, stable suspensions can be produced, which is a requirement for the seeding step.

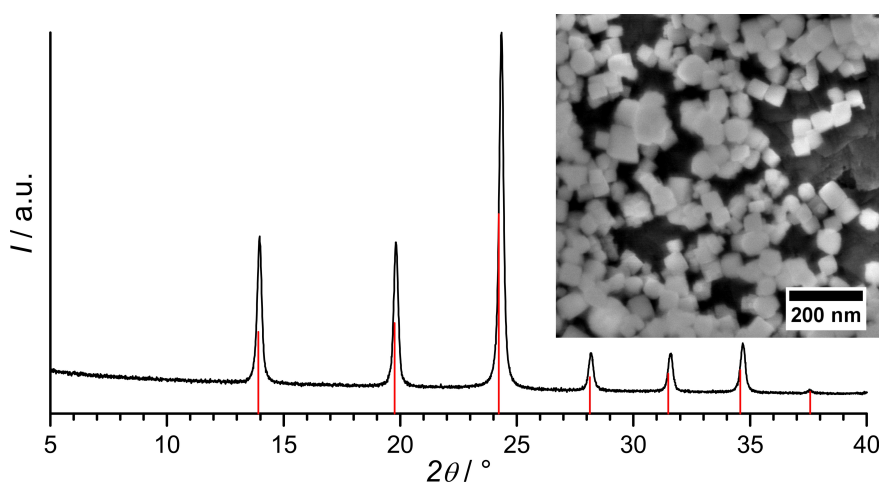


Fig. 1: PXRD pattern of the synthesized TMA-AlSi-SOD nanocrystals with corresponding powder diffraction file (pdf-card [22-1809]) and SEM micrograph of the sample.

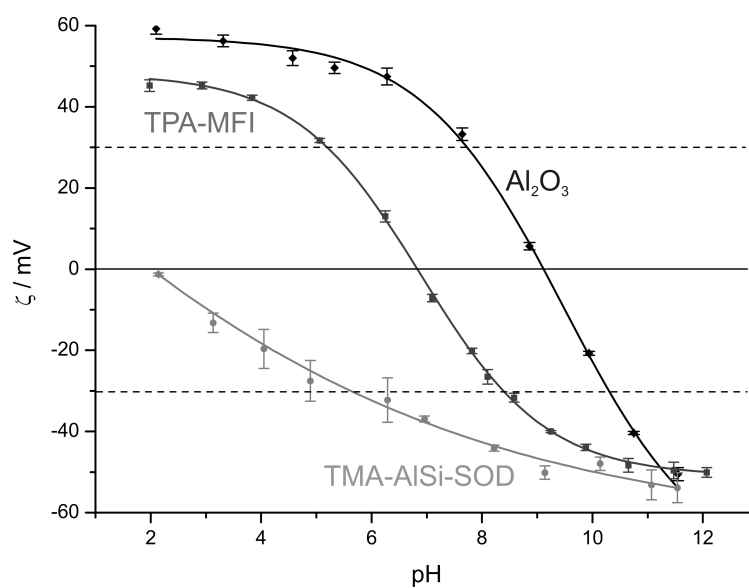


Fig. 2: Zeta potentials of  $\alpha$ -alumina, TMA-AlSi-SOD nanocrystals and TPA-MFI nanocrystals plotted against the pH-value of the suspension.

To determine the pH-value suitable for the seeding of the TMA-AlSi-SOD nanocrystals onto the  $\text{Al}_2\text{O}_3$  support by electrostatic adhesion the zeta-potentials of both materials were measured in a range of pH 2 – 11.5 (Fig. 2). As a rule of thumb a suspension is supposed to be stable if the zeta potential of the dispersed species lies either above +30 mV or below -30 mV and a reasonably strong adhesion between two differently charged species takes place if the zeta potentials differ for at least 60 mV (that is one above +30 mV the other below -30 mV).  $\text{Al}_2\text{O}_3$  and TMA-AlSi-SOD meet these criteria at a pH-value between 5.5 and 8. That is why a pH-value of 6.5 was chosen for the seeding step.

Fig. 3 shows the X-ray diffraction patterns of the membrane support after the seeding and after the second crystallization step in comparison to a pattern of the untreated support and a bulk-sample of sodalite synthesized with ethylamine as SDA (ET-SOD). After the electrostatic adhesion of the TMA-AlSi-SOD nanocrystals reflections of very low intensity are visible which can be attributed to the sodalite-phase. These reflections become much more intense after the second crystallization step, which clearly demonstrates the success of this two-step synthesis procedure. SEM-micrographs of this sample (Fig. 4) reveal that in fact an intergrown layer of cubic sodalite crystals was formed on top of the support. There are no cracks or holes visible in the layer. The cross-section image of the membrane shows a densely intergrown layer with a thickness of 4.5  $\mu\text{m}$ .

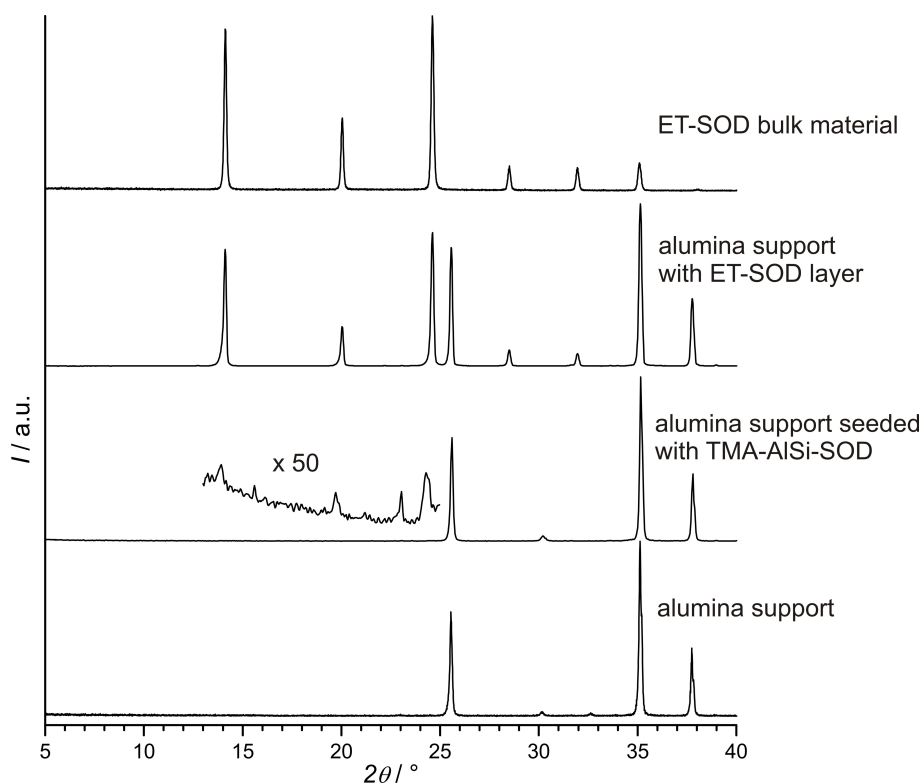


Fig. 3: X-ray diffraction patterns of the  $\alpha$ -alumina support, the support after seeding with TMA-AlSi-SOD nanocrystals, after the hydrothermal crystallization step and of a bulk sample of ET-SOD.

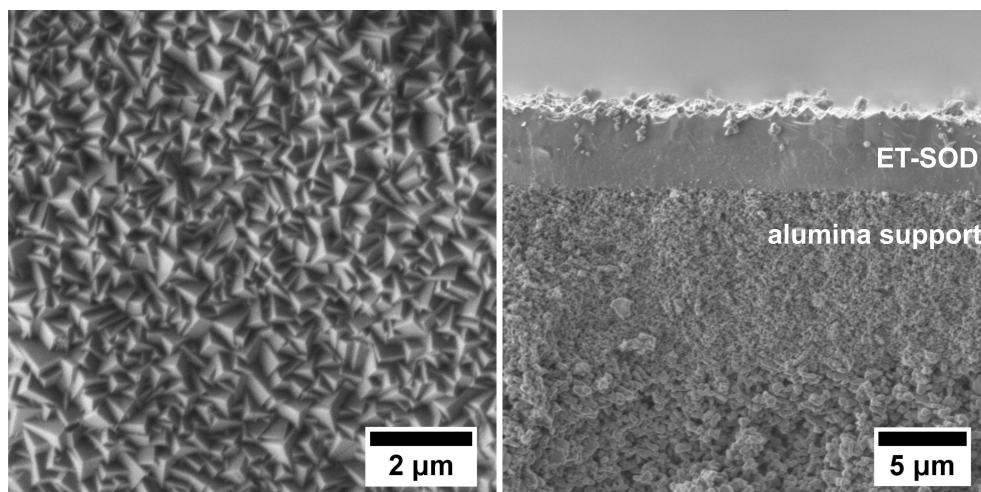


Fig. 4: SEM micrographs of the as-synthesized sodalite layer grown directly on the asymmetric  $\alpha$ -alumina support (left: top view, right: cross section).

To actually use such a layer for separation purposes it is necessary to remove the SDA from the pores of the structure, in this case ethylamine. In the case of sodalite this is a rather demanding task because of the quite small pore opening size of the sodalite-cages of approx. 2.8 Å. Diffusion in these narrow pores is strongly hindered. Oxygen, which is needed for the decomposition of the organic template, as well as decomposition products like CO or CO<sub>2</sub> possess kinetic diameters which are larger than the six-membered ring openings in sodalite materials. A removal of the templates is only possible due to the unusual structural features of sodalite. By a cooperative rotation of the tetrahedra without reconstructive changes in the structure at very high temperatures, which leads to a nearly complete expansion of the SiO<sub>2</sub> framework, the removal of the template is facilitated. Nonetheless the detemplation is often incomplete especially in micrometer-sized crystals caused by the strong influence of the length of diffusion paths. These materials show a coloration ranging from light grey to black. The color indicates the presence of larger defects in the framework in which carbon fragments have accumulated to form coke.

Testings of different calcination techniques with bulk material of ET-SOD have shown that the best results with regard to completeness of detemplation can be achieved with a heating and cooling rate of 2 K min<sup>-1</sup> and a temperature of 1273 K for 48 h. Thereby a white powder was obtained which exhibited split reflection in the powder XRD-pattern. The splitting up of the reflections is caused by a change in the symmetry in the framework material upon removal of the SDA. This calcination program was also used for the template removal from the produced supported silica-sodalite layers. The resulting sample showed a white color. Comparing the diffraction patterns of the SOD-layer before and after the heat-treatment, the described splitting up of the reflections can be observed (Fig. 5).

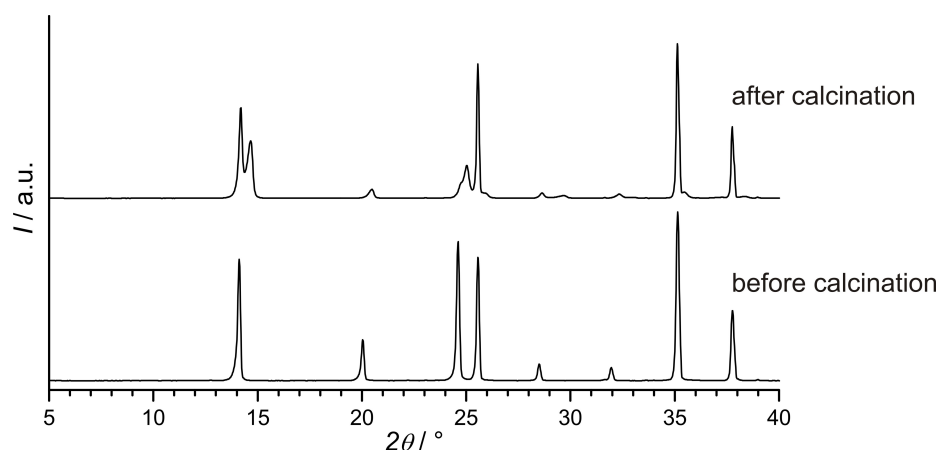


Fig.5: Comparison of the X-ray diffraction patterns of the alumina supported sodalite layer before and after the heat treatment at 1273 K for 48 h (heating and cooling rate of 2 K min<sup>-1</sup>).

Hence it is safe to assume that the removal of the ethylamine was near to complete. Unfortunately severe cracks have occurred in the material which were visible to the naked eye. The sodalite layer has started to fall off of the alumina support after the heat treatment. This can also be observed in the SEM micrographs (Fig. 6). These cracks are possibly caused by a mismatch in the thermal expansion coefficients of the sodalite and the corundum support. We therefore thought about introducing a layer of another zeolitic material between the support and the SOD-layer. The material we chose for this purpose is the silicalite-1 (MFI-topology) for it has a channel-like pore system with larger pore openings and thus its detemplation is much easier. So next silicalite-1 membranes were synthesized and characterized.

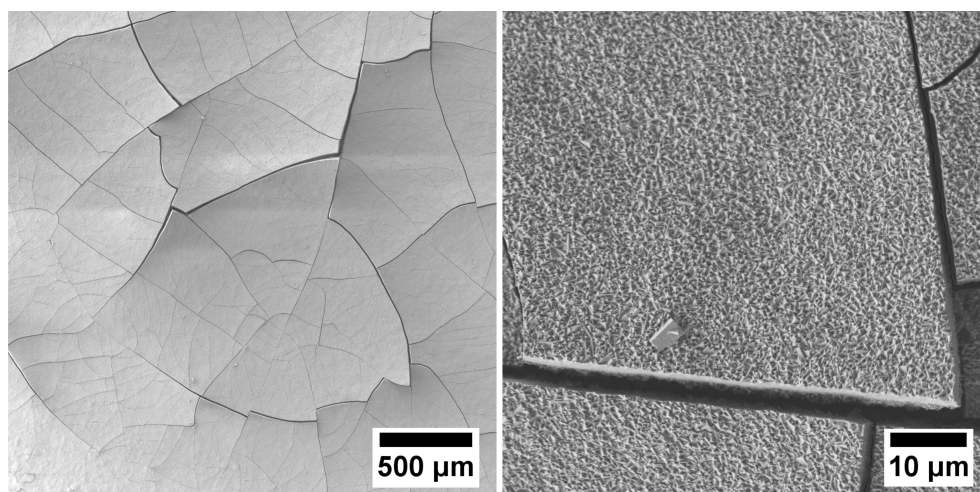


Fig. 6: SEM micrographs of the calcined alumina supported ET-SOD layer (1273 K for 48 h, heating and cooling rate of 2 K min<sup>-1</sup>).



### *Alumina supported silicalite-1 membranes*

The alumina supported silicalite-1 membranes were synthesized by using a two step crystallization consisting of a seeding of nanocrystals and a second crystallization to grow these into dense layers. The nanocrystals as well as the layers were produced with TPAOH as SDA and are of pure siliceous nature. The powder diffraction pattern of the nanoparticles shows a good agreement with the powder diffraction file (pdf card [43-322]) for MFI (Fig. 7). Deviations in the patterns are due to the fact, that the particles are a still templated silicalite-1 while the pdf-card refers to the sodium aluminum silicate with MFI-topology. From the SEM-micrographs (Fig. 7) of the sample the particle size cannot be determined clearly as the ball-shaped particles with a size of approx. 80 – 100 nm seem to consist of even smaller primary particles. Using Scherrer's equation a particle size of 45 nm can be calculated.

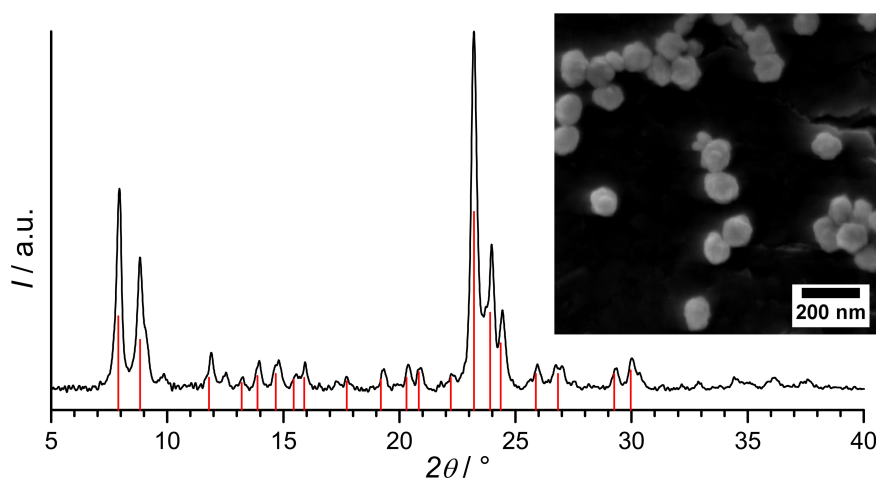


Fig. 7: PXRD pattern of the synthesized TPA-MFI nanocrystals with corresponding powder diffraction file (pdf-card [43-322]) and SEM micrograph of the sample.

Looking at the zeta-potentials of the TPA-MFI in comparison to that of aluminum oxide (Fig. 2) it becomes clear that a seeding by electrostatic adhesion would not work in this case. The curve progressions of the zeta-potentials of the two materials are too similar to lead to an adhesion strong enough. Therefore a different seeding method was chosen in this case. First a stable suspension of the TPA-MFI particles was prepared by dispersing the material in 0.1 M ammonia solution using ultrasound. This suspension was then dropped onto the alumina support to form a preferably thin liquid film. The sample was then dried and the excess of particles was brushed off. The XRD-pattern of the seeded supports in fact shows reflections of quite low intensity that can be assigned to the MFI (Fig. 8), which demonstrates the successful seeding. The support-discs seeded by this “dropping and brushing” method were then incorporated in a hydrothermal second crystallization step. After this step, the typical MFI-reflections can be found in the diffraction pattern. In comparison to the pattern of a bulk-sample it can be noticed that especially the (101), (102) and the (303) reflections show an increased intensity in the pattern of the membrane. Since the pattern was collected

in theta-theta geometry this means that the crystals in the layer have a preferred orientation with the *c*-axis oblique to the surface of the support. This is a well known phenomenon in MFI-layers. The *c*-axis is the fastest growing direction in the TPA-MFI. In the competitive growth-mechanism the seeds exhibiting an oblique orientation can outgrow the seeds showing other orientations in early stages of growth. This orientation can also be observed in the SEM-micrographs of the membrane shown in Fig. 9. The crystals can be found standing on the elongated *c*-axis and in the top-view of the layer the rounded tops of the crystals are pointing towards the observer. The cross-section image shows a columnar, intergrown layer with a thickness of approx. 2.5  $\mu\text{m}$ .

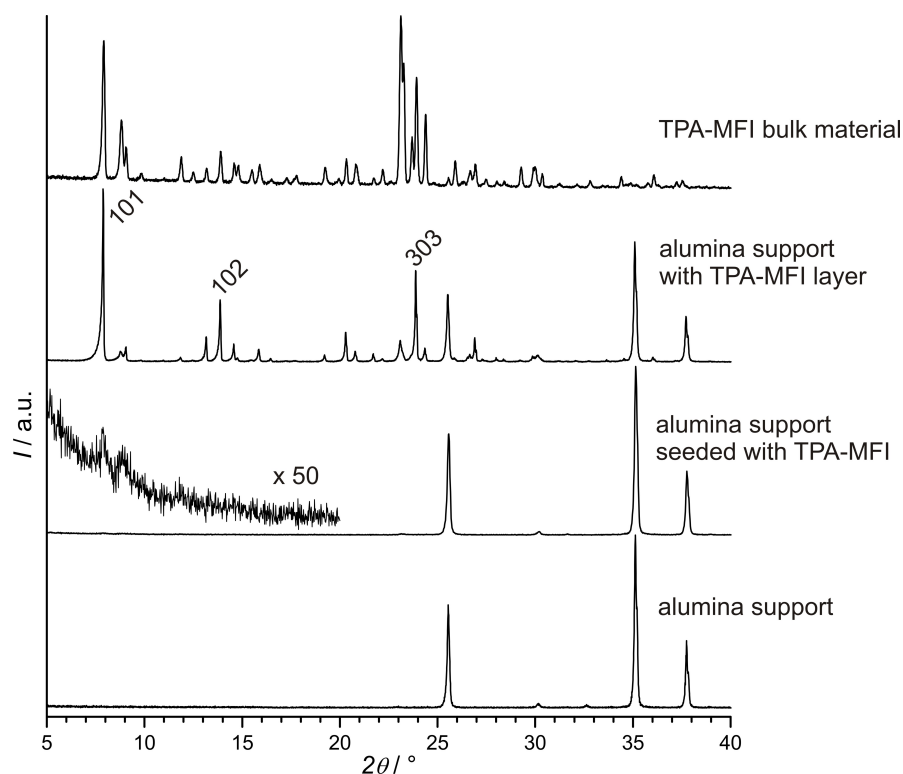


Fig. 8: X-ray diffraction patterns of the  $\alpha$ -alumina support, the support after seeding with TPA-MFI nanocrystals, after the hydrothermal crystallization step and of a bulk sample of TPA-MFI.

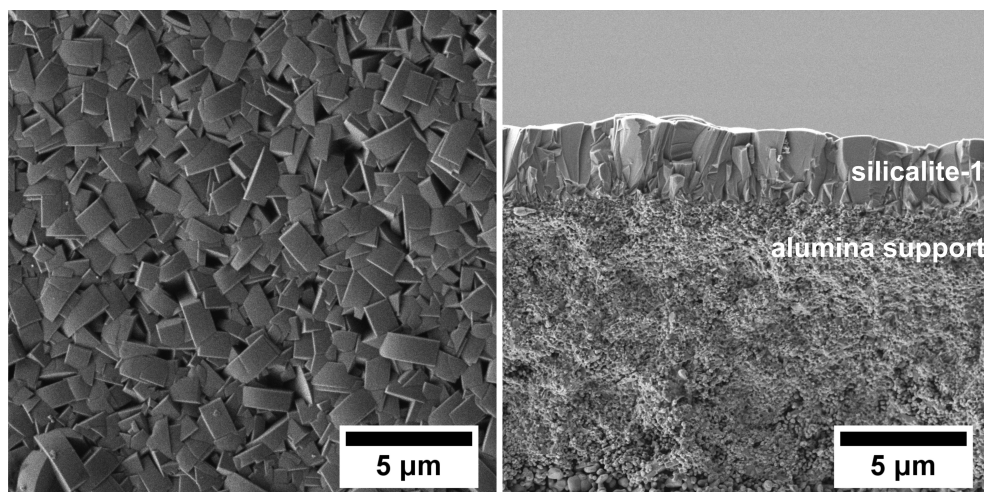


Fig. 9: SEM micrographs of the as-synthesized TPA-MFI membrane on  $\alpha$ -alumina support (left: top view, right: cross section).

To judge the quality of the produced silicalite-1 membranes, single gas permeation measurements were done with  $\text{H}_2$ ,  $\text{CH}_4$ ,  $i\text{-C}_4\text{H}_{10}$  and  $\text{SF}_6$  at room temperature. The permeances ( $P$ ) for gases with small kinetic diameters are high (Fig. 10). For example the permeance of hydrogen reaches  $3.3 \times 10^{-6} \text{ mol m}^{-2} \text{ s}^{-1} \text{ Pa}^{-1}$ . Compared to values found in the literature (see Table 1) the flux found in our membrane is quite high. This is probably caused by the small thickness of the active separation layer of only  $2.5 \mu\text{m}$ . Testing larger gases like  $\text{SF}_6$  with a kinetic diameter  $5.5 \text{ \AA}$ , similar to the diameter of the pores in MFI, the values for the permeance decrease dramatically to  $4.2 \times 10^{-8} \text{ mol m}^{-2} \text{ s}^{-1} \text{ Pa}^{-1}$  (Fig. 10). From the determined single gas permeances the ideal separation factors were calculated as  $\alpha = P_{(\text{gas1})} / P_{(\text{gas2})}$ . When comparing these separation factors to the Knudsen separation factors (Table 1) which can be calculated from the molecular masses as  $\alpha_{(\text{Knudsen})} = (M_{(\text{gas1})}/M_{(\text{gas2})})^{1/2}$  one can notice that the ideal separation factors for  $\text{H}_2 / i\text{-C}_4\text{H}_{10}$  and  $\text{H}_2 / \text{SF}_6$  differ markedly from the Knudsen separation factors. This means that a true molecular sieving effect is taking place in the produced membrane. Despite the relatively high permeances the ideal separation factor for  $\text{H}_2 / \text{SF}_6$  reaches a value of 78.5 which is a reasonably good value considering the small thickness of the separating layer.

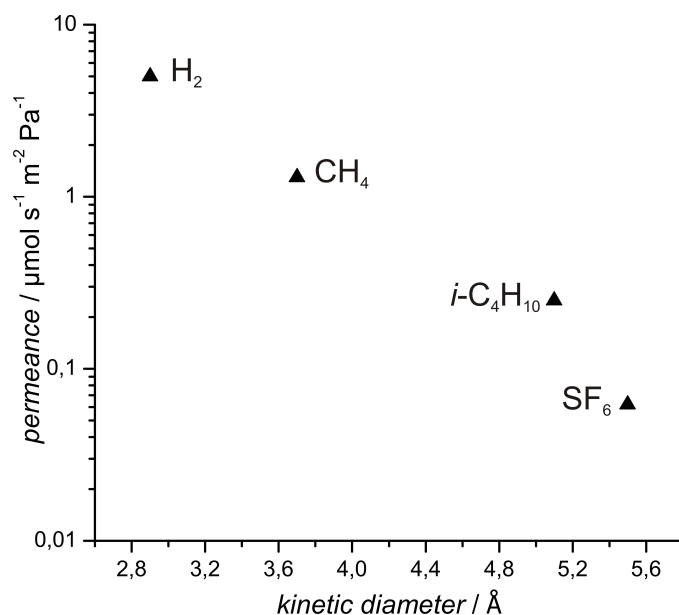


Fig. 10: Single gas permeances of  $H_2$ ,  $CH_4$ ,  $i-C_4H_{10}$  and  $SF_6$  through the silicalite-1 membrane plotted against the kinetic diameters of the gas molecules.

Table 1: Comparison of single gas permeances ( $P$ ) and ideal separation factors ( $\alpha$ ) for different MFI membranes reported in literature.

Support	d ( $\mu\text{m}$ )	P ( $10^{-7} \text{ mol m}^{-2} \text{ s}^{-1} \text{ Pa}^{-1}$ )			$\alpha$		T (K)	Ref.
		$H_2$	$i-C_4H_{10}$	$SF_6$	$H_2 / i-C_4H_{10}$	$H_2 / SF_6$		
$\alpha\text{-Al}_2\text{O}_3$	2.5	33	1.6	0.42	20.6	78.5	298	this work
$\alpha\text{-Al}_2\text{O}_3$	6-8	16.4	0.63	0.23	25.86	71.14	298	[39]
$\alpha\text{-Al}_2\text{O}_3$	15	0.39	-	0.0072	-	54.63	298	[39]
$\gamma\text{-Al}_2\text{O}_3$	5	0.34	-	0.0025	-	136	298	[40]
$\alpha\text{-Al}_2\text{O}_3$	0.5	219	-	13	-	17	298	[29]
$\alpha\text{-Al}_2\text{O}_3$	-	16	1.8	0.24	8.9	67	295	[41]
					4.9	8.3		Knudsen diffusion

### Sodalite layers on top of silicalite-1 membranes

The sodalite layers on top of the described silicalite-1 membranes were prepared by a two step crystallization as well. It was also tried to directly grow a sodalite film on top of the silicalite-1, but without an additional seeding step no crystallization was observed. Very much like the seeding step in the preparation of the silicalite-1 membrane on  $\alpha$ -alumina supports, a seeding by electrostatic adhesion was not possible due to the similar zeta potentials of TPA-MFI and TMA-AlSi-SOD (Fig. 2). So again the “dropping and brushing” method was used on the calcined silicalite-1 membranes with a suspension of the TMA-AlSi-SOD nanocrystals. In the diffraction pattern recorded of the seeded silicalite-1 membrane (Fig.11) there are no visible reflections that could be attributed to the TMA-AlSi-SOD phase. The intensities of these reflections would probably be so low

that they are not noticeable with all the reflections of the silicalite-1 present in the diffraction pattern. After the hydrothermal second crystallization step on the other hand additional reflections of the ET-SOD phase emerge (Fig.11). Since this does not happen when no seeding step is applied it can be stated that the seeding must have been successful.

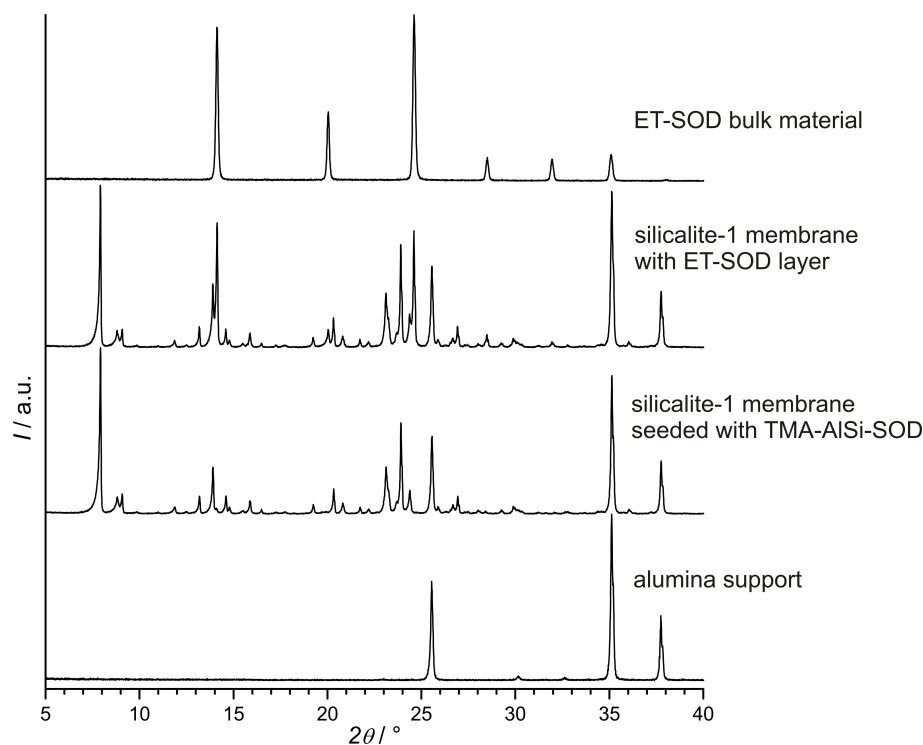


Fig. 11: X-ray diffraction patterns of the  $\alpha$ -alumina support, the supported silicalite-1 membrane after seeding with TMA-AlSi-SOD nanocrystals, after the hydrothermal crystallization step of ET-SOD and of a bulk sample of ET-SOD.

The SEM micrographs recorded after the coating with ET-SOD (Fig.12) show that the surface is covered with cubic sodalite crystals. In the cross-section image two different layers are visible on the  $\alpha$ -alumina support. The first layer is the silicalite-1 membrane and the layer on top corresponds to sodalite. Both layers exhibit a similar thickness of approx. 2.5  $\mu\text{m}$ . Although the same reaction conditions were chosen for the syntheses of ET-SOD on silicalite-1 and directly on  $\alpha$ -alumina, the film thickness is not the same for both cases. This might be due to the different seeding techniques used. When the TMA-AlSi-SOD nanocrystals are attached directly to the ceramic support by electrostatic adhesion, the final membrane has a thickness of 4.5  $\mu\text{m}$  while the layer grown on silicalite-1 after seeding by “dropping and brushing” is 2  $\mu\text{m}$  thinner.

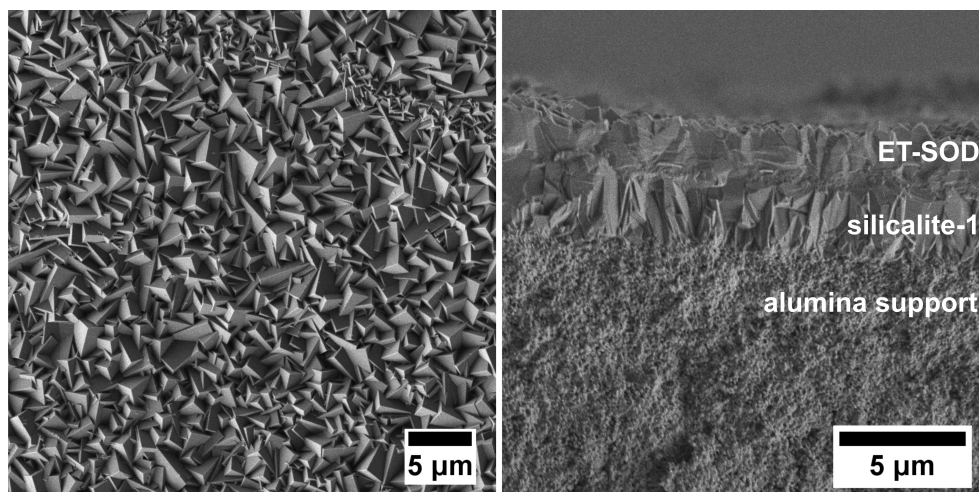


Fig. 12: SEM micrographs of the as-synthesized ET-SOD layer on top of the silicalite-1 membrane on  $\alpha$ -alumina support (left: top view, right: cross section).

For the calcination of the sodalite layer in the two-layered membranes different conditions were used. At first the same calcination method as for the sodalite layers on alumina was used (calcination at 1273 K for 48 h with a heating and cooling rate of 2 K min<sup>-1</sup>). The diffraction pattern (Fig. 13) demonstrates that the template removal was successful since the reflections of the SOD are split up after the heat treatment. Moreover the pattern shows that the silicalite-1 has survived these harsh calcination conditions unchanged. A photograph of the calcined membrane is shown in Fig. 14 a. Unfortunately the zeolitic layer is heavily damaged and is even falling off of the support. That is why other calcination temperatures and heating rates were tried to see if the procedure can be optimized in such a way, that a detemplated and intact membrane can be obtained. Reducing the heating rate from 2 K min<sup>-1</sup> to 0.5 K min<sup>-1</sup> and the time at 1273 K from 48 h to 24 h resulted in a layer with less cracks than the one described before, but still quite large gaps of several μm are visible in the SEM micrographs (Fig.14 c, d). In another attempt the same calcination process as for the silicalite-1 was used. That is a heating to 623 K for 6 h and another heating step to 723 K for another 6 h with a heating rate of 0.3 K min<sup>-1</sup>. XRD measurements of these samples showed that the template cannot be removed from the sodalite at such low temperatures. A repetition of this heating program showed no improvement of that fact. The best results could be achieved with a heating rate of 0.5 K min<sup>-1</sup> and a reduction of the temperature to 1073 K for only 12 h. In that case the diffraction pattern showed the typical split up reflections which indicate the successful removal of the SDA, but cracks are still visible in the SEM image (Fig. 14 b) even though the cracks are smaller than in all other attempts.

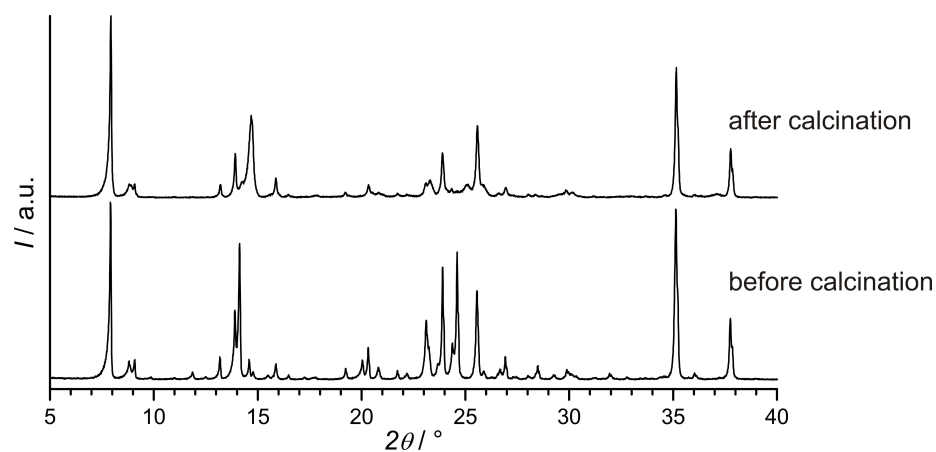


Fig. 13: Comparison of the X-ray diffraction patterns of the alumina supported silicalite-1 sodalite double-layer before and after the heat treatment at 1273 K for 48 h (heating and cooling rate of 2 K  $\text{min}^{-1}$ ).

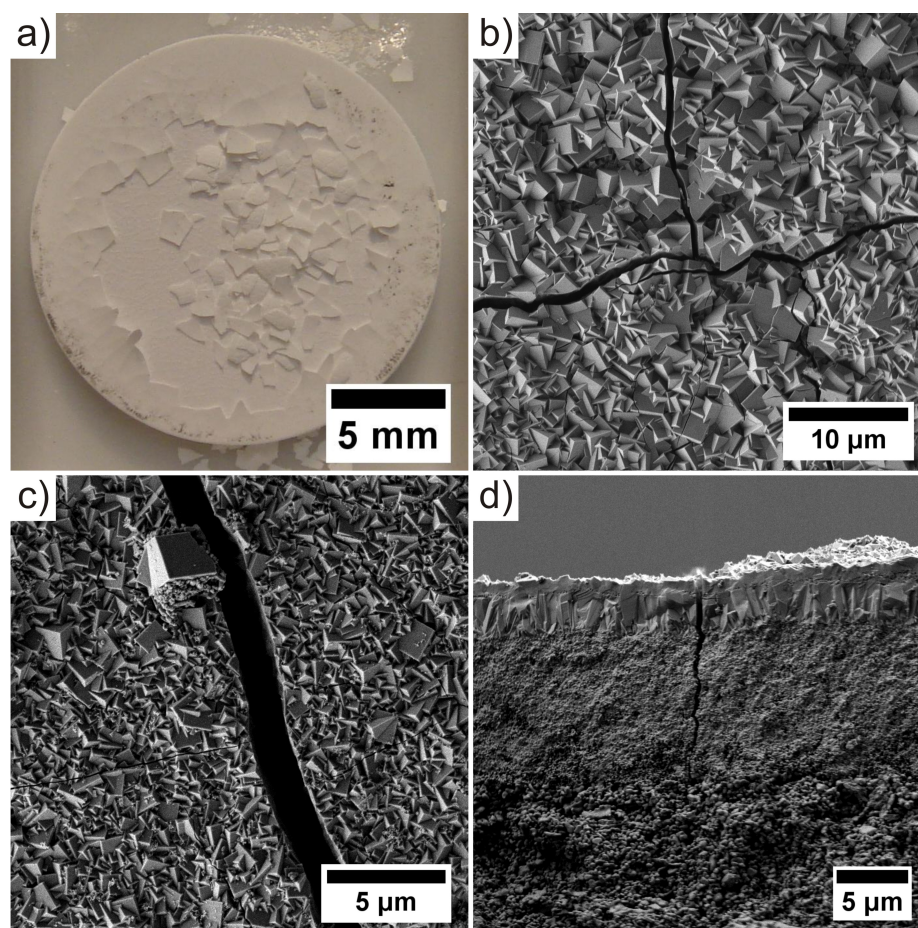


Fig. 14: Pictures of alumina supported silicalite-1 sodalite double-layers after different calcination processes (a: photograph of a sample heated to 1273 K for 48 h with 2 K  $\text{min}^{-1}$ , b: SEM micrograph of a sample heated to 1073 K for 12 h with 0.5 K  $\text{min}^{-1}$ , c (top view) and d (cross section): SEM micrographs of a sample heated to 1273 K for 24 h with 0.5 K  $\text{min}^{-1}$ ).

## Summary

Our ambitions in producing a purely siliceous sodalite membrane for a possible use in the separation of small molecules like hydrogen failed for the calcination of the sodalite needs very high temperatures. At these temperatures of at least 1023 K the thermal expansion in the materials leads to the formation of cracks in the zeolite layer. The attempt to overcome these problems by adding a layer of silicalite-1 between the support and the sodalite did not bring the improvement in the calcination step that we hoped for. Various temperature profiles were tried for the calcination of the two layered membrane. Either the template was not removed at low temperatures or cracks appeared in the layer at high temperatures. Although it was not our primary goal, we were able to produce silicalite-1 membranes with a quite small thickness that shows good ideal separation factors that differ significantly from the Knudsen separation factors.

We could also show that it is possible to synthesize multilayers of different zeolites on porous ceramic substrates by using seeded synthesis. The seeding step can be done in an easy and quick way by the described “dropping and brushing” method. This could be an interesting approach for other combinations of different zeolites. It might be possible to build up a multilayer system in which the first layer might serve as a size selective membrane whereas the second layer could be a catalyzing one.

## References

- [1] J. Caro, M. Noack, *Microporous Mesoporous Mater.* **115** (2008) **215**.
  - [2] K. Kusakabe, T. Kuroda, A. Murata, S. Morooka, *Ind. Eng. Chem. Res.* **36** (1997) **649**.
  - [3] K. Kusakabe, T. Kuroda, K. Uchino, Y. Hasegawa, S. Morooka, *AIChE J.* **45** (1999) **1220**.
  - [4] H. Kita, T. Inoue, H. Asamura, K. Tanaka, K. Okamoto, *Chem. Commun.* (1997) **45**.
  - [5] M. Lassinantti, J. Hedlund, J. Sterte, *Microporous Mesoporous Mater.* **38** (2000) **25**.
  - [6] V. Nikolakis, G. Xomeritakis, A. Abibi, M. Dickson, M. Tsapatsis, D. G. Vlachos, *J. Membr. Sci.* **184** (2001) **209**.
  - [7] M.A. Salomón, J. Coronas, M. Menendez, J. Santamaria, *Chem. Commun.* (1998) **125**.
  - [8] Y. Kim, P.K. Dutta, *Res. Chem. Intermed.* **30** (2004) **147**.
-



- [9] Y. Lee, P.K. Dutta, *J. Phys. Chem. B* **106** (2002) **898**.
- [10] M.A. Salomón, J. Coronas, M. Menendez, J. Santamaria, *Chem. Commun.* (1998) **125**.
- [11] E. Piera, M.A. Salomón, J. Coronas, M. Menendez, J. Santamaria, *J. Membr. Sci.* **149** (1998) **99**.
- [12] X. Lin, E. Kikuchi, M. Matsukata, *Chem. Commun.* (2000) **957**.
- [13] A. Tavoraro, A. Julbe, C. Guizard, A. Basile, L. Cot, E. Drioli, *J. Mater. Chem.* **10** (2000) **1131**.
- [14] S. Yamazaki, K. Tsutsumi, *Microporous Mater.* **5** (1995) **245**.
- [15] N. Nishiyama, T. Matsufuji, K. Ueyama, M. Matsukata, *Microporous Mater.* **12** (1997) **293**.
- [16] T. Matsufuji, S. Nakagawa, N. Nishiyama, M. Matsukata, K. Ueyama, *Microporous Mesoporous Mater.* **38** (2000) **43**.
- [17] H. Lee, P.K. Dutta, *Microporous Mesoporous Mater.* **38** (2000) **151**.
- [18] J.C. Poshusta, V.A. Tuan, J.L. Falconer, R.D. Noble, *Ind. Eng. Chem. Res.* **37** (1998) **3924**.
- [19] L.X. Zhang, M.D. Jia, E.Z. Min, *Prog. Zeolite Microporous Mater. Proc. Int. Zeolite Conf. 11th*, 1996, Part A–C **105** (1997) **2211**.
- [20] J.C. Lin, M.Z. Yates, *Chem. Mater.* **18** (2006) **4137**.
- [21] M. Kazemimoghadam, T. Mohammadi, *Desalination* **181** (2005) **1**.
- [22] A. Julbe, J. Motuzas, F. Cazevielle, G. Volle, C. Guizard, *Sep. Purif. Technol.* **32** (2003) **139**.
- [23] S.-R. Lee, Y.-H. Son, A. Julbe, J.-H. Choy, *Thin Solid Films* **495** (2006) **92**.
- [24] X. Xu, Y. Bao, C. Song, W. Yang, J. Liu, L. Lin, *Microporous Mesoporous Mater.* **75** (2004) **173**.
- [25] A. van Niekerk, J. Zah, J.C. Breytenbach, H.M. Krieg, *J. Membrane Sci.* **300** (2007) **156**.
- [26] S. Khajavi, F. Kapteijn, J.C. Jansen, *J. Membr. Sci.* **299** (2007) **63**.
- [27] S. Khajavi, J.C. Jansen, F. Kapteijn, *J. Membr. Sci.* **326** (2009) **153**.
- [28] M.C. Lovallo, A. Gouzinis, M. Tsapatsis, *AIChE J.* **44** (1998) **1903**.
-

- 
- [29] J. Hedlund, J. Sterte, M. Anthonis, A.-J. Bons, B. Carstensen, N. Corcoran, D. Cox, H. Deckman, W.D. Gijst, P.-P. de Moor, F. Lai, J. McHenry, W. Mortier, J. Reinoso, J. Peeters, *Microporous Mesoporous Mater.* **52** (2002) **179**.
- [30] T.C. Bowen, H. Kalipcilar, J.L. Falconer, R.D. Noble, *J. Membr. Sci.* **215** (2003) **235**.
- [31] W.J.W. Bakker, L.J.P. van den Broeke, F. Kapteijn, J.A. Moulijn, *AIChE J.* **43** (1997) **2203**.
- [32] A.J. Burggraaf, Z.A.E.P. Vroon, K. Keizer, H. Verweij, *J. Membr. Sci.* **144** (1998) **77**.
- [33] M. Noack, P. Kölsch, J. Caro, M. Schneider, P. Toussaint, I. Sieber, *Microporous Mesoporous Mater.* **35-36** (2000) **253**.
- [34] U. Illgen, R. Schäfer, M. Noack, P. Kölsch, A. Kühnle, J. Caro, *Catal. Commun.* **2** (2001) **339**.
- [35] J. Caro, M. Noack, P. Kölsch, R. Schäfer, *Microporous Mesoporous Mater.* **38** (2000) **3**.
- [36] S. Münzer, J. Caro, P. Behrens, *Microporous Mesoporous Mater.* **110** (2008) **3**.
- [37] W. Song, R.E. Justice, C.A. Jones, V.H. Grassian, S.C. Larsen, *Langmuir* **20** (2004) **4696**.
- [38] M.C. Lovallo, M. Tsapatsis, *AIChE Journal* **42** (1996) **3020**.
- [39] Q. Zao, J. Wang, N. Chu, X. Yin, J. Yang, C. Kong, A. Wang, J. Lu, *J. Membr. Sci.* **320** (2008) **303**.
- [40] C. Bai, M.-D. Jia, J.L. Falconer, R.D. Noble, *J. Membr. Sci.* **105** (1995) **79**.
- [41] W.T. Gibbons, Y. Zhang, J.L. Falconer, R.D. Noble, *J. Membr. Sci.* **357** (2010) **54**.
-

### 3.2 Investigating the Influence of Different Monocarboxylic Acid Modulators on the Synthesis of Zr-*bdc* MOF (UiO-66)

#### *Preface*

The work presented in this section deals with the influence of different monocarboxylic acids as modulators on the synthesis of UiO-66. The driving force behind these investigations was to find a suitable synthesis to yield intergrown UiO-66 crystals of a sufficient size. All syntheses of this Zr-MOF published up to date have resulted in nanoparticles (either aggregated or isolated ones). For the production of polycrystalline supported membranes it is mandatory to find synthesis parameters that lead to the formation of larger crystals in the micrometer size range. The monocarboxylic acid 3-chloropropanoic acid was found to facilitate not only the formation of large UiO-66 crystals but also to evoke a strong tendency to intergrowth and heterogeneous nucleation. It was observed that 3-chloropropanoic acid can react with the solvent dimethylformamide to form *N,N*-dimethyl-beta-alanine and also acrylic acid. Correspondingly, the modulating effects of these two species were investigated as well. It became apparent from comparing the results of all syntheses that the intergrowth of the crystals that could be observed when high amounts of 3-chloropropanoic acid were used, were actually caused by the presence of *N,N*-dimethyl-beta-alanine.

This section will be submitted as an original research article. The authors are Imke Bremer, Andreas Schaate, Simon Dühren, Thomas Preuße, Adelheid Godt and Peter Behrens. Dr. A. Schaate provided general advice on the synthesis of Zr-MOFs. S. Dühren identified *N,N*-dimethyl-beta-alanine in the reaction solution. T. Preuße from the group of Prof. Dr. A. Godt at the Department of Chemistry at the Universität Bielefeld performed the <sup>1</sup>H-NMR spectroscopic analyses.

---



## Investigating the Influence of Different Monocarboxylic Acid Modulators on the Synthesis of Zr-*bdc* MOF (UiO-66)

Imke Bremer,<sup>1</sup> Andreas Schaate,<sup>1</sup> Simon Dühren,<sup>1</sup> Thomas Preuße,<sup>2</sup> Adelheid Godt,<sup>2</sup> and Peter Behrens<sup>1</sup>

<sup>1</sup> Institute of Inorganic Chemistry, Leibniz University Hannover, Callinstr. 9, 30167 Hannover

<sup>2</sup> Department of Chemistry, Bielefeld University, Universitätsstr. 25, 33615 Bielefeld

### Abstract

We have investigated the effects of the addition of different monocarboxylic acids, which can act as a modulator, on the synthesis of Zr-*bdc* MOF (UiO-66). Modulators can influence the crystal size and the degree of aggregation and intergrowth of the crystallites which is of interest for various applications. Without the addition of a monocarboxylic acid, the synthesis of Zr-*bdc* MOF yields aggregated and intergrown small nanosized particles. Here, we describe the modulating effects of different monocarboxylic acids, namely benzoic acid, 3-chloropropanoic acid (which has a pK<sub>A</sub> value similar to that of benzoic acid), *N,N*-dimethyl-beta-alanine hydrochloride and acrylic acid (both of which were found to be formed in the synthesis mixture of the reaction with 3-chloropropanoic acid). Of special interest are the morphologies formed in the presence of 3-chloropropanoic acid and *N,N*-dimethyl-beta-alanine: The formation of strongly intergrown micrometer-sized crystallites can serve as a basis for the formation of dense films and membranes.

### Keywords

metal-organic framework – microporous materials – modulator approach – Zr-MOF – Zr-terephthalate – UiO-66

### Introduction

The interest in porous coordination polymers (PCPs) or metal-organic frameworks (MOFs) has dramatically increased over the past years. These porous materials are constructed of metal ions or metal clusters that are interconnected by bridging organic linkers and usually exhibit very high specific surface areas.<sup>[1,2]</sup> One of the advantages of these materials is the fact that the linkers can readily be interchanged, opening a way to tailor not only the porosity by varying the linker

---

length<sup>[3,4]</sup> but also the properties of the MOFs by adding functional groups.<sup>[5]</sup> This makes them promising candidates for applications such as gas separation,<sup>[6,7]</sup> gas storage,<sup>[8]</sup> sensing devices,<sup>[9]</sup> and catalysis.<sup>[10]</sup>

A major setback of many MOFs is their insufficient stability towards atmospheric air, water, other chemicals or temperature. The synthesis of an isorecticular series of more stable Zr<sup>4+</sup>-containing MOFs has been published.<sup>[11]</sup> These contain a stable secondary building unit (SBU) with the formula [Zr<sub>6</sub>O<sub>4</sub>(OH)<sub>4</sub>]<sup>12+</sup> and feature a high degree of interconnectivity between these SBUs (each SBU is connected to twelve other SBUs by linear dicarboxylate linkers to form a face centered cubic arrangement), all based on strong zirconium-oxygen bonds, resulting in high chemical and thermal stability. The zirconium-oxo-hydroxo clusters corresponding to the SBUs have also been described as isolated molecules when saturated with monocarboxylate ligands,<sup>[12,13]</sup> which further emphasizes their high stability. The first materials of this type are UiO-66 (Zr-*bdc*, H<sub>2</sub>*bdc*: terephthalic acid), UiO-67 (Zr-*bpdc*, H<sub>2</sub>*bpdc*: biphenyl dicarboxylic acid) and UiO-68 (Zr-*tpdc*, H<sub>2</sub>*tpdc*: triphenyl dicarboxylic acid). It was demonstrated by Guillerm *et al.* that the methacrylate-terminated cluster Zr<sub>6</sub>O<sub>4</sub>(OH)<sub>4</sub>(maa)<sub>12</sub> (maa: CH<sub>2</sub>=C(CH<sub>3</sub>)COO<sup>-</sup>) can in fact be used as a precursor in the synthesis of UiO-66 and an isostructural MOF containing the muconic acid dianion as linker.<sup>[14]</sup>

In order to make use of these materials it is necessary to gain control over the synthesis and be able to selectively influence the morphological properties of the products like, for example, the crystal size and shape as well as the state of aggregation and intergrowth: Whereas single crystals are important for X-ray structural analysis and for the exploitation of certain physical properties and individual nanoparticles can be of interest for chemical sensing devices or biomedical applications, micrometer-sized and densely intergrown crystals are requested in the formation of dense supported layers, as used for example in separation membranes. Following the modulation approach originally described by the group of Kitagawa<sup>[16,17]</sup>, we added monocarboxylic acids to the synthesis mixtures. On the one hand, this addition allowed us to increase the reproducibility and the crystallinity of the products. Furthermore, it provided the possibility to synthesize novel MOFs which were not accessible without using a modulator, including several with UiO-type topology (Zr-*fum*-MOF, H<sub>2</sub>*fum*: fumaric acid, *trans*-butene-1,4-dicarboxylic acid;<sup>[18]</sup> Zr-*abdc*-MOF, H<sub>2</sub>*abdc*: azobenzenedicarboxylic acid)<sup>[19]</sup> and the family of PIZOFs (porous interpenetrated Zr-organic frameworks).<sup>[20]</sup> Most importantly, by applying the modulation approach we also gained a certain degree of control about the crystal size in the products of Zr-MOF syntheses.<sup>[18,21]</sup> Using different amounts of benzoic acid as the modulator, we were able to selectively vary the crystal size of UiO-66 nanocrystals, to obtain micrometer-sized UiO-67 crystals in a highly reproducible fashion, and to produce the first single crystals of a Zr-MOF.<sup>[21]</sup> The use of formic acid as the modulating agent in the synthesis of the Zr-*fum* MOF also allowed a certain degree of control over the size of the nanocrystals. Generally, it was observed that with increasing

the amount of modulator, the crystallites appeared more isolated, i.e. aggregation and intergrowth decreased. These findings can be explained by the idea of “coordination modulation”, which is based on a competition between monocarboxylic acids (modulators) and dicarboxylic acids (linkers) for the coordination sites at the SBUs. In this way, modulators can slow down the rate of nucleation as well as of growth. A reduced nucleation rate should lead to fewer and larger crystals, a reduced growth rate should lead to more defect-free crystals and enhanced crystallinity.

Here we report on the effects of different monocarboxylic acids as modulators in the synthesis of UiO-66. Benzoic acid was chosen as a modulator because of its similarity to the linker molecules (terephthalic acid) and 3-chloropropanoic acid was chosen because it has a  $pK_A$  value of 4.1, which is very similar to that of benzoic acid (4.17). *N,N*-dimethyl-beta-alanine hydrochloride and acrylic acid were found to be formed during the course of the synthesis reaction involving 3-chloropropanoic acid. Hence, these two species were also investigated as possible modulators.

## Experimental

*N,N*-dimethyl-beta-alanine hydrochloride was purchased from TCI (Tokyo Chemical Industries), all other chemicals were obtained from Sigma-Aldrich. All chemicals were used as received without further purification.

### *Syntheses of UiO-66*

The synthesis of UiO-66 was performed by dissolving  $ZrCl_4$  (0.429 mmol, 1 eq) and  $H_2bdc$  (0.429 mmol, 1eq) in 25 mL *N,N*-dimethylformamide (DMF) in a 100 mL glass flask at room temperature. To these mixtures 0 – 30 equivalents of benzoic acid, 3-chloropropanoic acid (3-cpa), *N,N*-dimethyl-beta-alanine hydrochloride (dmba) and acrylic acid were added to investigate the influence of these monocarboxylic acids as a modulator. The glass flask was then sealed with a Teflon lined screw cap and heated to 120 °C for 72 h. After cooling the white precipitate was collected by centrifugation and was washed with 15 mL DMF and 15 mL ethanol, respectively. The washing steps were carried out by repeated redispersion and centrifugation. The resulting white powders were then dried at 60 °C overnight. Activation of the samples was done by a Soxhlet extraction with ethanol overnight and drying at 120°C in a convection oven.

---

### *Characterization*

Powder X-ray diffraction (PXRD) patterns were collected using a Stoe Stadi P transmission diffractometer with Ge(111)-monochromized  $\text{CuK}\alpha_1$  radiation with a wavelength of  $\lambda = 1.54060 \text{ \AA}$ . When applicable, Scherrer's equation was used to calculate the particle size using the first (and most intense) reflection of the diffraction pattern. A silicon standard was measured under the same conditions to determine the reflection broadening caused by the instrumental setup.

Scanning electron micrographs were recorded using a JEOL JSM-6700F field-emission scanning electron microscope operated with an acceleration voltage of 2 kV at a working distance of 8 mm using a LEI-detector and 3 mm using a SEI-detector respectively. Samples were prepared by suspending the material in ethanol and dropping the suspension on a graphite block.

Thermogravimetric analysis (TGA) measurements were carried out using a Netzsch STA 429 thermoanalyser. The samples were heated in corundum crucible in air with a heating rate of  $5 \text{ K min}^{-1}$  to a maximum temperature of  $1000 \text{ }^\circ\text{C}$ .

Argon sorption isotherms were measured on a Quantachrome Autosorb-1 instrument. Prior to the sorption experiment, the samples were purified by Soxhlet extraction with ethanol for 24 h, dried at  $120^\circ\text{C}$  and outgassed at  $120 \text{ }^\circ\text{C}$  in vacuum for 72 h.

## **Results and discussion**

In the following the amount of modulator used will be stated as molar equivalents in relation to the amount of  $\text{ZrCl}_4$ . For example, a synthesis performed with benzoic acid in a molar ratio of 10:1 in relation to  $\text{ZrCl}_4$  will be denoted as "10 eq benzoic acid".

In Figure 1 and 2 the PXRD patterns of the products of the syntheses with different amounts of benzoic acid and 3-cpa are shown (for benzoic acid-modulated syntheses, which had been carried out with syntheses periods of 24 h, similar results have been described in ref. [21]). Independent of the type and amount of modulator used in the synthesis of UiO-66, a full set of reflections can be found in all diffraction patterns. All reflections can be attributed to the UiO-66 phase. Using no modulator or small amounts of modulator, the reflections are broadened. From this reflection broadening, the crystallite sizes can be calculated using Scherrer's equation (Table 1). In syntheses with low amounts of modulator, the particle sizes decrease at first; they increase dramatically when 5 eq or more of the modulator were used. Interestingly, this behavior is the same for both benzoic acid and 3-cpa, and particle sizes calculated from the broadening of the reflections are very similar for the same amount of modulator used. SEM micrographs of the products



obtained with low amounts of modulators (up to 10 eq) are also similar for products from both, benzoic acid- (Fig. 1) and 3-cpa-modulated (Fig. 2) syntheses.

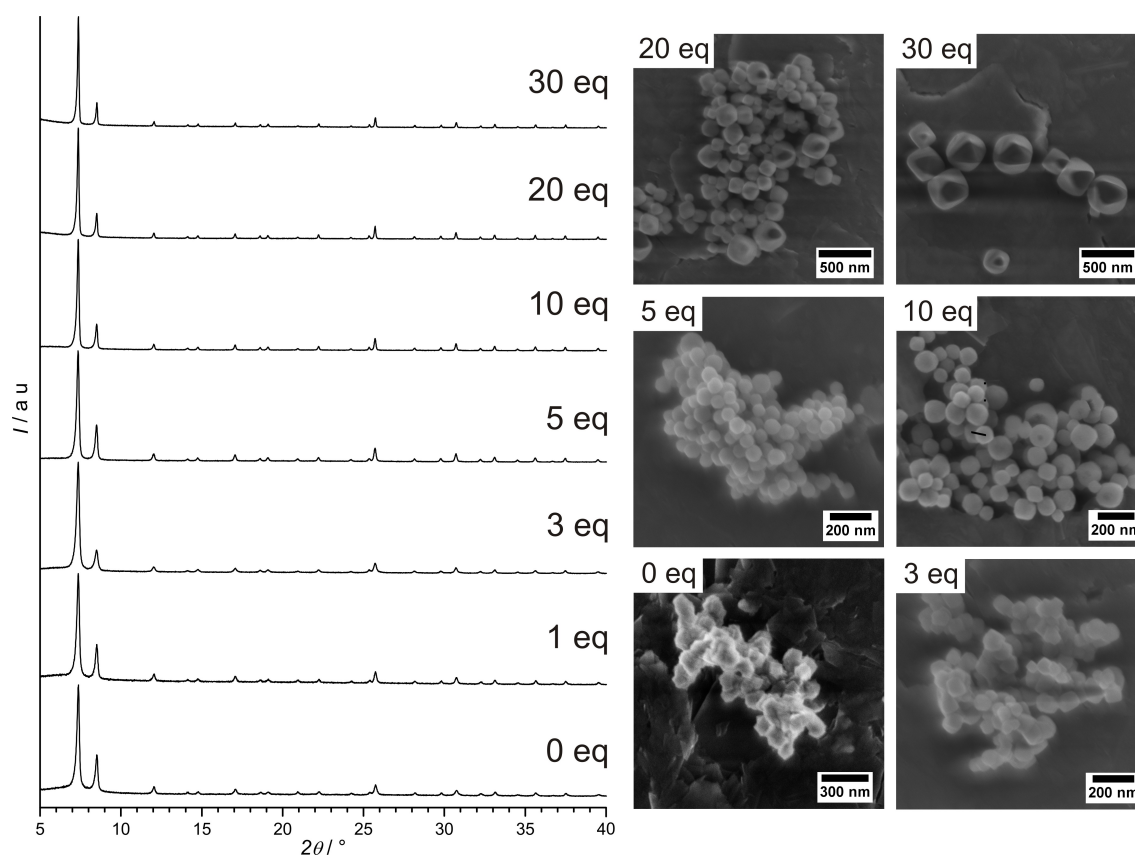


Fig. 1: Powder XRD patterns of Zr-*bdc* MOF synthesized with different amounts of benzoic acid (0 – 30 eq) and corresponding SEM micrographs of the samples.

When no modulator is used intergrown aggregates of very small crystallites are obtained (Fig. 1, 0 eq). With an increasing amount of modulator the particles become more individualized and crystal faces become visible in the SEM micrographs. This is especially the case for benzoic acid where this trend continues up to the highest modulator concentrations used here (Fig. 1). With 3-cpa as modulator, this trend towards more individual crystals can only be observed for small amounts of modulator of up to 10 eq (Fig. 2). When more than 10 eq (i.e. 20 eq or 30 eq) of 3-cpa are added in the syntheses, a tremendous change in the product morphology can be noted. In contrast to the products obtained with benzoic acid, which are isolated octahedrally shaped crystals with sizes of approx. 200 - 300 nm (Fig. 1, 30 eq), in the case of 3-cpa the crystals are strongly intergrown (Fig. 2, 30 eq). The primary crystals are several  $\mu\text{m}$  in size and also show indications of an octahedral shape.

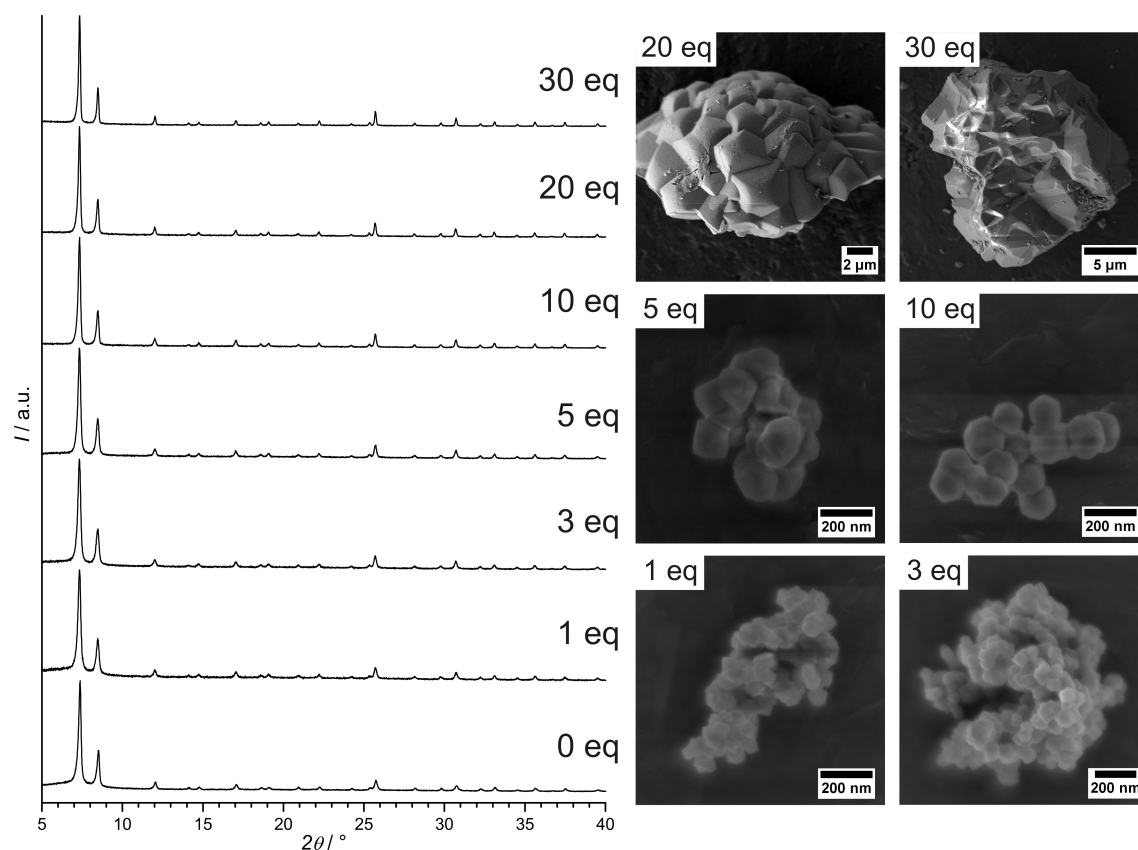


Fig. 2: Powder XRD patterns of Zr-*bdc* MOF synthesized with different amounts of 3-chloropropanoic acid (0 – 30 eq) and corresponding SEM micrographs of the samples.

Table 1: Crystal sizes of UiO-66 prepared with different amounts of benzoic acid and 3-chloropropanoic acid as modulators determined by Scherrer's equation and SEM micrographs.

amount of modulator	benzoic acid		3-chloropropanoic acid	
	$d_{\text{Scherrer}} / \text{nm}$	$d_{\text{SEM}} / \text{nm}$	$d_{\text{Scherrer}} / \text{nm}$	$d_{\text{SEM}} / \text{nm}$
0 eq	55.8	- <sup>b</sup>	55.8	- <sup>b</sup>
1 eq	52.3	40 - 60	52.3	40 - 60
3 eq	49.1	50 - 80	46.4	50 - 70
5 eq	58.9	50 - 100	52.0	100 - 150
10 eq	76.7	70 - 130	68.5	120 - 170
20 eq	90.1	80 - 180	- <sup>a</sup>	several $\mu\text{m}$
30 eq	- <sup>a</sup>	200 - 300	- <sup>a</sup>	several $\mu\text{m}$

<sup>a</sup>: Crystal sizes are too large for the application of Scherrer's equation.

<sup>b</sup>: Crystal sizes cannot be evaluated from SEM micrographs due to aggregation.

During the syntheses with 20 and 30 eq 3-cpa, it can be observed that crystallization takes place quite late (typically during the last 12 of 72 h) and mainly on the surface of the glass. This fact and the strong intergrowth are indications that a heterogeneous crystallization takes place unlike to the case of benzoic acid-modulated reactions, where crystallization starts within several minutes (at most 2 h with 30 eq benzoic acid) mainly in the solution and not on the

glass walls of the vessel. Also, reaction solutions to which large amounts of 3-cpa had been added, show a yellow color after the reaction treatment and a gas is escaping from the solution upon opening the reaction vessels.

Summarizing, the results from reactions modulated with small to medium amounts of benzoic acid or 3-cpa show similar outcomes, in line with the similarity of the  $pK_a$  values of both acids. However, for large amounts of modulator, the reactions and their products are rather different for benzoic acid versus 3-cpa. In fact, similar results as obtained with the use of benzoic acid as a modulator can also be produced with many other simple acids like for example acetic acid or formic acid. Also the additional observations described above suggest that 3-cpa plays a special role in product formation. The yellow coloration of the synthesis mixture after reaction, the delayed formation of the product and the liberation of a gas indicated to us that 3-cpa probably undergoes reactions in the synthesis mixture which lead to some species that disseminate a modulating effect different from that of a simple monocarboxylic acid.

To clarify this proposal, a mixture of DMF, 3-cpa and  $ZrCl_4$  (750 : 30 : 1) without any linker was heated to 120 °C for 72 h in a closed vessel. After cooling the mixture to room temperature, a white precipitate formed. The PXRD pattern of the precipitate showed no similarity to any of the reactants but was identified as *N,N*-dimethyl-beta-alanine (dmba) (Fig. 4). This species is formed in a reaction of 3-cpa with dimethylamine (DMA). DMA forms when the solvent DMF decomposes upon contact with water and heating (Fig.3). Evaluation of a  $^1H$ -NMR spectrum of the reaction solution revealed the presence of acrylic acid (aa). Either dmba or 3-cpa can undergo an elimination of DMA or HCl, respectively, to form aa (Fig. 3). Interestingly no residual 3-cpa was found to be present in the reaction solution.

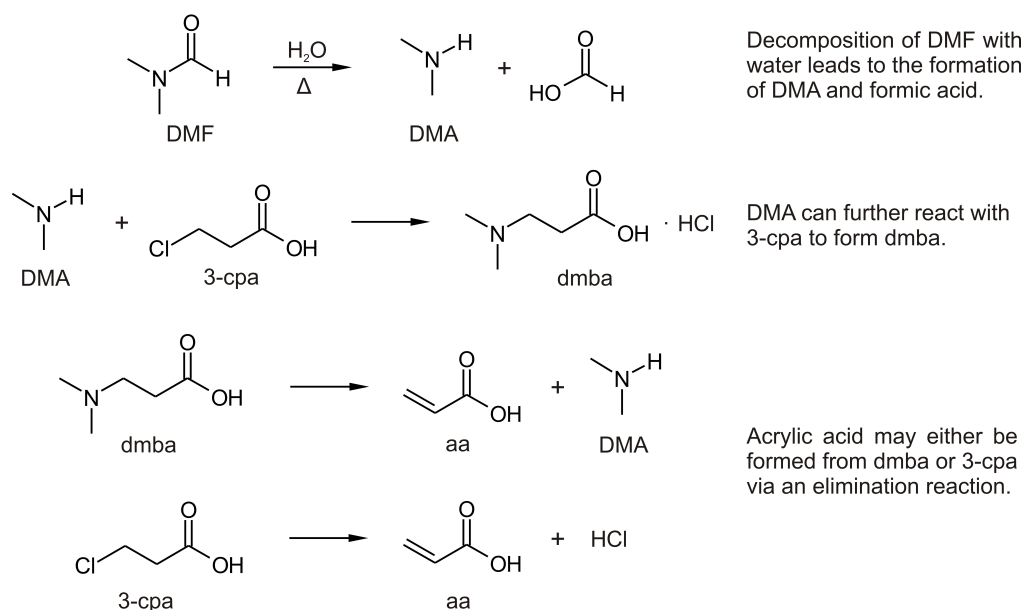


Fig. 3: Reaction scheme clarifying the formation mechanisms of *N,N*-dimethyl-beta-alanine(dmba) and acrylic acid (aa).

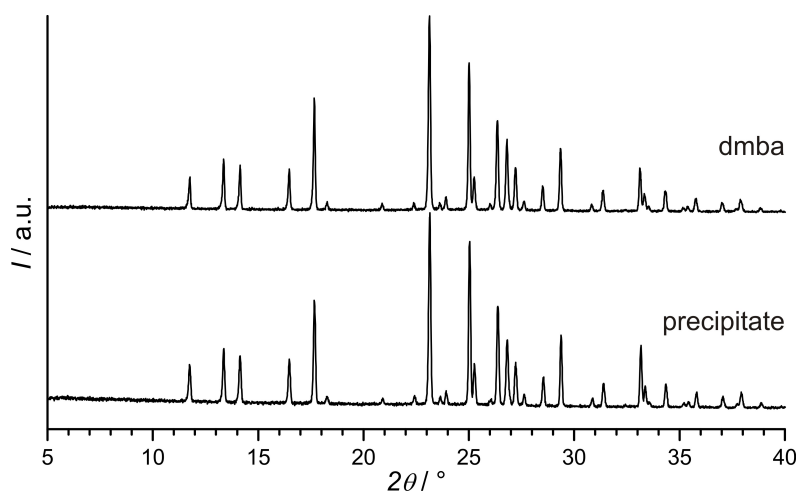


Fig. 4: Comparison of the PXRD patterns of the precipitate formed a mixture of DMF, 3-cpa and  $ZrCl_4$  without any linker and the commercially available *N,N*-dimethyl-beta-alanine hydrochloride.

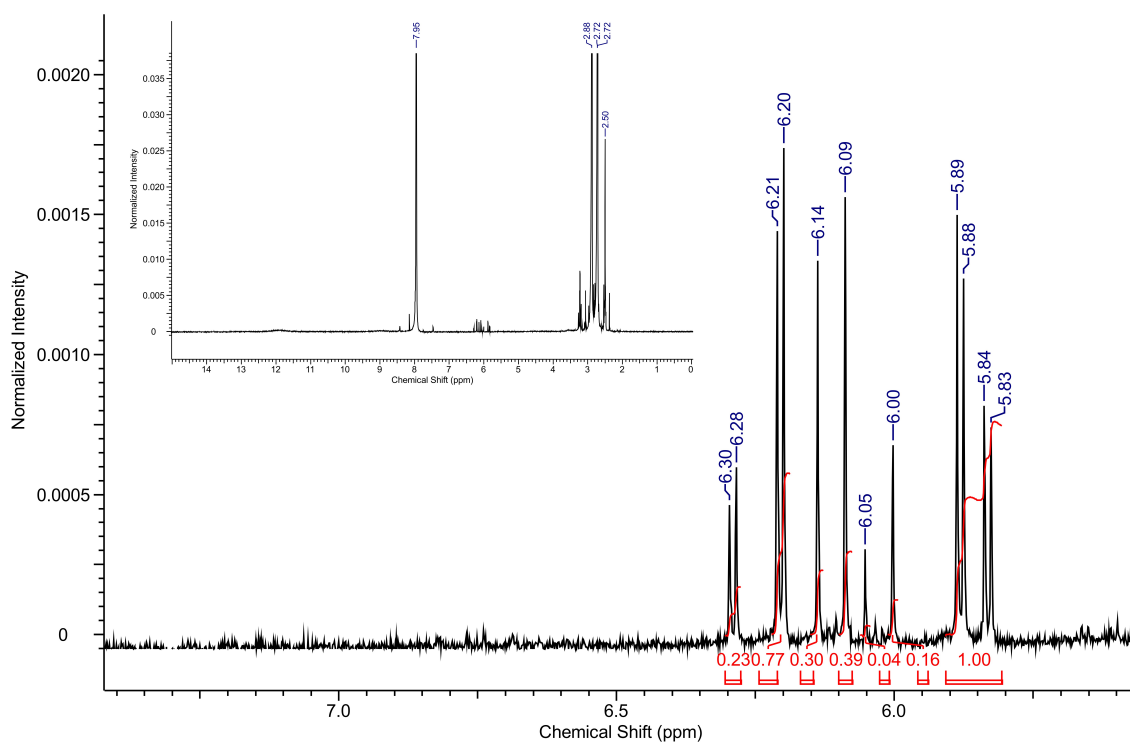


Fig. 5:  $^1H$ -NMR of a reaction solution (without  $ZrCl_4$ , heated to 120 °C for 72 h) shows the presence of acrylic acid ( $^1H$ -NMR (200 MHz,  $DMSO-d_6$ )  $\delta$  = 5.86 (dd,  $J$  = 9.79, 2.26 Hz, 1H), 6.07 (dd,  $J$  = 17.32, 9.79 Hz, 1H), 6.25 (dd,  $J$  = 17.07, 2.30 Hz, 1H) ppm). Signals of dmba are superimposed by the very intense DMF signals.

Since acrylic acid and dmba were found in the reaction mixture when 3-cpa was used as a modulator, the modulating properties of these acid were also studied by a set of reactions with different amounts of aa and dmba introduced to the synthesis batches.

When acrylic acid is added to the reaction, it can be judged from the broadening of the reflections in the PXRD patterns (Table 2) as well as from the SEM micrographs (Fig. 6) of the samples that nanoparticles without defined shape and with a small degree of aggregation are obtained in all syntheses regardless of the amount of aa

added. These findings are very much unlike the observations made with 3-cpa as modulator, where micrometer-sized intergrown crystals are formed with high modulator concentrations of 20 – 30 eq. From the comparison of these results it can be stated that acrylic acid is obviously not accountable for the intergrown nature of the crystals and therefore not the ‘true’ modulator in the modulated reaction with 3-cpa.

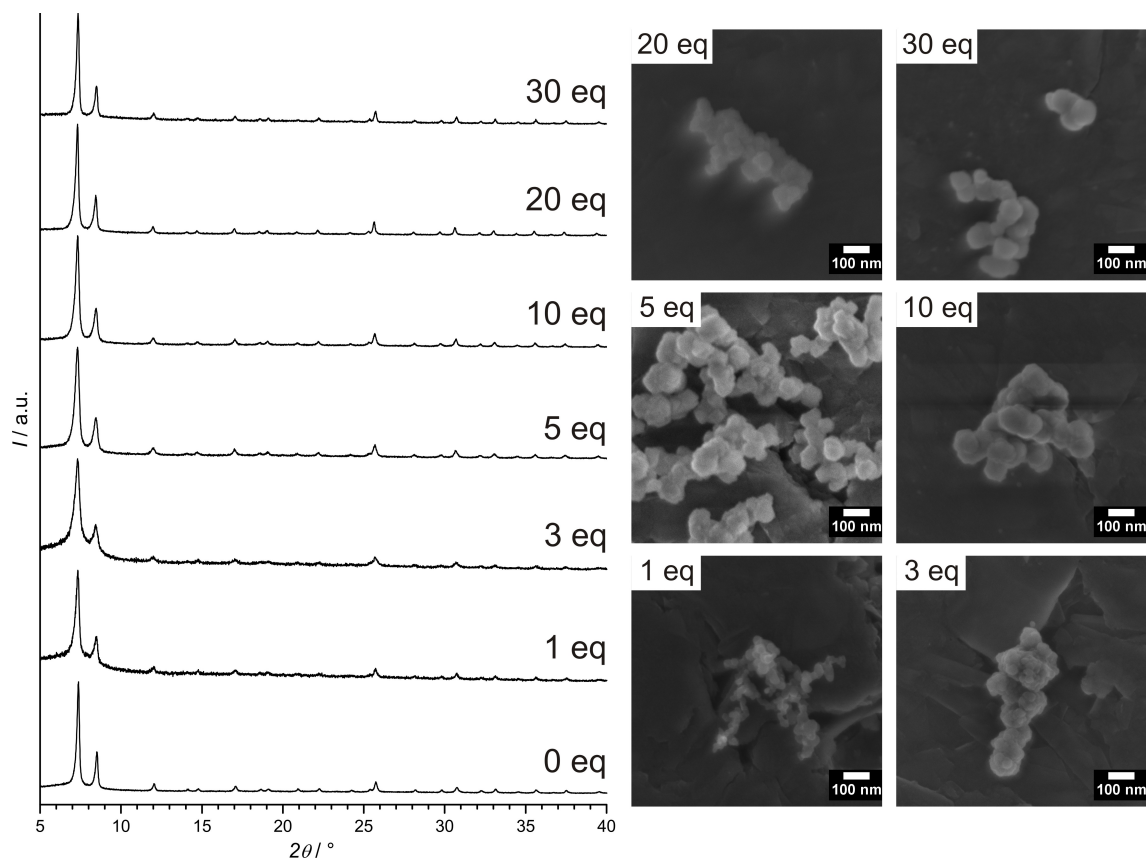


Fig. 6: Powder XRD patterns of Zr-*bdc* MOF synthesized with different amounts of acrylic acid (0 – 30 eq) and corresponding SEM micrographs of the samples.

Table 2: Crystal sizes of UiO-66 prepared with different amounts of acrylic acid as modulator determined by Scherrer’s equation and SEM micrographs.

amount of acrylic acid	$d_{\text{Scherrer}} / \text{nm}$	$d_{\text{SEM}} / \text{nm}$
1 eq	37.3	20 - 30
3 eq	25.4	25 - 35
5 eq	32.4	35 - 50
10 eq	37.4	40 - 60
20 eq	46.8	40 - 55
30 eq	55.4	60 - 90

Dmba carries a carboxylic acid group as well and could thus also act as a modulator. To investigate this idea further, syntheses with different amounts of the commercially available *N,N*-dimethyl-beta-alanine hydrochloride were carried

out. The PXRD patterns shown in Fig. 7 display the presence of an amorphous background for products obtained at low dmbs concentrations (1 – 5 eq). In this range of concentrations, the presence of dmbs does not seem to unfold a modulating effect, but rather to interfere with the synthesis in a way that amorphous products are formed. With higher concentrations of 10 – 30 eq, on the other hand, highly crystalline products are formed, which show no amorphous background and exhibit reflections with a narrow half-width in the PXRD pattern. The samples prepared with high modulator concentrations consist of large intergrown particles (Fig. 7, 20 eq, 30 eq) and look very similar to those prepared with high amounts of 3-cpa (Fig. 2, 20 eq, 30 eq) in the SEM micrographs.

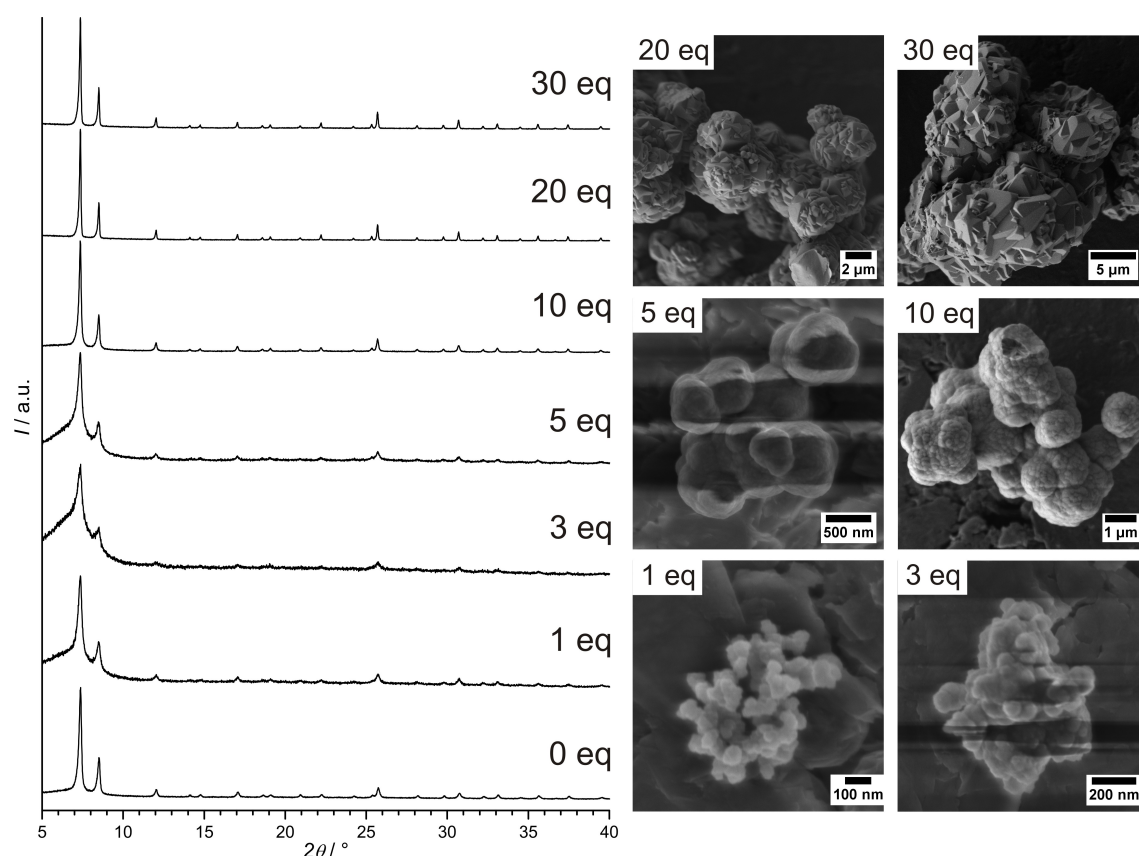


Fig. 7: Powder XRD patterns of Zr-*bdc* MOF synthesized with different amounts of *N,N*-dimethyl-beta-alanine hydrochloride (0 – 30 eq) and corresponding SEM micrographs of the samples.

These results allow the assumption that dmbs is the actual modulator also in the syntheses carried out with 3-cpa. This would also explain the prolonged reaction times in 3-cpa modulated reactions. First dmbs has to be formed before the crystallization of the Zr-*bdc* MOF can start.

The intergrown nature of the products obtained with dmbs is probably caused by the presence of the additional amine function which will to a large part be protonated under the strongly acidic conditions of the synthesis. Assuming that in the synthesis solution growing crystallites are capped with dmbs molecules by coordinating with their carboxylate functionality, these crystallites would carry the ammonium functions of the dmbs molecules. The strong interaction of

alkylammonium moieties with glass surfaces is well known and could thus explain the heterogeneous nucleation on the vessel surface. Also, particles of UiO-66 prepared in the presence of 30 eq of benzoic acid show a negative zeta potential of  $-40$  mV (measured in water at a pH value of 7; the sample was washed with DMF and dried prior to the measurement, but was not Soxhlet extracted), which explains the formation of individual particles due to electrostatic repulsion. This negative surface charge is probably caused by the presence of unprotonated *bdc* linkers on the surface of the crystallites. When growing particles in *dmba*-modulated syntheses carry *dmba* molecules with protonated amine groups on their surface, the negative charge of the particles would decrease, explaining the observed aggregation and intergrowth of the primary crystallites (schematic illustration in Fig. 8). Moreover the decreased negative surface charge would probably facilitate the addition of deprotonated carboxylate-linkers and thereby lead to the observed larger crystal sizes. At low modulator concentrations this charge compensation is obviously not sufficient so that smaller crystals are formed eventually. To gain a more detailed insight into the surface characteristics of the particles forming in *dmba*-modulated syntheses, zeta potential measurements would be desirable. Unfortunately, the large particle sizes make it impossible to obtain stable suspensions of the materials, which are required for zeta potentials measurements.

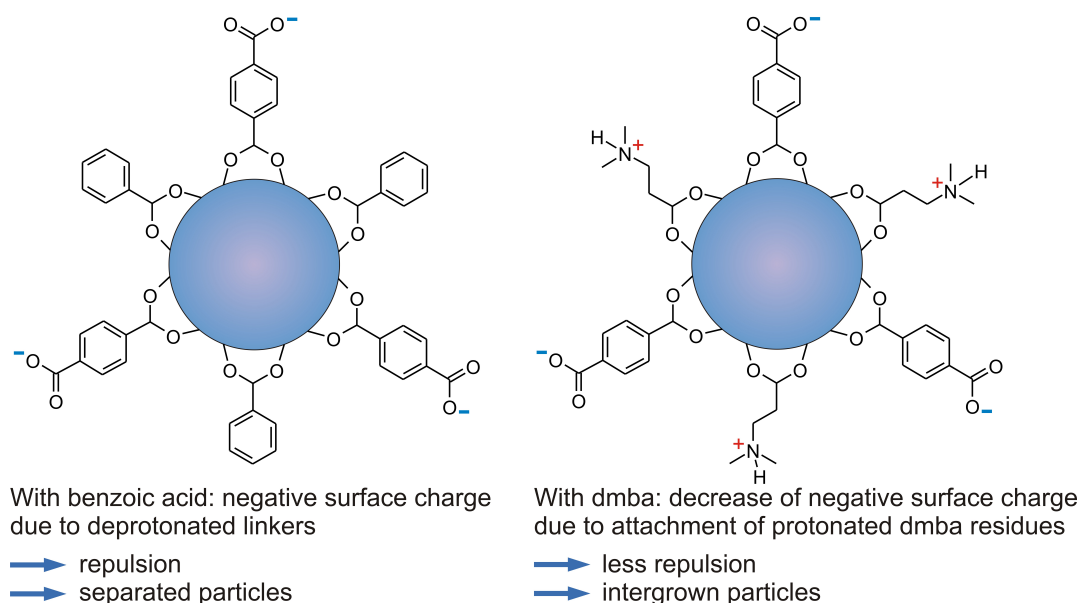


Fig. 8: Schematic illustration of the possible mechanism for the reduction of the surface charge of UiO-66 particles prepared in syntheses with 3-*cpa* (or *dmba*) as modulator.

The BET surface areas of the samples prepared with different modulators were determined from argon sorption isotherms (Figs. 9 and 10). Without any modulator the UiO-66 shows a surface area of  $840 \text{ m}^2 \text{ g}^{-1}$ , whereas the surface areas of the materials prepared with 30 eq of the different modulator lie in a range of  $1100 \text{ m}^2 \text{ g}^{-1}$ . The determined surface area for the sample prepared with 30 eq of

3-cpa is exceptionally high with  $1580 \text{ m}^2 \text{ g}^{-1}$ . These results prove that the porosity of the materials prepared with the use of modulating agents is preserved.

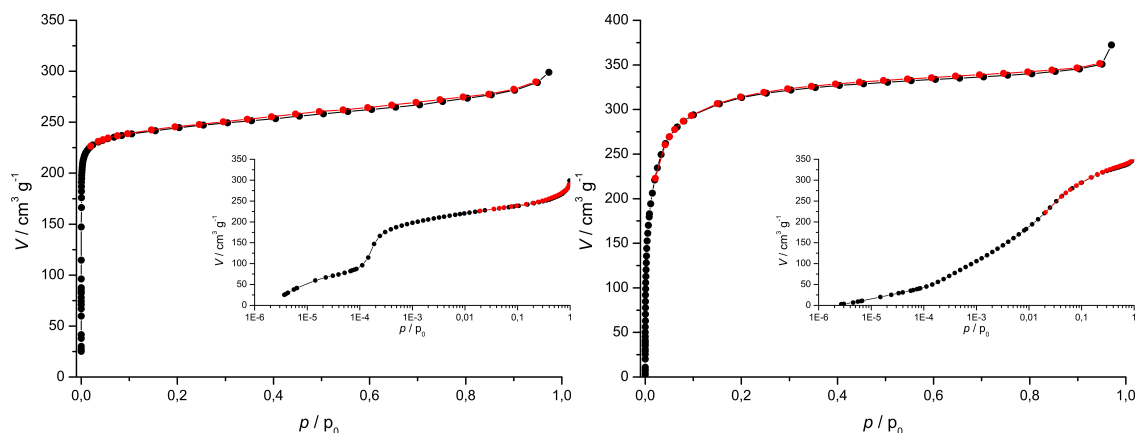


Fig. 9: Argon sorption isotherm in linear and logarithmical (inset) plotting of a sample prepared without modulator (left); Argon sorption isotherm in linear and logarithmical (inset) plotting of a sample prepared with 30 eq of benzoic acid (right)

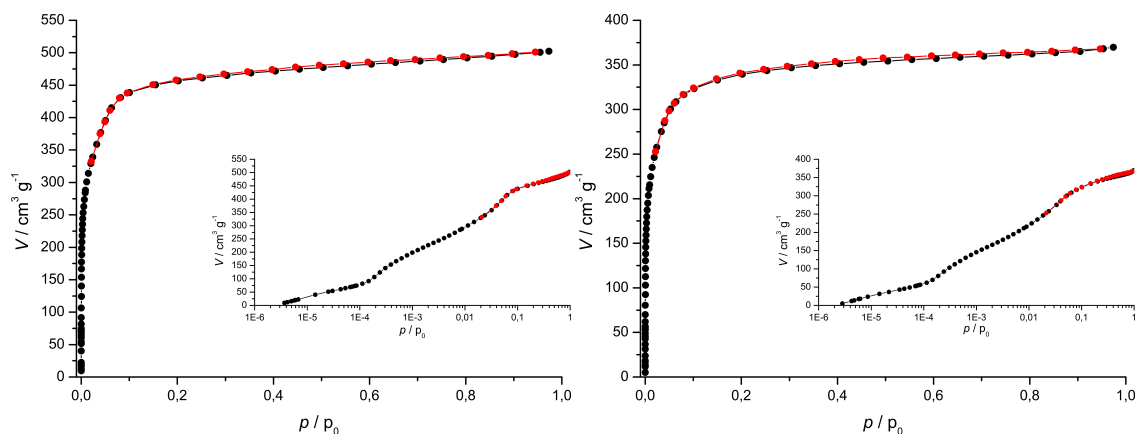


Fig. 10: Argon sorption isotherm in linear and logarithmical (inset) plotting of a sample prepared with 30 eq of 3-chloropropanoic acid (left); Argon sorption isotherm in linear and logarithmical (inset) plotting of a sample prepared with 30 eq of *N,N*-dimethyl beta alanine (right).

## Summary

We have shown that the size and morphology of UiO-66 crystals can be tuned by the choice of the monocarboxylic acid used as a modulator. With the use of benzoic acid it is possible to obtain separated nanocrystals while the use of 3-chloropropanoic acid leads to micrometer-sized and strongly intergrown crystals. This observation was at first surprising since both acids possess a very similar  $\text{pK}_a$  value. Further investigation led to the result that 3-chloropropanoic acid reacts with dimethylamine that is liberated from the solvent DMF to form *N,N*-dimethyl-beta-alanine (dmba). We assume that it is this species that accounts for the intergrowth of the crystals, since pure dmba as modulator led to similarly intergrown products. It is probably the amine-functionality (that is protonated and therefore positively charged in the acidic synthesis solution) that leads to positive



electrostatic interactions with deprotonated linker species that are present in the growing MOF particles.

With this ability to adjust the size and state of intergrowth of Zr-*bdc*-MOF crystals, this material can be tailored for different types of applications. For example, in applications where nanoparticles are desired, e.g. in sensing devices, the synthesis can be carried out by modulation with benzoic acid; on the other hand, for the preparation of gas-separating membranes, for which intergrown crystals are necessary, the synthesis should be carried out in the presence of *dmba* or *3-cpa*.

## References

- [1] S. Kitagawa, R. Kitaura and S. Noro, *Angew. Chem. Int. Ed.* **43** (2004) **2334**.
  - [2] G. Férey, *Chem. Soc. Rev.* **37** (2008) **191**.
  - [3] O. Yaghi, M. O'Keeffe, N.W. Ockwig, H.K. Chae, M. Eddaoudi and J. Kim, *Nature* **42** (2003) **3705**.
  - [4] R. Robson, *Dalton Trans.* **38** (2008) **5113**.
  - [5] K.K. Tanabe and S.M. Cohen, *Chem. Soc. Rev.* **40** (2011) **498**.
  - [6] J.-R. Li, R.J. Kuppler and H.C. Zhou, *Chem. Soc. Rev.* **38** (2009) **1477**.
  - [7] B. Chen, S. Xiang and G. Qian, *Acc. Chem. Res.* **43** (2010) **1115**.
  - [8] L.J. Murray, M. Dinca and J.R. Long, *Chem. Soc. Rev.* **38** (2009) **1294**.
  - [9] O. Shekhan, J. Liu, R.A. Fischer and C. Wöll, *Chem. Soc. Rev.* **40** (2011) **1081**.
  - [10] L. Ma and W. Lin, *Top. Curr. Chem.* **293** (2010) **175**.
  - [11] J.H. Cavka, S. Jakobsen, U. Olsbye, N. Guillou, C. Lamberti, S. Bordiga and K.P. Lillerud, *J. Am. Chem. Soc.* **130** (2008) **13850**.
  - [12] G. Kickelbick and U. Schubert, *Chem. Ber.* **130** (1997) **473**.
  - [13] P. Piszczek, A. Radtke, A. Grodzicki, A. Wojtczak and J. Chojnacki, *Polyhedron* **26** (2007) **679**.
  - [14] V. Guillermin, S. Gross, C. Serre, T. Devic, M. Bauer and G. Férey, *Chem. Commun.* **46** (2010) **767**.
  - [15] L. Valenzano, B. Civalleri, S. Chavan, S. Bordiga, M.H. Nilsen, S. Jakobsen, K.P. Lillerud and C. Lamberti, *Chem. Mater.* **23** (2011) **1700**.
  - [16] T. Tsuruoka, S. Furukawa, Y. Takashima, K. Yoshida, S. Isoda and S. Kitagawa, *Angew. Chem. Int. Ed.* **48** (2009) **4739**.
-

- [17] S. Diring, S. Furukawa, Y. Takashima, T. Tsuruoka and S. Kitagawa, *Chem. Mater.* **22** (2010) **4531**.
- [18] G. Wißmann, A. Schaate, I. Bremer and P. Behrens, *Microporous Mesoporous Mater.* **152** (2012) **64**.
- [19] A. Schaate, S. Dühren, G. Platz, S. Lilienthal, A.M. Schneider, P. Behrens, *Eur. J. Inorg. Chem.* (2012) **790**.
- [20] A. Schaate, P. Roy, T. Preuße, S.J. Lohmeier, A. Godt, P. Behrens, *Chem. Eur. J.* **17** (2011) **9320**.
- [21] A. Schaate, P. Roy, J. Lippke, F. Waltz, M. Wiebcke, A. Godt and P. Behrens, *Chem. Eur. J.* **17** (2011) **6643**.
-

### 3.3 Deposition of Zr-MOF Layers on Different Ceramic Support Materials

#### *Preface*

The work presented in this chapter deals with the investigation of the influence of different ceramic support materials on the deposition of polycrystalline Zr-MOF layers. The ultimate goal was the preparation of supported layers of Zr-MOFs, especially of PIZOFs, for the use as membranes. Since the linkers for the PIZOFs are not commercially available and as their synthesis is laborious, we have decided to first explore suitable preparation techniques for polycrystalline layers of the Zr-MOF UiO-66 as a model substance. Different support materials ( $\alpha$ -alumina, titania, and amino functionalized  $\alpha$ -alumina) and different monocarboxylic acid modulators were tested. The reaction principles found were then transferred to PIZOF-2 as a representative of the PIZOF family. As the synthesis conditions for the different PIZOFs (nineteen members of this family are known up to date) are rather similar, it can be presumed that a reproducible pathway of producing PIZOF-2 layers should work for other PIZOFs as well.

All produced Zr-MOF layers presented in this work showed cracks, which restricts their use as membranes. These cracks probably arise during the drying of the samples. Different drying methods were therefore tested, but none yielded defect-free membranes. However, the dense layers prepared in this work open possibilities for a variety of other applications, for example as selective layers for sensors or as coatings on implants, using the pore space for the delivery of bioactive substances.

This section will be submitted as an original research article. The authors are Imke Bremer, Andreas Schaate, Thomas Preuße, Adelheid Godt and Peter Behrens. Dr. A. Schaate provided general advice on the synthesis of Zr-MOFs. T. Preuße from the group of Prof. Dr. A. Godt at the Department of Chemistry at the Universität Bielefeld synthesized the linker for PIZOF-2. This work was part of a collaboration within the DFG priority program "Porous Metal-Organic Frameworks" (SPP 1362).

---



## Deposition of Zr-MOF Layers on Different Ceramic Support Materials

Imke Bremer,<sup>1</sup> Andreas Schaate,<sup>1</sup> Thomas Preuße,<sup>2</sup> Adelheid Godt,<sup>2</sup> and Peter Behrens<sup>1</sup>

<sup>1</sup> Institute of Inorganic Chemistry, Leibniz University Hannover, Callinstr. 9, 30167 Hannover

<sup>2</sup> Department of Chemistry, Bielefeld University, Universitätsstr. 25, 33615 Bielefeld

### Abstract

We have investigated the influence of different ceramic support materials for the deposition of UiO-66 as a simple representative of the family of Zr-based MOFs. The results of these experiments were further compared to experiments of depositing PIZOF-2 on the same support materials. Optimized conditions for the production of supported Zr-MOFs were found. All densely intergrown MOF layers investigated here have shown cracks probably caused during drying by capillary stress. Modified protocols for drying the materials did not lead to an improvement in preventing the formation of cracks. Therefore none of the materials could be tested for possible applications in gas separation.

### Keywords

metal-organic framework – modulator approach – Zr-MOF – UiO-66 – PIZOFs – MOF layers – MOF membranes

### Introduction

The deposition of layers of porous materials on supports is of interest for a variety of applications. Most notably, membranes can provide the basis for energy- and cost-efficient separation processes, either utilizing a size-discriminating sieving effect or a functionalized pore volume to specifically interact with the analytes or a combination of both. In either case, a well defined pore size and uniform pore structure is desired. Other requirements for membrane materials are a sufficient chemical and thermal stability. A material class that fulfills these requirements are zeolites. Many examples of membranes prepared of different zeolite topologies have been reported in the literature.<sup>[1]</sup> However their application fields are limited due to the restricted chemical variability of silicates and aluminosilicates and

---

practical use in industrial scale is still scarce. Supported layers of microporous and mesoporous materials can also be of interest for other applications, for example in sensing devices or as protective coatings. For the construction of sensors, the deposition of microporous films on substrates like gold (as present in the sensing element of quartz crystal microbalances) or on the silica surface layer of silicon wafers is of interest. In the biomedical field, the application of a mesoporous silica coating on prostheses has opened the way for tissue engineering and the implant-based local delivery of drugs or growth factors.<sup>[2]</sup>

Over the last decade a new type of porous materials has drawn great attention, the porous coordination polymers (PCPs)<sup>[3]</sup> or metal organic frameworks (MOFs).<sup>[4]</sup> These hybrid materials consist of inorganic building blocks of metal clusters or discrete metal ions (the so-called secondary building units; SBUs) and organic linkers which connect these building blocks to form open framework structures. The application potential of these materials seems to be nearly unrestricted since MOFs can cover a wide range of pore sizes and the organic linkers feature the possibility for various pre- and post-synthetic functionalizations<sup>[5]</sup> utilizing the wide scope of organic chemistry. These two features make metal organic frameworks promising candidates for gas separation<sup>[6,7]</sup>, gas storage<sup>[8]</sup>, sensing<sup>[9]</sup> and catalysis.<sup>[10]</sup> A drawback in many metal-organic framework materials with carboxylate linkers is their insufficient stability towards water and hydrothermal conditions.<sup>[11,12]</sup> Some materials are not even stable towards atmospheric moisture.<sup>[13]</sup>

Several papers have recently reported on the enhanced stability of Zr<sup>4+</sup>-based MOFs. The compounds from the series of isorecticular MOFs with the UiO-66 topology (as UiO-66 and UiO-67)<sup>[14]</sup> contain a very stable secondary building unit (SBU), a zirconium-oxo-hydroxo cluster, which is interlinked by dicarboxylic acids: benzene dicarboxylic acid (*bdc*) in case of UiO-66, diphenylene dicarboxylic acid (*bpdc*) in case of UiO-67. Since the first report on these MOFs<sup>[14]</sup>, a number of other compounds with this topology has been described. These often feature outstanding temperature resistance as well as insensitivity to atmospheric moisture.<sup>[14,15]</sup> Some of these MOFs can even be stirred in water or aqueous solutions without loss in crystallinity.<sup>[16]</sup> This high stability can be explained by the strong zirconium-oxygen bonds present in the SBU and the high degree of interlinking between these SBUs (each SBU is linked to twelve others). Zirconium-oxo-hydroxo clusters saturated with monocarboxylate ligands have been described in the literature before as isolable molecules,<sup>[17-19]</sup> which further emphasizes the high stability of the corresponding SBU.

We have recently reported of an extension of the class of Zr-based MOFs with long rodlike dicarboxylic acid linkers of the type HO<sub>2</sub>C[PE-P(R<sup>1</sup>,R<sup>2</sup>)-EP]CO<sub>2</sub>H (P = phenylene, E = ethynylene), which are named porous interpenetrated zirconium organic frameworks (PIZOFs).<sup>[20]</sup> These MOFs feature broadly variable substituents R<sup>1</sup> and R<sup>2</sup> (e.g. alkyl, O-alkyl, oligo(ethylene glycol), alkyne) and are

---

therefore possibly applicable for a variety of sensing, separation and catalysis purposes.

In preceding work we have shown that the concept of modulation as proposed by Kitagawa and co-workers<sup>[21,22]</sup> is especially fruitful in the synthesis of Zr-based MOFs. The modulation approach consists in the addition of a monocarboxylic acid to the synthesis mixture. This modulator then competes with the linker molecules for the coordination sites at the metal cations, leading to a reduced nucleation rate. This in turn leads to increased crystal size and increased crystallinity. Also, established synthesis procedures become more reproducible.<sup>[23]</sup> Many Zr-MOFs only become accessible by the application of modulated syntheses.<sup>[20]</sup> Recently, we have shown that the type of modulator also affects the aggregation tendency and degree of intergrowth between the formed crystals.

This work describes the preparation of polycrystalline layers of Zr-based MOFs. We use the archetype UiO-66 as a model substance to evaluate the synthetic conditions suitable for the preparation of supported Zr-MOF layers. Somewhat more restricted investigations have been performed on PIZOF-2 ( $R^1 = R^2 = \text{OMe}$ ) as an exemplary representative of the PIZOF family of materials, due to the fact that the linkers of the PIZOFs cannot be commercially purchased. Our investigations used the modulation approach.

## Experimental

All chemicals were purchased from Sigma-Aldrich and were used without further purification. Asymmetric porous alumina and titania support discs with a diameter of 18 mm and a thickness of 1 mm were purchased from Inoceramic, Germany.

### *Chemical modification of alumina support discs*

Prior to some of the preparation procedures of the layers, alumina support discs were surface modified with 3-aminopropyl-triethoxysilane (APTES) to form an amino-functionalized surface. This was done to evaluate the influence of the surface characteristics on the crystallization of the Zr-MOFs. For that purpose the alumina discs were immersed into a solution of 5 ml APTES in 20 ml ethanol. The mixture was heated to 60 °C for 2 h in a convection oven. After cooling to room temperature, the alumina discs were thoroughly washed with fresh ethanol and dried under ambient conditions.

---

### *Preparation of UiO-66 layers*

Two different monocarboxylic acids were tested as modulators for the deposition of UiO-66 layers on alumina, APTES-modified alumina, and titania supports. In a typical synthesis with benzoic acid as modulator a solution containing  $ZrCl_4$ , terephthalic acid, benzoic acid and DMF in a molar composition of 1 : 1 : 30 : 188 was prepared. Different supports were placed vertically into the solution using a Teflon holder to prevent sedimentation of material formed in the solution and to minimize crystallization on the back of the support. The mixture was then placed in a convection oven at 120 °C for 24 h.

For the syntheses with 3-chloropropanoic acid (3-cpa) as modulator a solution containing  $ZrCl_4$ , terephthalic acid, 3-cpa and DMF in a molar ratio of 1 : 1 : 30 : 750 was prepared. Again the support discs were placed vertically into the solution by using a Teflon holder. These mixtures were then placed into a convection oven at 120 °C for 96 h.

After the reaction, reacted discs were collected from the solution rinsed with fresh DMF and put into 25 ml of fresh DMF for 24 h. The samples were then activated by Soxhlet extraction with ethanol over night and dried under ambient conditions thereafter.

### *Preparation of PIZOF-2 layers*

For the preparation of PIZOF-2 layers on alumina, APTES-modified alumina or titania supports a solutions containing  $ZrCl_4$ , linker and benzoic acid in DMF in a molar ratio of 1 : 1 : 30 : 750 were produced. The supports were put into the solution held by a Teflon holder. The mixtures were placed in a convection oven at 120 °C for 24 h and after that treated the same way as described for UiO-66 layers.

3-cpa was tested as a modulating agent in the synthesis of PIZOF-2 layers as well. In this case only titania supports were used. The reaction mixtures contained  $ZrCl_4$ , linker, 3-cpa and DMF in a molar ratio of 1 : 1 : 30 : 750. The titania supports were put vertically into the solution and the mixture was then heated to 120 °C for 96 h. The drying and washing steps were the same as described before.

### *Modified drying method*

In addition to drying the supported layers simply under ambient conditions, a surfactant assisted drying process adopted from literature was tested.<sup>[24]</sup> In this method after the washing steps the samples were put in a solution containing 2 g of Span® 80 in 20 ml ethanol for 24 h and afterwards rinsed with ethanol. The samples were then kept in 25 ml of fresh ethanol for another 24 h before drying them at nearly saturated condition. For that purpose the wet samples were put in a

---



glass chamber with a beaker of ethanol. The chamber was covered with a watchglass to form a small opening. The samples were kept in this construction under nearly saturated conditions with ethanol until all ethanol was evaporated (approx. 4 days).

### *Characterization*

X-ray diffraction (XRD) patterns of the membranes were recorded using a Stoe Theta-Theta diffractometer with  $\text{CuK}\alpha$  radiation and a graphite-[002] secondary monochromator.

Scanning electron micrographs were recorded using a JEOL JSM-6700F field-emission scanning electron microscope operated with an acceleration voltage of 2 kV at a working distance of 8 mm using a LEI-detector. Samples were prepared by applying the supported membrane to a copper holder with graphite adhesive pads.

Argon sorption isotherms were recorded using a Quantachrome Autosorb-1. Prior to the measurements the samples were outgased in vacuum at 120 °C for 72 h.

## **Results and discussion**

### *UiO-66 with benzoic acid modulator*

In Fig. 1 the diffraction patterns of the UiO-66 layers grown on bare alumina, on APTES modified alumina, and on titania with the use of benzoic acid as a modulator are shown. All three patterns show the reflection set typical for phase pure UiO-66 in addition to the reflections that are caused by either the alumina or the titania supports. A comparison of the intensities caused by the MOF to those caused by the support gives a first hint for the coverage of the surface with crystalline material. The higher the intensities of the UiO-66 reflections in relation to the alumina / titania reflections, the more MOF is present and hence the better the coverage is. Following this argument, the X-Ray diffraction patterns indicate the best surface coverage in the case of APTES functionalized alumina whereas crystallization on bare alumina gives the lowest intensities and therefore the lowest coverage.

---

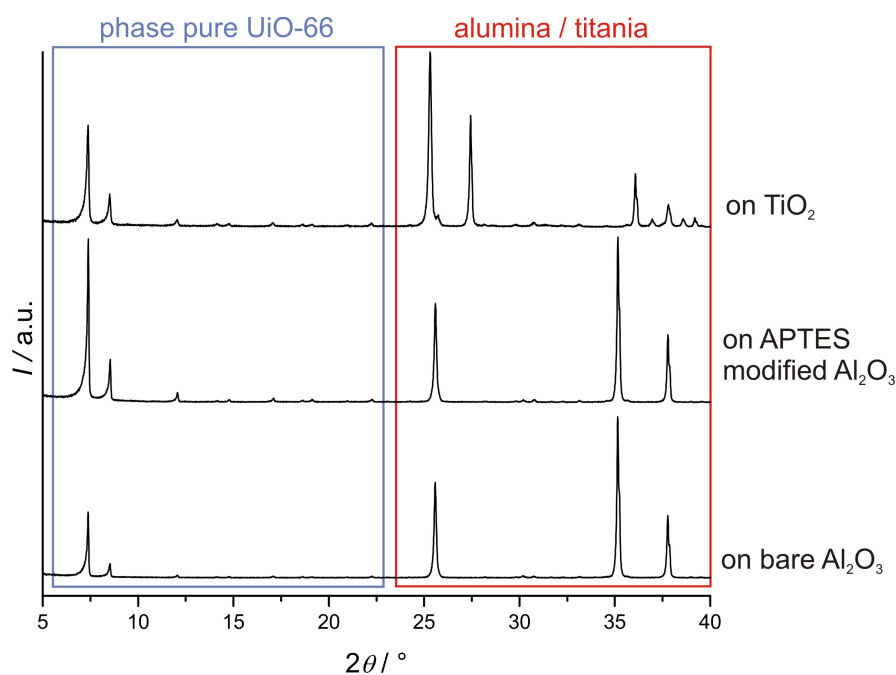


Fig.1: Diffraction patterns of UiO-66 layers grown on different support materials with using benzoic acid modulator.

These guesses can be confirmed by the SEM images taken of the samples (Fig. 2). On the bare alumina support (Fig. 2 a) large areas of the support are uncovered. Interestingly, in those regions where there is coverage with the typical octahedrally shaped UiO-66 crystals, the crystals are well intergrown. This is not the case for the titania support. Here the coverage shows clearances as well, but the crystals are much more homogeneously distributed over the surface, but crystallization sites are simply not dense enough to show a sufficient degree of intergrowth. The SEM micrograph of the layer grown on the APTES functionalized alumina support (Fig. 2 c) reveals a dense covering of the surface with intergrown crystals. When looking closer at the surface, it becomes obvious that cracks have formed in the layer, which makes the sample inapplicable as a membrane. These cracks probably occur during the drying process. The cross section (Fig. 2 d) shows a layer thickness of approximately only 1  $\mu\text{m}$ .

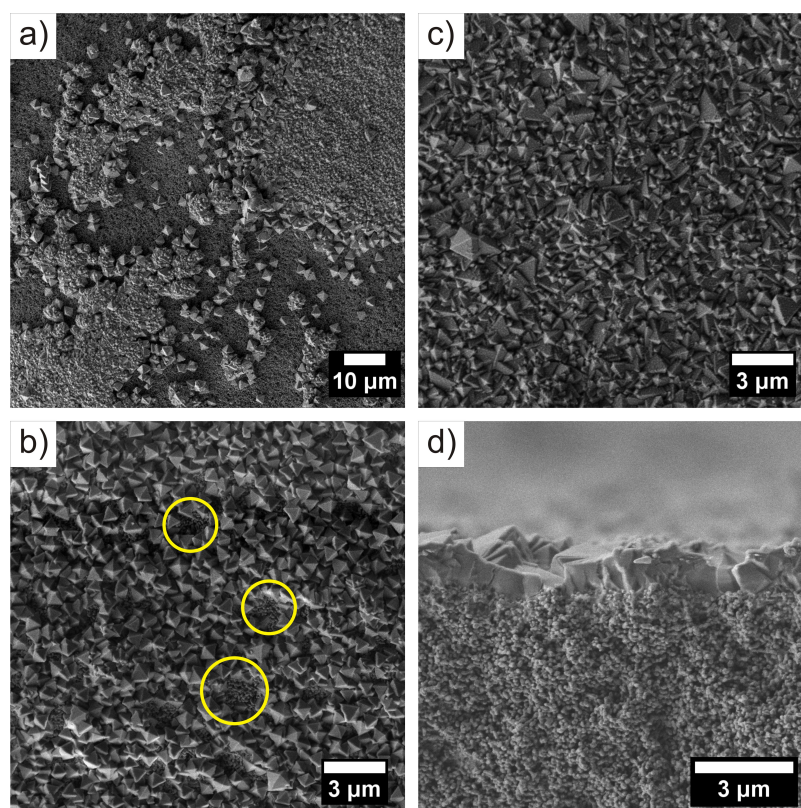


Fig. 2: Scanning electron micrographs of UiO-66 grown on different supports with benzoic acid modulator. a) on bare alumina, b) on titania (yellow circles indicate some spots where the support material is still visible), c) and d) on APTES modified alumina (top view and cross section respectively).

From these experiments it becomes obvious that the Zr-MOF shows a favored nucleation in the presence of amino-groups. This behavior may be explained by an electrostatic attraction between the support and the growing crystals. In the acidic reaction mixture the APTES functionalized alumina support would carry a positive surface charge due to a protonation of the amino groups. The nuclei of the Zr-MOF on the other hand are negatively charged because of deprotonated dicarboxylic acid linkers that have to be present on the surface of the particles during the growth process. The growing MOF particle could therefore be bound to the substrate by electrostatic adhesion and an “*in situ* seeding” of the alumina surface would occur.

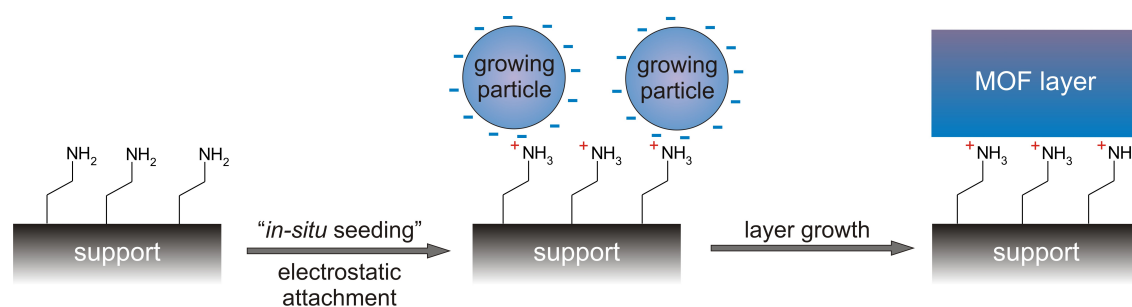


Fig. 3: Possible mechanism of “*in situ* seeding” by electrostatic adhesion that may occur when APTES modified alumina is used as support material.

*PIZOF-2 with benzoic acid modulator*

The same principles (benzoic acid modulator, same support materials) as in the syntheses of UiO-66 layers were applied to the synthesis of PIZOF-2 layers as an exemplary member of the PIZOF family of Zr-MOFs. The diffraction patterns in Fig. 4 show that phase pure PIZOF-2 was deposited regardless of the substrate material. Similar to the results of the UiO-66 again the X-ray diffraction pattern of the sample crystallized on bare alumina shows the lowest ratio between the intensities caused by the MOF and those of the alumina whereas a similar ratio is found with APTES modified alumina and titania. This means that the amount of crystals on bare alumina is the lowest out of the three.

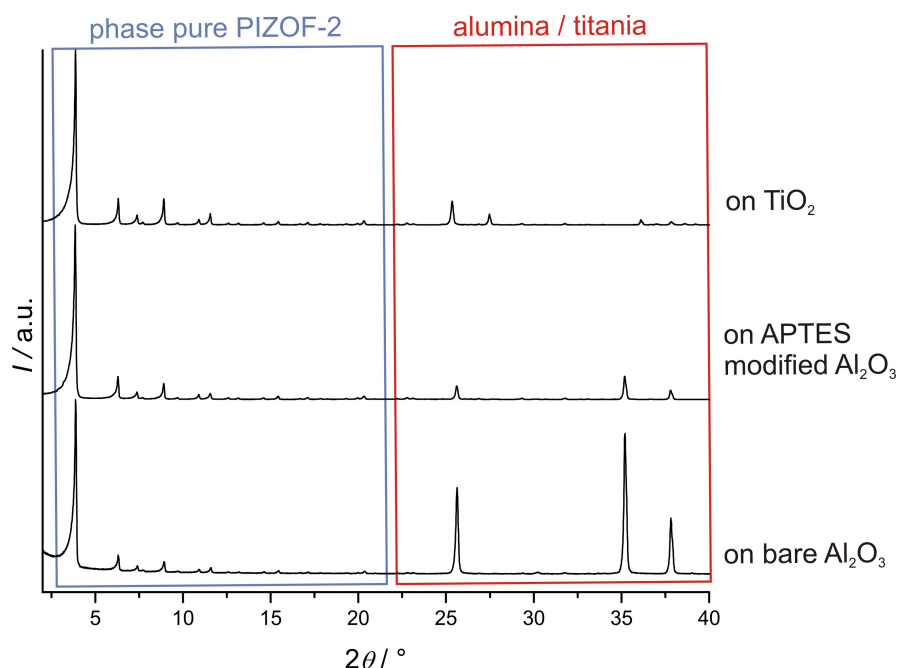


Fig. 4: Diffraction patterns of PIZOF-2 layers grown on different support materials with using benzoic acid modulator.

SEM images of the samples confirm this. With bare alumina (Fig. 4 a) only few and mostly isolated octahedral crystals are found. The crystal size is much larger than in the case of UiO-66. This is not surprising since large crystal sizes were reported before for precipitated PIZOF-2 as well.<sup>[20]</sup> In comparison to that the SEM image of the sample grown on APTES functionalized alumina shows the presence of similarly large PIZOF-2 crystals, but in addition to that smaller crystals occupying the surface between the large ones can be observed. This shows once more that the amino function facilitates the crystallization of Zr-dicarboxylates. The most homogeneous PIZOF-2 layer was obtained on titania substrate. The scanning electron micrographs (Fig. 5 c and d) show a layer of intergrown crystals (but with cracks) with a thickness of approx. 5  $\mu\text{m}$ . In that case of UiO-66 a homogeneous distribution of relatively small crystals was found on the titania support that were not intergrown. Although it seems contradictory at first, these observations are accordable. The crystal size of PIZOF-2 is at least 10 times bigger than that of UiO-

66. When the number of uniformly distributed crystallization sites is equal for both materials, an intergrown layer can form when the crystals reach a sufficient size. This is the case for PIZOF-2, but not for UiO-66.

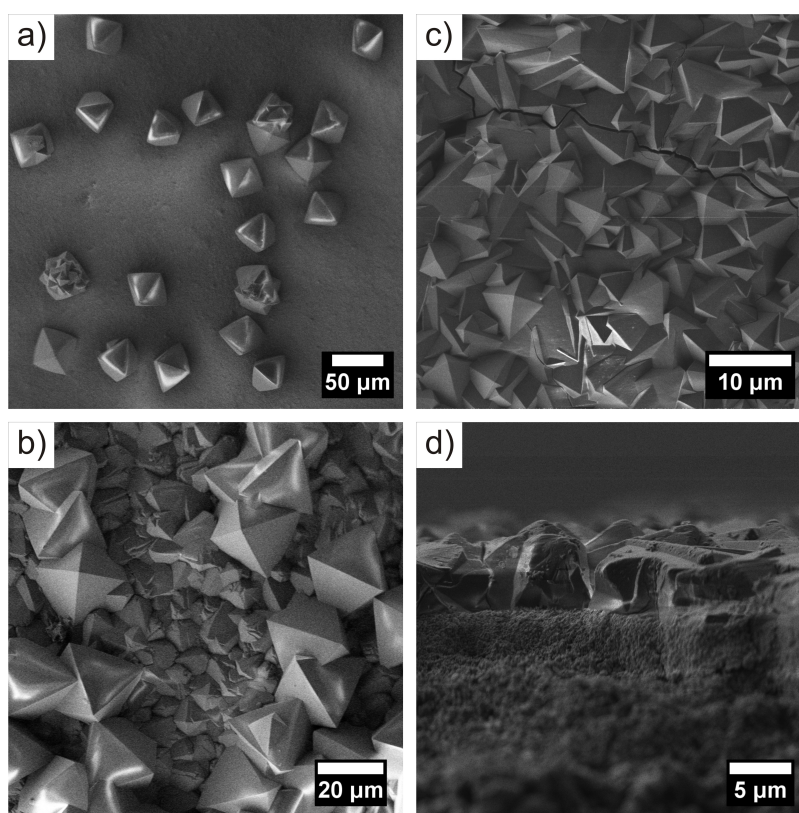


Fig. 5: Scanning electron micrographs of PIZOF-2 grown on different supports with benzoic acid modulator. a) on bare alumina, b) on APTES modified alumina, c) and d) on titania (top view and cross section respectively).

The very similar results of the crystallization of UiO-66 and PIZOF-2 on different support materials indicate a good transferability of principle reaction and crystallization mechanisms from one Zr-MOF to another. Therefore similar results can be expected for other UiO-type MOFs and other members of the PIZOF family of MOFs.

#### *UiO-66 with 3-cpa modulator*

The use of 3-chloropropanoic acid as modulator in the synthesis of UiO-66 has proven to promote the formation of large and intergrown crystals in our laboratory before. With the use of 3-cpa mainly heterogeneous nucleation on the walls of the reaction vessel is observed. These two characteristics seem very well suited for the deposition of layers.

With 3-cpa as modulator, the X-ray diffraction patterns (Fig. 6) of the samples prepared with different substrates look all very similar. In all three cases, no additional reflections besides those of the MOF and of the support are visible. From

comparing the intensities of the UiO-66 reflections to those caused by the supports it becomes clear that a high amount of material was deposited in all three cases. Moreover from comparing the intensities in the final product with those in a simulated powder pattern (Fig. 7), a preferred orientation with the (100) planes parallel to the surface can be found. This means that the octahedrally shaped crystals are pointing out of the surface of the membrane with their vertices. This can be explained by the competitive growth model.<sup>[25]</sup> When the density of crystal nuclei in random orientations on the surface is high enough, the crystals oriented with the fastest growing direction perpendicular to the surface will simply outgrow the other orientations.

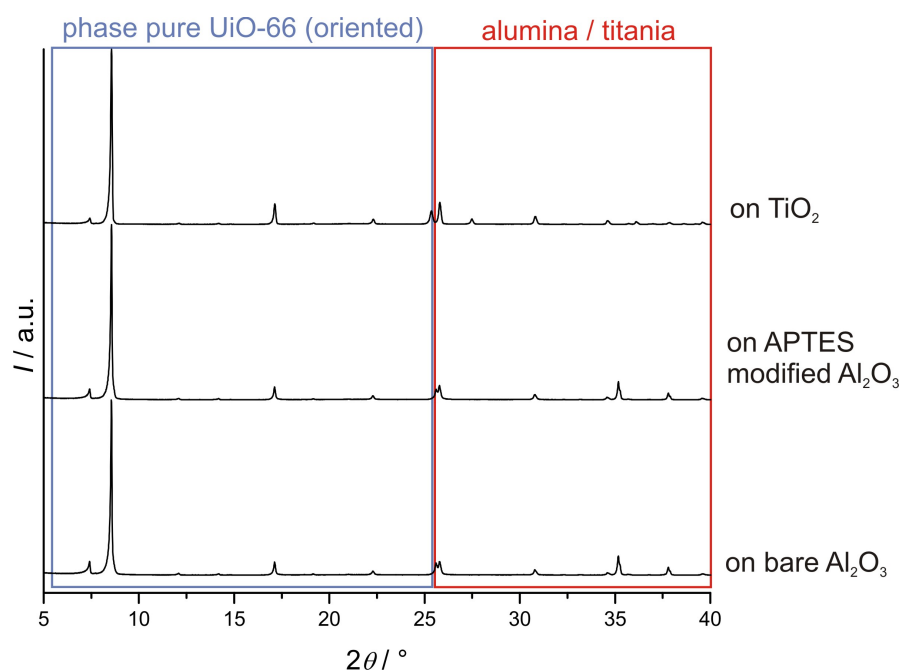


Fig. 6: Diffraction patterns of UiO-66 layers grown on different support materials with using 3-cpa modulator.

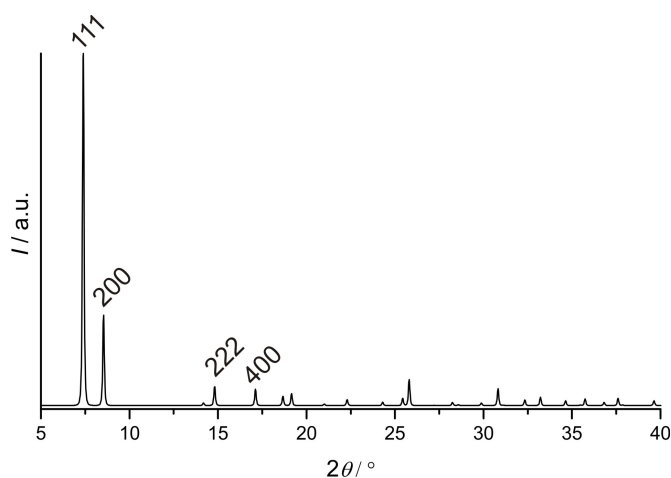


Fig. 7: Simulated powder pattern of UiO-66 with  $hkl$  indices of some mayor reflections.

Like the diffraction patterns the SEM images (Fig. 8) of the three samples look similar as well. They all show intergrow layers of UiO-66 with a thickness of 7 –

8  $\mu\text{m}$ . Again all samples show (possibly drying) cracks favorably running along grain boundaries. The orientation of the crystals becomes apparent in the micrographs as well. In the top view images, the vertices of the octahedral crystals are pointing out of the layer.

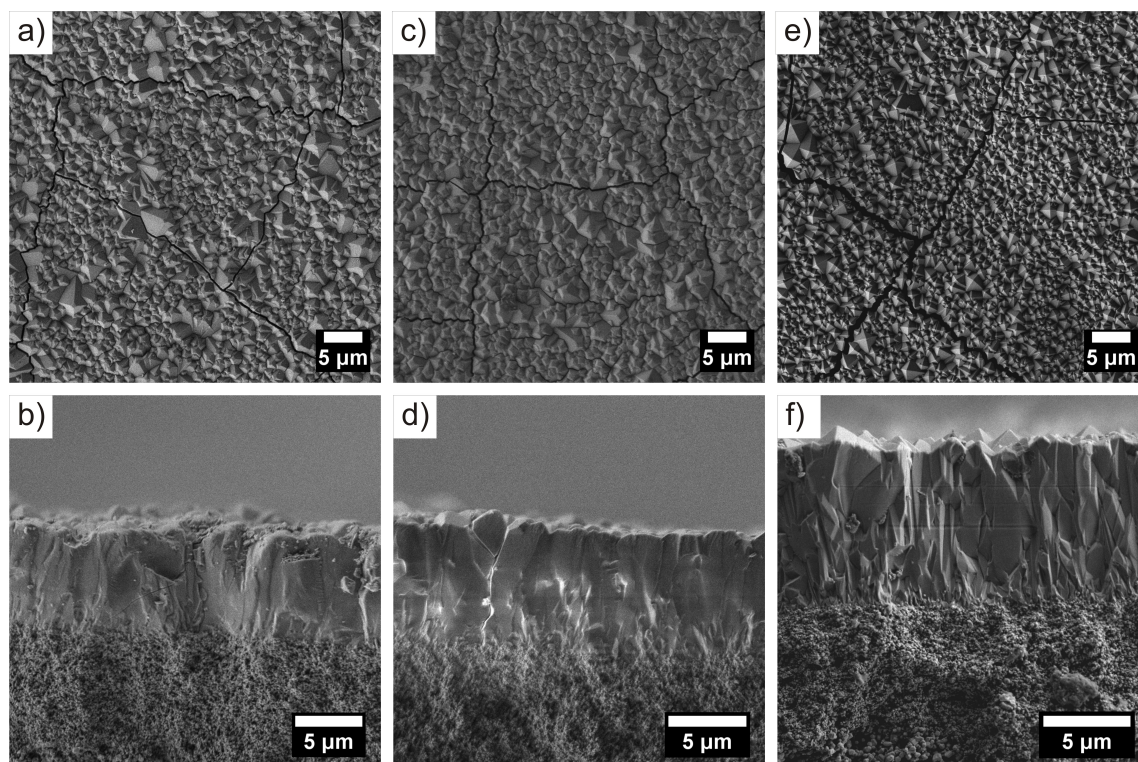


Fig. 8: Scanning electron micrographs of UiO-66 grown on different supports with 3-cpa modulator. a) and b) on bare alumina (top view and cross section), c) and d) on titania (top view and cross section), e) and f) on APTES modified alumina (top view and cross section).

These results show that the kind of support is irrelevant for the crystallization of UiO-66 when 3-chloropropanoic acid is used for the modulating effect. Regardless of the substrate material preferentially oriented layers with the same thickness are formed.

#### *PIZOF-2 with 3-cpa modulator*

Since the use of 3-cpa modulator yielded thick and intergrown layers in the synthesis of UiO-66, it was also tested for PIZOF-2. This time solely titania supports were used because the amount of linker was limited and experiments with benzoic acid modulator had shown the best results on this kind of substrate.

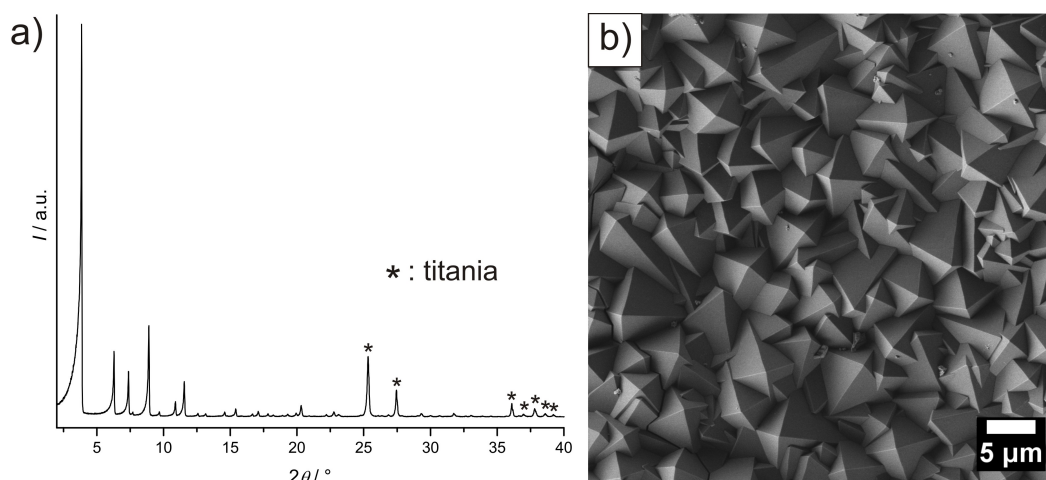


Fig. 8: X-ray diffraction pattern (a) of PIZOF-2 layer on titania prepared with 3-cpa modulator and corresponding SEM micrograph (b).

XRD pattern of the sample (Fig. 8 a) confirms once more that the MOF was crystallized phase pure and in a high amount on the support. An intergrown layer of PIZOF-2 crystals can be seen in the SEM image (Fig. 8 b). Again fine cracks are running through the sample. These results confirm once more the transferability of suitable reaction parameters from the synthesis of UiO-66 to PIZOF-2.

#### *Alternative drying methods*

Since all layers produced with drying the samples under ambient conditions have shown the presence of cracks, alternative drying approaches were tested for UiO-66 and PIZOF-2.

To evaluate the accessibility of the pore system after the drying step with Span<sup>®</sup> 80, powder samples of UiO-66 and PIZOF-2 (obtained from a synthesis with 3-cpa) were dried under the same conditions as the membranes (two samples of each material; one dried under ambient conditions, the other in a surfactant assisted drying procedure). Argon sorption measurements were carried out with all samples. The isotherms of the UiO-66 sample dried with surfactant in comparison to the one dried without surfactant are shown in Fig. 9. The BET surface area determined from the data for the material dried with the surfactant of  $1400 \text{ m}^2 \text{ g}^{-1}$  is only slightly lower than the surface area of the material dried without the use of a surfactant which amounts to  $1600 \text{ m}^2 \text{ g}^{-1}$ . The form of the isotherm remains unchanged. This indicates that the pore system is still accessible.



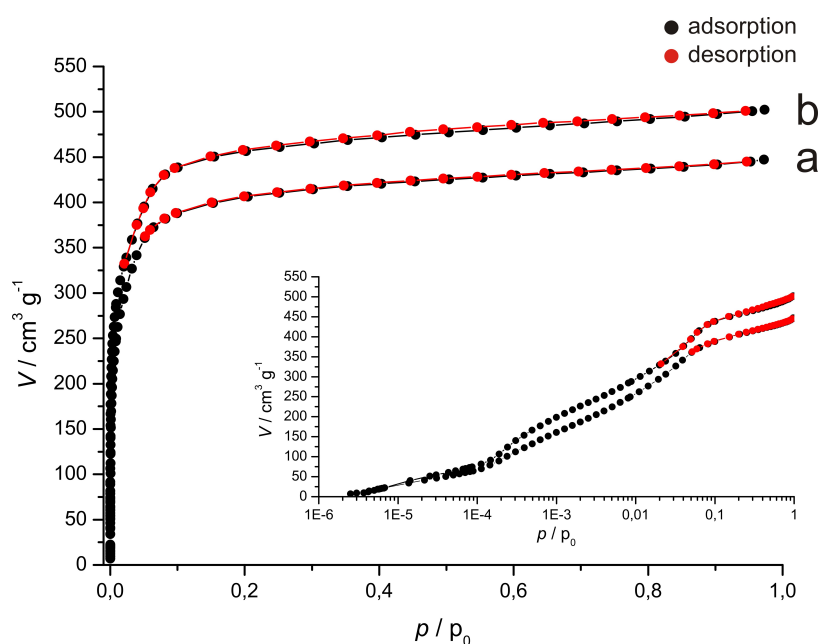


Fig. 9: Argons sorption isotherms of UiO-66 dried under ambient conditions (b) and with a surfactant assisted drying process (a). The inset shows the same isotherms plotted logarithmical.

Similar observations can be made in the argon sorption of the two differently dried samples of PIZOF-2 (Fig. 10). Although the surface area is reduced from approx.  $1890 \text{ m}^2 \text{ g}^{-1}$  to  $1530 \text{ m}^2 \text{ g}^{-1}$  with the use of a surfactant, the slopes of the isotherms remain unchanged. This means that the pore characteristics like pore diameter and geometry are not affected by the surfactant adsorbed by the MOF. It is particularly interesting to note that the desorption branch of the isotherm recorded of the material dried with Span<sup>®</sup> 80 does not meet the adsorption branch. This clearly shows that the desorption of argon is affected by the surfactant, which in fact was the intention in using this drying method. A similar hysteresis can be observed in sorption isotherms of polymers.<sup>[26]</sup> This observation therefore gives the hint, that the adsorbed Span<sup>®</sup> 80 behaves similar to a polymer on the surface of PIZOF-2.

Since the sorption experiments for both UiO-66 and PIZOF-2 have proven no negative influence of the surfactant assisted drying method (like a plugging of the pores for example), layers of both materials were crystallized. In these experiments only the materials synthesized with 3-cpa on titania were tested.

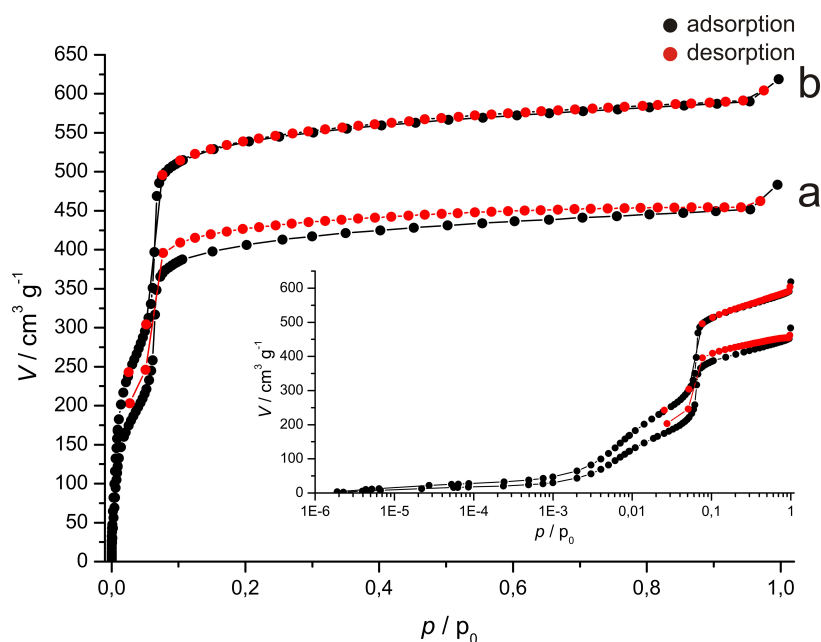


Fig. 10: Argons sorption isotherms of PIZOF-2 dried under ambient conditions (b) and with a surfactant assisted drying process (a). The inset shows the same isotherms plotted logarithmical.

Fig. 11 shows the diffraction pattern and the corresponding scanning electron micrograph of the UiO-66 layer dried with surfactant. The XRD pattern shows all reflections of the MOF with the previously described preferred orientation. In addition to these reflections, only those of the titania support are apparent. No additional phase has formed during the modified drying process. Unfortunately the SEM image shows the presence of cracks in the layer. The surfactant assisted drying step is obviously not capable of preventing the formation of these cracks, even though they seem to be smaller than in the material dried under ambient conditions (Fig. 8 e).

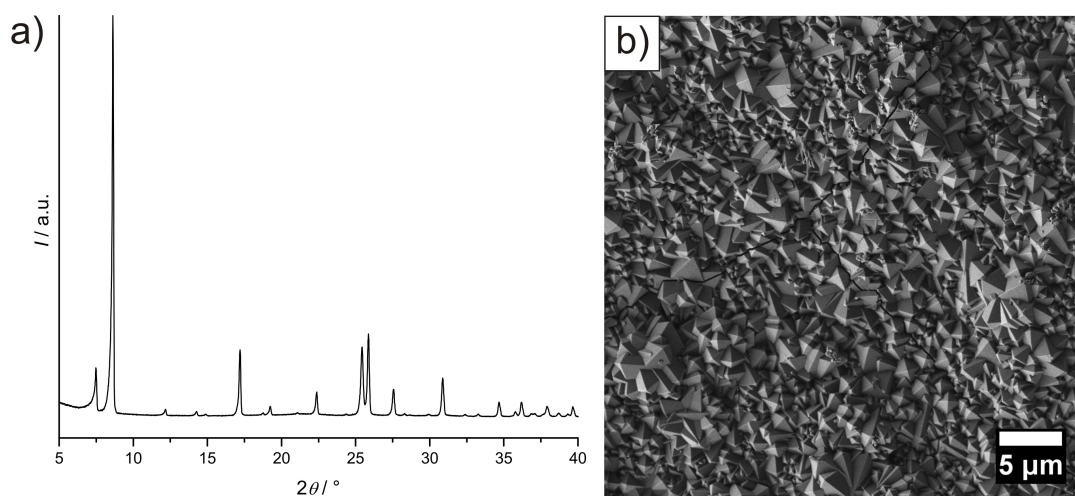


Fig. 11: X-ray diffraction pattern (a) and corresponding SEM image (b) of a UiO-66 layer on titania dried with the use of the surfactant Span® 80.

The results of the corresponding experiments with PIZOF-2 are similar to those of UiO-66. The XRD pattern presented in Fig. 12 a exhibit no hint for an additional phase formed during the drying as well. Only the reflections caused by PIZOF-2 and those of the titania support can be found. The SEM micrograph in Fig. 12 b again shows the presence of cracks in the PIZOF-2 layer.

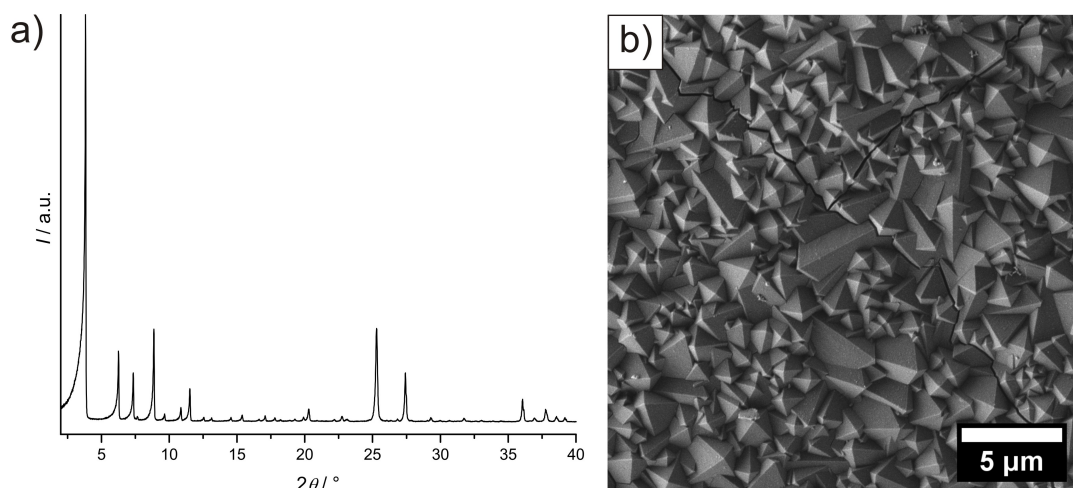


Fig. 12: X-ray diffraction pattern (a) and corresponding SEM image (b) of a PIZOF-2 layer on titania dried with the use of the surfactant Span® 80.

## Summary

The investigations on the influence of different ceramic support materials on the layer growth of Zr-MOFs have show a preference of amino-functionalized surfaces. This may be explained by electrostatic interactions between the substrate surface and the MOF nuclei which could lead to “*in situ* seeding”.

The choice of modulator for the synthesis of Zr-MOF layers of course also has an influence in respect to crystal size and therefore layer thickness and degree of intergrowth of the layers. The best results were obtained with 3-chloropropanoic acid as modulator. In this case heterogeneous nucleation is so pronounced that the choice of support material becomes subordinate. Intergrown layers with comparable thicknesses are obtained regardless of the substrate materials. Unfortunately it was not possible to prevent the formation of drying cracks in all MOF layers. A modified drying protocol with the use of a surfactant and slower evaporation of the solvent did not prove successful.

## References

- [1] J. Caro, M. Noack, *Microporous Mesoporous Mater.* **115** (2008) **215**.
- [2] N. Ehlert, P.P. Mueller, M. Stieve, T. Lenarz, P. Behrens, *Chem. Soc. Rev.* **42** (2013) **3847**.
- [3] S. Kitagawa, R. Kitaura, S. Noro, *Angew. Chem. Int. Ed.* **43** (2004) **2375**.
- [4] O.M. Yaghi, M. O'Keeffe, N.W. Ockwig, H.K. Chae, M. Eddaoudi, J. Kim, *Nature* **432** (2003) **705**.
- [5] K.K. Tanabe, S. Cohen, *Chem. Soc. Rev.* **40** (2011) **498**.
- [6] J.-R. Li, R.J. Kuppler, H.C. Zhou, *Chem. Soc. Rev.* **38** (2009) **1477**.
- [7] B. Chen, S. Xiang, G. Qian, *Acc. Chem. Res.* **43** (2010) **1115**.
- [8] L.J. Murray, M. Dinca, J.R. Long, *Chem. Soc. Rev.* **38** (2009) **1294**.
- [9] O. Shekhan, J. Liu, R.A. Fischer, C. Wöll, *Chem. Soc. Rev.* **40** (2011) **1081**.
- [10] L. Ma, W. Lin, *Top. Curr. Chem.* **293** (2010) **175**.
- [11] K.A. Cychoz, A.J. Matzger, *Langmuir* **26** (2010) **17198**.
- [12] J.J. Low, A.I. Benin, P. Jakubczak, J.F. Abrahamian, S.A. Faheem, R.R. Willis, *J. Am. Chem. Soc.* **131** (2009) **15834**.
- [13] S.S.Kaye, A. Dailly, O.M. Yaghi, J.R. Long *J. Am. Chem. Soc.* **129** (2007) **14176**.
- [14] J.H. Cavka, S. Jakobsen, U. Olsbye, N. Guillou, C. Lamberti, S. Bordiga, K.P.Lillerud, *J. Am. Chem. Soc.* **130** (2008) **13850**.
- [15] L. Valenzano, B. Civalieri, S. Chavan, S. Bordiga, M.H. Nilsen, S. Jakobsen, K.P. Lillerud, C. Lamberti, *Chem. Mater.* **23** (2011) **1700**.
- [16] G. Wißmann, A. Schaate, S. Lilienthal, I. Bremer, A.M. Schneider, P. Behrens, *Microporous Mesoporous Mater.* **152** (2012) **64**.
- [17] G. Kickelbick, U. Schubert, *Chem. Ber.* **130** (1997) **473**.
- [18] P. Piszczek, A. Radtke, A. Grodzicki, A. Wojtczak, J. Chojnacki, *Polyhedron* **26** (2007) **679**.
- [19] V. Guillermin, S. Gross, C. Serre, T. Devic, M. Bauer, G. Férey, *Chem. Commun.* **46** (2010) **767**.
- [20] A. Schaate, P. Roy, T. Preuße, S.J. Lohmeier, A. Godt, P. Behrens, *Chem. Eur. J.* **17** (2011) **9320**.
-

- 
- [21] T. Tsuruoka, S. Furukawa, Y. Takashima, K. Yoshida, S. Isoda, S. Kitagawa, *Angew. Chem. Int. Ed.* **48** (2009) **4739**.
- [22] S. Diring, S. Furukawa, Y. Takashima, T. Tsuruoka, S. Kitagawa, *Chem. Mater.* **22** (2010) **4531**.
- [23] A. Schaate, P. Roy, A. Godt, J. Lippke, F. Waltz, M. Wiebcke, P. Behrens, *Chem. Eur. J.* **17** (2011) **6643**.
- [24] Y. Yoo, V. Varela-Guerrero, H.-K. Jeong, *Langmuir* **27** (2011) **2652**.
- [25] A. van der Drift, *Philips Research Report* **22** (1967) **267**.
- [26] J. Weber, J. Schmidt, A. Thomas, W. Böhlmann, *Langmuir* **26** (2010) **15650**.
-



## 4 Conclusion and Outlook

The first part of this work deals with the fabrication of silica sodalite layers. In order to use a microporous material as a membrane, the pores have to be accessible and empty. In the case of zeolitic materials this is accomplished by a calcination process. The narrow pores of sodalite which on the one hand make this material especially interesting for the separation of small gases (hydrogen in particular) are on the other hand a major drawback when it comes to activating the material. For a successful calcination, oxygen has to enter the pores and the combustion products have to leave the pores. In the case of sodalite this is only possible when high temperatures (1000 °C) are used and the breathing effects of the framework become distinct enough to let larger molecules pass. Such harsh conditions resulted in the formation of cracks in the sodalite membranes probably due to a mismatch in the thermal expansion between active layer and ceramic support. A two-layered membrane consisting of silicalite-1 and sodalite was successfully synthesized using simple and fast seeding steps by rubbing nanocrystalline seeds on the substrates. Single gas permeation experiments have shown that the silicalite-1 membranes produced in this work were of good quality. Unfortunately, the introduction of the additional layer of the robust zeolite silicalite-1 (which has larger pores) did not have the effect hoped for. It could not act as a mediator between the sodalite and the alumina support and cracks were apparent after fully template removal of the sodalite again.

Nonetheless the presented work has shown the possibility of producing multi-layered zeolite membranes by using a simple seeding method which has worked for both sodalite and silicalite-1. Multi-layered zeolite membranes (with other combinations of materials) could be very interesting in building membrane reactors serving different purposes at the same time. It could for example be possible to build up a sequence of materials in which the first layer might serve as a size selective membrane whereas the second layer could be a catalyzing one or the other way around.

---

The work presented has clearly shown that the calcination temperature of 1000 °C that is necessary to obtain a fully activated silica sodalite eventually leads to cracks in the sodalite layer. It is therefore doubtful if silica sodalite membranes can be produced using a space filling agent in the synthesis of SOD. It might be possible to find reaction parameters for the synthesis of silica sodalite layers prepared by a template-free secondary growth. This concept has for example worked out for the synthesis of MFI-type membranes,<sup>[1]</sup> but has not been reported for sodalite thus far. Another possibility that could be tested for the synthesis of silica sodalite membranes is the use of other space filling agents. Silica sodalite prepared with ethylene glycol was reported to be free of the space-filler after heating the material to only 680 °C under nitrogen.<sup>[2]</sup> However, earlier work in our group had shown that the pores of an ethylene glycol silica sodalite treated this way are still largely blocked by carbonaceous residues. It therefore appears doubtful whether the application of such a low calcinations temperature is suited for the preparation of crack-free and activated silica sodalite membranes.

The second part of this thesis deals with the investigation of the influence of different monocarboxylic acid modulators on the synthesis of UiO-66. The modulation idea was originally published by and adopted from the group of KITAGAWA<sup>[3]</sup> and then successfully transferred by our group to the synthesis of Zr-based MOFs. The aim of the presented work was to find suitable reaction parameters that yield large aggregates of the Zr-MOF crystallites. Up to date all published syntheses for UiO-66 lead to the formation of nanoparticles. To eventually be able to synthesize supported membranes of UiO-66 it is necessary to be able to produce larger micrometer-sized crystals. Otherwise the intergrowth in the layers may not be sufficient. In fact the modulator 3-chloropropanoic acid was found to not only facilitate the formation of larger crystals but also yield strongly intergrown products at the same time. Further investigation led to the finding that in fact *N,N*-dimethyl-beta-alanine that is formed in a reaction between the dimethylamine (derived from the solvent *N,N*-dimethylformamide by decomposition) and 3-chloropropanoic acid is actually accountable for these findings. With increasing amounts of 3-chloropropanoic acid the crystallization occurs preferably on the walls of the reaction vessel. This is a good hint that

---

[1] M. Pan, S.Y. Lin, *Microporous Mesoporous Mater.* **43** (2001) **319**.

[2] R.S.P. King, S.E. Dann, M.R.J. Elsegood, P.F. Kelly, R.J. Mortimer, *Chem. Eur. J.* **15** (2009) **5441**.

[3] T. Tsuruoka, S. Furukawa, Y. Takashima, K. Yoshida, S. Isoda, S. Kitagawa, *Angew. Chem. Int. Ed.* **48** (2009) **4739**.



heterogeneous nucleation becomes more pronounced. To investigate the nucleation mechanisms in more detail, *in situ* experiments like time-resolved *in situ* X-ray diffraction using synchrotron radiation would be helpful. This method has already been used in clarifying formation parameters like induction times, rate constants, formation of a precursor phase, or the type of reaction control for some MOFs.<sup>[4,5]</sup>

In our explanatory approach for the modulation effects we assume that clusters similar to the SBUs finally found in the Zr-MOFs are formed in solution which are terminated by the monocarboxylic acids added to the reaction mixtures. Crystal structures of similar complexes were already described in literature.<sup>[6-8]</sup> In some cases the solvents used for crystallizing the complexes are incorporated in the final structure by additionally coordinating the Zr-cluster. None of the reported clusters was synthesized in DMF which is the common solvent in the synthesis of Zr-containing MOFs. It would therefore be interesting to investigate on the possibility of synthesizing such complexes from DMF to shed some light on the theory of modulating effects of monocarboxylic acids in DMF. We have already done some experiments concerning this idea in our laboratory. The data obtained from single crystal X-ray structural analyses of precipitates formed from solutions containing ZrCl<sub>4</sub>, monocarboxylic acid and DMF was not fully evaluable. But it does give reason to believe that Zr-clusters containing the monocarboxylic acid modulator form in DMF containing solutions as well.

In the third part of this thesis the influence of different substrates on the crystallization of Zr-MOF layers is evaluated. In addition to that two different modulators were tested. With benzoic acid modulator, crystal sizes remain too small in the case of UiO-66 to reliably form dense layers. However the influence of the surface properties of different substrates becomes evident with this modulator. Pristine alumina surfaces do not lead to the formation of a dense layer of crystals, but crystal growth occurs only spot-wise. Titania surfaces on the other hand lead to a more homogeneously distributed arrangement of nucleation sites over the whole surface of the support.

---

[4] F. Millange, M.I. Medina, N. Guillou, G. Férey, K.M. Golden, R.I. Walton, *Angew. Chem. Int. Ed.* **49** (2010) **763**.

[5] J. Cravillon, C.A. Schröder, R. Nayuk, J. Gummel, K. Huber, M. Wiebcke, *Angew. Chem. Int. Ed.* **50** (2011) **8067**.

[6] G. Kickelbick, P. Wiede, U. Schubert, *Inorg. Chim. Acta* **284** (1999) **1**.

[7] F.R. Kogler, M. Jupa, M. Puchberger, U. Schubert, *J. Mater. Chem.* **14** (2004) **3133**.

[8] P. Piszczek, A. Radtke, A. Grodzicki, A. Wojtczak, J. Chojnacki, *Polyhedron* **26** (2007) **679**.

It was also clearly shown that an amino-functionalized alumina surface strongly influences the nucleation. Possibly because of electrostatic interactions nucleation occurs preferentially on such surfaces. The transferability of these basic findings from UiO-66 to structurally related PIZOFs was proven drawing on the example of PIZOF-2, a prototypical member of this family of Zr-MOFs. The finding from the second part of this work, namely that 3-chloropropanoic acid can be used to obtain larger and more intergrown UiO-66 crystals led to a well reproducible synthesis route for the deposition of UiO-66 layers. The pronounced tendency to heterogeneous nucleation with this modulator favors the formation of dense layer so much that the surface properties of the support are no longer relevant. The layer thickness of UiO-66 remained the same on all tested supports. Similar effects (intergrowth and heterogeneous nucleation) were observed for PIZOF-2 synthesized with 3-chloropropanoic acid as well. Here again the use of this modulator leads to improvements in terms of reproducibility and reliability of the synthesis.

All Zr-MOF layers that were produced in the course of this work have shown cracks. These were probably caused during the drying step by capillary stress. A surfactant assisted drying method that was reported to be beneficial in reducing such drying cracks in IRMOF-3 layers<sup>[9]</sup> was tested but did not improve the results. That is why the membranes could not be tested for possible separation tasks. Possibly, other means of drying the layers can be tested in the future. We have already done some first experiments with extracting the solvents with supercritical CO<sub>2</sub>. Further experiments varying different parameters like extraction time and speed are necessary to fully evaluate the quality of this method for Zr-MOF layers. Until now it seems to produce even larger cracks in the UiO-66 films, but for PIZOF-2 films the early results looked promising.

Even the cracked layers may find applications in other fields than membranes. Since PIZOFs are highly modular due to their tunable linkers they may be promising candidates for sensing devices. In this field of application a layer of the active material is for example deposited on a quartz crystal microbalance. When a tested gaseous species is taken up into the pore system of the active layer, the slight shift in weight can be detected by a shift in the resonance frequency of the quartz. The linker in the PIZOF may be equipped with very specific side chains to

---

[9] Y. Yoo, V. Varela-Guerrero, H.-K. Jeong, *Langmuir* **27** (2011) **2652**.

exhibit tailored sorption properties for particular gases. Also for biomedical applications like local drug delivery from an implant-bound film, the coatings do not have to be crack-free.

---



## 5 Curriculum Vitae

**Imke Bremer**

**Date of birth** February 02, 1983

**Place of birth** Twistringen

**Family status** Single

**Nationality** German

### Education

**Since December 2008** **Dissertation** at the Institut für Anorganische Chemie of the Leibniz Universität Hannover in the group of Prof. Dr. Peter Behrens.

**October 2002 – November 2008** **Study** of Chemistry (Diplom)  
Diplom in November 2008 at the Institut für Anorganische Chemie of the Leibniz Universität Hannover  
Final grade: sehr gut  
Titel of diploma thesis: "Strategien zur Oberflächenmodifizierung amorpher und kristalliner Silica-Nanopartikel"

**September 1995 – June 2002** **School Education** at the Gymnasium Syke  
Abitur (A-levles)

**September 1993 – June 1995** **School Education** at the Orientierungsstufe Twistringen

**September 1989 – June 1993** **School Education** at the Grundschule Twistringen

---

## 6 List of Publications

### Articles

F. Heinroth, I. Bremer, S. Münzer, P. Behrens, C. Reinhardt, S. Passinger, C. Orth, B. Chichkov, *Microporous Mesoporous Mater.* **119** (2009) **104**; Titel: "Microstructured templates produced using femtosecond laser pulses as templates for the deposition of mesoporous silicas"

G. Wissmann, A. Schaate, S. Lilienthal, I. Bremer, A.M. Schneider, P. Behrens, *Microporous Mesoporous Mater.* **152** (2012) **64**; Titel: "Modulated synthesis of Zr-fumarate MOF"

### Scientific Talks

23. *Deutsche Zeolith-Tagung* Erlangen, Germany. Authors: I. Bremer, A. Schaate, P. Roy, T. Preuße, A. Godt, P. Behrens. Title: "Preparation of Zr-MOF Layers for Possible Membrane Application Using Modulated Synthesis"

24. *Deutsche Zeolith-Tagung* Magdeburg, Germany. Authors: G. Wissmann, A. Schaate, I. Bremer, A.M. Schneider, P. Behrens. Title: "Modulated Synthesis of Zr-fumarate MOF"

### Poster Presentations

21. *Deutsche Zeolith-Tagung* Kiel, Germany. Authors: I. Bremer, P. Behrens. Title: "Enabling Mesoporous Materials for Click Chemistry"

22. *Deutsche Zeolith-Tagung* München, Germany. Authors: I. Bremer, S. Münzer, F. Waltz, J. Caro, P. Behrens. Title: "Preparation of Dense Sodalite Layers on Top of Alumina Supported Silicalite-1 Membranes"

5<sup>th</sup> *International Zeolite Membrane Meeting* Loutraki, Greece. Authors: I. Bremer, S. Münzer, J. Caro, P. Behrens. Title: "Preparation of Dense Sodalite Layers on Top of Silicalite-1 Membranes"

---

*1<sup>st</sup> International Workshop ENMIX* Antwerp, Belgium. Authors: I. Bremer, A. Schaate, P. Behrens. Title: "Preparation of Alumina Supported Zr-MOF Layers Using Modulated Synthesis"

*Hybrid Materials 2011* Strasbourg, France. Authors: I. Bremer, A. Schaate, P. Roy, T. Preuße, A. Godt, P. Behrens. Title: "Preparation of Supported Zr-MOF layers Using Modulated Synthesis"

*5<sup>th</sup> International FEZA Conference* Valencia, Spain. Authors: I. Bremer, A. Schaate, P. Roy, T. Preuße, H. Bux, J. Caro, A. Godt, P. Behrens. Title: "Using Modulated Synthesis to Prepare the First Supported Zr-based MOF Membranes"

*LNQE Nanoday 2011* Hannover, Germany. Authors: I. Bremer, A. Schaate, P. Roy, T. Preuße, H. Bux, J. Caro, A. Godt, P. Behrens. Title: "Using Modulated Synthesis to Prepare the First Supported Zr-based MOF Membranes"

*24. Deutsche Zeolith-Tagung* Magdeburg, Germany. Authors: P. Zerner, A. Schaate, I. Bremer, P. Behrens. Title: "Studies on the Synthesis of Porous Coordination Polymers Based on Titanium(IV)"

*MOF2012* Edinburgh, Great Britain. Authors: G. Wißmann, S. Schaate, S. Lilienthal, I. Bremer, A.M. Schneider, P. Behrens. Title: "A Water-born Zr-based Porous Coordination Polymer: Modulated Synthesis of Zr-fumarate MOF"

*IMMS 2013* Awaji, Japan. Authors: P. Behrens, G. Wißmann, J. Lippke, P. Zerner, I. Bremer, S. Lilienthal, F. Kempf, A.M. Schneider. Title: "Modulation Effects in the Synthesis of MOFs"

---